

**Localizing a diffusion source on graphs:  
analysis and design of node selection strategies**

Submitted in partial fulfillment of the requirements for  
the degree of  
Doctor of Philosophy  
in  
Department of Electrical and Computer Engineering

Sabina Zejnilović

M.Sc. Electrical and Computer Engineering,  
University of Sarajevo, Bosnia and Herzegovina

B.Sc. Electrical and Computer Engineering,  
University of Sarajevo, Bosnia and Herzegovina

Carnegie Mellon University  
Pittsburgh, PA

May 2016



*To my parents.*



Copyright ©2016 Sabina Zejnilović

All rights reserved.



## Acknowledgments

This research was supported by Fundação para a Ciência e a Tecnologia (project FCT [UID/EEA/50009/2013] and a Ph.D. grant from the Carnegie Mellon-Portugal program no. SFRH/BD/51567/2011).

I would like to thank my advisers, João Pedro Gomes and Bruno Sinopoli for their continuous guidance and unwavering encouragement throughout this Ph.D. journey. I am also grateful to João Xavier for his creative input and willingness to immerse into details. I would also like to thank the remaining members of my dissertation committee: Pulkit Grover, Massimo Franceschetti and João Sobrinho for their valuable comments. My gratitude also goes to Dieter Mitsche whose enthusiasm and meticulousness were instrumental for part of this work. João Paulo Costeira and José Moura played a fundamental role within CMU|Portugal program, and I thank them for their continued trust and support.

I would also like to thank Ana Mateus who has carried a significant burden of the administration associated with a dual degree program. A very special thanks goes to my numerous friends and colleagues, both from the 7th floor of ISR and from Porter Hall, for making Ph.D. an enjoyable and enriching experience. Thank you for all our coffee breaks, homework consultation and commiseration, practice presentations, TTLs and Friday lunches... Especially, I am grateful to Susana Brandão and Pinar Ekim Oguz for their friendship and support. I am also thankful to Agović family without whom Pittsburgh would not have felt like home.

Finally, my deepest gratitude goes to my family for their love and faith in me. I am especially thankful to my late parents, Jasmo and Biljana, my sisters, Jasmina and Nermina, my husband Leid and our amazing children, Tamer and Taira.



# Abstract

Many different phenomena, such as spreading of infectious diseases in networks and dissemination of information through social networks are modeled as a diffusion over a network of nodes. Localizing the source of diffusion becomes crucial for quarantine efforts, as well as for identifying trendsetters. In many real world networks, due to their size, it is unfeasible to observe the infection times of all nodes. In this case, identification of the source node is carried out based only on a subset of nodes, called observer nodes. The choice of observer nodes heavily impacts the accuracy of source localization.

In this thesis we specifically focus on the analysis and design of observer selection strategies with the goal of understanding which are the best nodes to observe that contribute the most to the disambiguation of the source on graphs for different diffusion scenarios. There are four main contributions of our work:

- We model the dynamics of network diffusion in a purely deterministic scenario as a linear time-varying system, and present a necessary and sufficient condition for exact source localization in the context of the proposed model, as well as in the context of graph theory. Relating the observer selection problem to a known problem in graph theory, we design observer selection strategies with performance guarantees.
- We present necessary and sufficient conditions for exact source localization when the network topology is not fully known as the edges between different communities are hidden, and the components are all trees, cycles, grids and complete graphs. We also give sufficient conditions when the components are of arbitrary structure.
- We formulate a metric, based on error exponents, that can be used to compare different observer subsets from the perspective of source localization error. We evaluate the metric for three different diffusion scenarios; in each, the infection times are modeled as random variables with different distributions: Gaussian, Laplace and exponential.
- We develop different sequential selection strategies, optimal and sub-optimal, for dynamic observer selection in both deterministic and stochastic setting, and demonstrate the applicability of one of the proposed strategies on a real-world dataset of a cholera outbreak.



# Contents

|          |  |           |
|----------|--|-----------|
| <b>1</b> | <b>Introduction</b>  | <b>1</b>  |
| 1.1      | A general network diffusion model . . . . .  | 2         |
| 1.2      | Related work . . . . .   | 3         |
| 1.3      | Thesis contributions . . . . .   | 11        |
| <b>2</b> | <b>Node selection for deterministic infection times</b>  | <b>13</b> |
| 2.1      | Block selection . . . . .  | 14        |
| 2.1.1    | Linear systems model . . . . .   | 15        |
| 2.1.2    | Graph theoretic model . . . . .  | 18        |
| 2.1.3    | A note on unknown activation time . . . . .  | 21        |
| 2.2      | Sequential selection . . . . .   | 22        |
| 2.2.1    | Optimal strategy . . . . .   | 23        |
| 2.2.2    | Greedy strategies . . . . .  | 27        |
| 2.2.3    | Simulation results . . . . .   | 33        |
| 2.2.4    | Extending the results to unknown activation time . . . . .   | 36        |
| 2.3      | Summary . . . . .  | 39        |
| <b>3</b> | <b>Node selection for deterministic infection times and in the presence of uncertainty in the network topology</b> | <b>41</b> |
| 3.1      | Block selection . . . . .  | 43        |
| 3.1.1    | Results for special graph classes . . . . .  | 44        |
| 3.1.2    | Results for general graph classes . . . . .  | 56        |

|          |  |            |
|----------|--|------------|
| 3.2      | Source localization using observed infection times . . . . .       | 60         |
| 3.3      | Summary . . . . .  | 64         |
| <b>4</b> | <b>Node selection for stochastic infection times</b>               | <b>67</b>  |
| 4.1      | Block selection . . . . .  | 68         |
| 4.1.1    | A general framework for deriving error exponents . . . . .         | 70         |
| 4.1.2    | Observations are modeled as Gaussian random variables . . . . .    | 77         |
| 4.1.3    | Observations are modeled as Laplace random variables . . . . .     | 87         |
| 4.1.4    | Observations are modeled as exponential random variables . . . . . | 95         |
|          | Properties of the exponent . . . . .                               | 98         |
| 4.1.5    | Simulation results . . . . .                                       | 101        |
| 4.2      | Sequential selection . . . . .                                     | 105        |
| 4.2.1    | Real-world case study: Cholera Outbreak . . . . .                  | 110        |
| 4.3      | Summary . . . . .  | 115        |
| <b>5</b> | <b>Thesis conclusions and future work</b>                          | <b>117</b> |
| 5.1      | Conclusions . . . . .  | 117        |
| 5.2      | Limitations and future work . . . . .                              | 120        |
| <b>6</b> | <b>Bibliography</b>  | <b>123</b> |

# List of Tables

|     |   |    |
|-----|---|----|
| 1.1 | Summary of related work with focus on source localization . . . . .   | 9  |
| 1.2 | Summary and comparison with related work with focus on observer selection . . . . .                               | 10 |
| 2.1 | A minimum number of nodes that achieves network observability for special graph classes .                         | 19 |
| 2.2 | The expected cost calculated for each node of the network in Figure 2.3a of being the first<br>observer . . . . . | 27 |
| 2.3 | RHS of (2.22): $\sum_{s \in S(O')} h_s(O', o)$ . . . . .  | 30 |



# List of Figures

|     |   |    |
|-----|---|----|
| 2.1 | Network observability for a tree network with 6 nodes . . . . .   | 18 |
| 2.2 | Performance of the Algorithm 1 for 500 Erdős-Rényi graphs with 20 nodes and different edge probabilities. . . . . | 21 |
| 2.3 | Analysis of source candidates . . . . .   | 24 |
|     | (a) An example network . . . . .  | 24 |
|     | (b) Observation diagram when node 1 is the source . . . . .   | 24 |
| 2.4 | The performance of dynamic programming and greedy approaches for solving the problem (2.8) . . . . .              | 34 |
|     | (a) Cost incurred by the proposed approaches compared to a benchmark . . . . .                                    | 34 |
|     | (b) Cost incurred by the optimal and greedy approaches . . . . .  | 34 |
| 2.5 | Time required by dynamic programming and the greedy approaches for solving the problem (2.8) . . . . .            | 35 |
| 2.6 | The performance of Algorithms 3 and 5 for larger sized networks . . . . .   | 35 |
| 2.7 | The performance of dynamic programming and greedy approaches for solving the problem (2.9) . . . . .              | 35 |
|     | (a) Number of source candidates . . . . .   | 35 |
|     | (b) Time required . . . . .   | 35 |
| 3.1 | Network observability illustrated on a partially known network with two components. . . . .                       | 44 |
|     | (a) Vertices $o_1, o_2$ and $o_3$ are included in the observed set $O$ . . . . .                                  | 44 |
|     | (b) Vertices $o_1, o_2, o_3, o_4$ and $o_5$ are included in the observed set $O$ . . . . .                        | 44 |

|      |   |    |
|------|---|----|
| 3.2  | Case I in the Proof of Theorem 9: Constructing trees $H_1$ and $H_2$ when both components $C_i$ and $C_j$ have at least two vertices. . . . . | 47 |
|      | (a) Both components have a leaf which is not included in $O$ . . . . .  | 47 |
|      | (b) All leaves of $C_i$ are in $O$ and $C_j$ is not a path. . . . .   | 47 |
|      | (c) All leaves of $C_i$ are in $O$ and $C_j$ is a path. . . . .   | 47 |
|      | (a) $C_j$ is a path. . . . .  | 47 |
|      | (b) $C_j$ is not a path. . . . .  | 47 |
| 3.4  | Proof of Theorem 10: Constructing trees $H_1$ and $H_2$ when both components $C_i$ and $C_j$ are complete graphs. . . . .                     | 49 |
|      | (a) $C_i$ is of size at least 3, with two vertices that are not included in $O$ . . . . .   | 49 |
|      | (b) $C_i$ is of size 2 and neither vertex is included in $O$ . . . . .  | 49 |
|      | (c) Both $C_i$ and $C_j$ , are size 2 and each have only one node in $O$ . . . . .  | 49 |
| 3.5  | Proof of Theorem 11: Constructing $H_1$ and $H_2$ when the components are grids. . . . .  | 52 |
|      | (a) The vertices $r_1^i$ and $r_2^i$ are not corner vertices and they differ in both coordinates. . . . .                                     | 52 |
|      | (b) The vertices $r_1^i$ and $r_2^i$ are not corner vertices and they differ in one coordinate. . . . .                                       | 52 |
|      | (c) The vertices $r_1^i$ and $r_2^i$ are two corner vertices with one identical coordinate. . . . .   | 52 |
| 3.6  | Case I in the Proof of Theorem 12: Both cycle components have an even number of vertices. . . . .   | 54 |
|      | (a) The vertices $p$ and $u$ lie in the same semi-cycle. . . . .  | 54 |
|      | (b) The vertices $p$ and $u$ lie in different semi-cycles. . . . .  | 54 |
| 3.7  | Proof of Theorem 12: Constructing $H_1$ and $H_2$ when the components are cycles. . . . .   | 54 |
|      | (a) The vertices $r_1^i$ and $r_2^i$ are exactly at distance $\frac{n_i}{2}$ . . . . .  | 54 |
|      | (b) The vertices $r_1^i$ and $r_2^i$ are not at distance $\frac{n_i}{2}$ . . . . .  | 54 |
| 3.8  | Proof of Theorem 14: Extending the shortest path $r - u$ to a shortest path $r - u'$ . . . . .  | 58 |
| 3.9  | Performance of the boundary bound . . . . .   | 60 |
| 3.10 | A tree network of 20 nodes with two unobserved edges . . . . .  | 63 |
| 3.11 | The effect of the number of observers on the optimization problem (3.9) for a 20 node tree with two unobserved edges. . . . .                 | 64 |
|      | (a) Time required to solve (3.9) . . . . .  | 64 |

|     |  |     |
|-----|--|-----|
| (b) | Number of possible solutions to (3.9)  | 64  |
| 4.1 | Unit ball in two-dimensional space for $\gamma(i, j)$ , centered at a point $\mathbf{a}^i = 1$ and $\mathbf{a}^j = 1$ denoted with a red circle.   | 100 |
| 4.2 | Relationship between error probability and error exponents for 200 trees of 20 nodes and 9 observers where infection times of the observers are modeled as variables with multivariate Gaussian distribution                             | 102 |
| (a) | Binned error exponents vs mean error probability for different levels of variation of propagation delay  | 102 |
| (b) | Error exponent vs error probability with each scatter point representing a different spanning tree   | 102 |
| 4.3 | Relationship between error probability and error exponents for 100 Erdős-Rényi graphs of 20 nodes and 500 different subsets of 5 observers where infection times of the observers are modeled as variables with exponential distribution | 103 |
| (a) | Error exponent vs mean error probability for different levels of observation noise   | 103 |
| (b) | Error exponent vs error probability with each scatter point representing a different subset of observers in one graph  | 103 |
| 4.4 | Comparison of performances of the proposed metric with centrality based approaches   | 103 |
| 4.5 | Map and a graph model of the Thukela river basin   | 112 |
| (a) | Hydrographic map of the Kwazulu-Natal province from [1]  | 112 |
| (b) | Graphical model of the Thukela river basin   | 112 |
| 4.6 | The results of applying Algorithm 7 to the dataset of Cholera outbreak in KwaZulu Natal  | 113 |
| (a) | 19 observers are selected until the stopping criterion is met  | 113 |
| (b) | Estimate of the source throughout the iterations of the Algorithm 7  | 113 |
| 4.7 | The performance of the random observer selection   | 114 |
| (a) | Histogram of the number of the selected observers  | 114 |
| (b) | Histogram of the distance of the true source to the source estimate  | 114 |



# List of Algorithms

|   |  |     |
|---|--|-----|
| 1 | Greedy algorithm for selecting the minimum number of observers needed for network observability . . . . .  | 20  |
| 2 | Greedy algorithm for selecting $r$ observers that lead to the smallest ambiguity in the source identity . . . . .  | 20  |
| 3 | Greedy algorithm for sequential selection of observers for source localization with the smallest cost based on adaptive submodularity . . . . .                    | 32  |
| 4 | Greedy algorithm for sequential selection of $r$ observers that lead to the smallest ambiguity in the source identity based on adaptive submodularity . . . . .    | 33  |
| 5 | Greedy algorithm for sequential selection of observers for source localization with the smallest cost based on minimizing the worst case . . . . .                 | 33  |
| 6 | Greedy algorithm for sequential selection of $r$ observers that lead to the smallest ambiguity in the source identity based on minimizing the worst case . . . . . | 34  |
| 7 | Greedy algorithm for sequential source localization when the infection times are stochastic .  | 109 |



# Chapter 1

## Introduction

Many different phenomena that are observed in today's technological, social and biological networks are modeled as network diffusion. Examples include: propagation of diseases in human populations [2], spreading of worms, email viruses and faults in communication networks [3] and dissemination of information and propagation of influence in social networks [4]. In disease propagation, individuals are modeled as the nodes, and the connections between them as the edges, as many diseases spread through contact of an infected individual with the disease-free ones. Similarly, in spreading of computer viruses, the communication equipment represents the nodes and the channels between them are the edges, while in rumor propagation, again, the individuals are the nodes, and the friendship ties between them are the network edges.

In all of the above examples of diffusion, localizing the source, i.e., the node that initiated the diffusion, plays a crucial role in limiting the damages or identifying trendsetters. Identifying patient zero, also referred as the index case, is helpful for understanding the origin of the disease and for prevention of further outbreaks. Localizing and isolating the computer hosting a virus is a key to curbing the infection, and also aids the authorities in apprehending the perpetrators. Similarly, law enforcement agencies may want to identify individuals who initiate industry rumors or publish malicious information on social network sites. On the other hand, marketing companies would like to single out influential individuals in peer networks, who initiate certain trends or purchasing behavior. Therefore, source localization represents a task of significant interest.

Often, information available for source localization includes the times when the nodes first became infected or informed. However, in many real-world networks, due to their size and the cost of data collection, as well as privacy issues, it is unfeasible to observe the infection times of all nodes [5, 6, 7, 8, 9, 10, 11]. In these cases, identification of the source node involves only observations of a subset of nodes, called

observer nodes. The choice of these observer nodes heavily impacts the ability to localize the source, hence, selection of observer nodes plays a critical role for the task of source localization in graphs. In this thesis we specifically focus on the analysis and design of observer selection strategies with the goal of understanding which are the best nodes to observe that contribute the most to disambiguation of the source on graphs for different diffusion scenarios.

## 1.1 A general network diffusion model

In this work, we refer to network diffusion to describe the process of a contagion spreading through a network, where the network is modeled as a graph. A contagion may correspond to a virus, a trend or information, and a network can be social, technological or biological. A network is represented using a graph  $G = \{V, E\}$ , where  $V = \{1, 2, \dots, N\}$  is the set of vertices representing the individuals or nodes and  $E \subseteq V \times V$  is the set of edges that may correspond to communication channels or personal ties. There is an edge between nodes  $i$  and  $j$ ,  $(i, j) \in E$ , if nodes  $i$  and  $j$  can communicate directly. If  $(i, j) \in E$  implies that  $(j, i) \in E$ , then the associated graph is called undirected. We will assume  $G$  to be undirected, as infections, rumors or viruses spread through channels and ties which are typically bidirectional. Additionally, we will consider that the diffusion spreads over a connected graph, meaning that there is a path between any two vertices in a network. If some network nodes were disconnected from the rest, the contagion could not reach them, and they would not be relevant to the diffusion process. Then, to study diffusion we would only consider the remaining part of the network, which is connected. In Chapters 2 and 4 we will assume to have complete knowledge of network topology: complete knowledge of nodes and edges between them. However, in Chapter 3 we relax this assumption and allow some uncertainty in our knowledge of the underlying graph. We still assume complete knowledge of network nodes, while we consider that some edges are hidden and remain unknown to us. In this case, the graph that we observe is disconnected, but the graph over which the contagion has propagated is in fact connected.

The distance between two vertices  $u$  and  $v$  in graph  $G$  represents the number of edges in a shortest path connecting them and will be denoted as  $d_G(u, v)$ . When there is no ambiguity in the identity of the graph that is referred to, the graph subscript will be dropped to simplify the notation and distance will be denoted as  $d(u, v)$ . The vector of graph distances of node  $u$  to a set of nodes  $O = \{o_1, \dots, o_r\}$  in a graph  $G$  will be denoted as  $\mathbf{d}_G(O, u) = [d_G(u, o_1), \dots, d_G(u, o_r)]^T$ . Again, subscript  $G$  will be dropped in case there is no uncertainty in the identity of the graph. The adjacency matrix  $\mathbf{A}$  of graph  $G$  is a  $N \times N$  symmetric matrix, with elements  $[\mathbf{A}]_{ij} = 1$  if  $(i, j) \in E$  and  $[\mathbf{A}]_{ij} = 0$  otherwise.

We assume a widely used *Susceptible-Infected propagation model* [12] that was initially used in modeling of epidemics. In this model, nodes can be in either one of two states: infected or not yet infected (susceptible).

In our setting, we will use the term *infected* node to denote a node to which a contagion has reached, regardless of what that contagion is: an infection, a computer virus, a rumor or a certain purchasing or social trend. Initially, only one infected node is present in the network and we denote it as the *source* node. Once a node becomes infected, it remains in that state indefinitely and continues spreading the contagion. As all nodes are susceptible to the contagion, after some time the whole network will become infected with probability 1.

The time when the first node became infected is referred to as the *activation time*,  $t_0$ . We will be considering several models for  $t_0$ : assuming it to be known, completely unknown and modeling it as a random variable with known distribution. Once a node  $u$  is infected at time  $t_u$ , it sends the information to its neighbor  $v$  at time  $t_v = t_u + \theta_{uv}$ , where  $\theta_{uv}$  denotes the *propagation delay* along the edge between nodes  $u$  and  $v$ . *Infection time* refers to the first time when a node receives the contagion. In Chapter 4 we will be making a distinction between a *true infection time*, which refers exactly to the time when a node became infected, and an *observed infection time*, which denotes a time when an individual exhibits symptoms of infection or reports knowing of a certain rumor. In Chapters 2 and 3, we will make no such distinction, as we assume both these times to be the same. We will also be considering several different models for the propagation delay along the edge. In Chapters 2 and 3, we will consider this delay to be a constant and identical for all the edges. In order to simplify the presentation, we will assume this constant to be exactly 1, as we can always normalize all the variables. In Chapter 4 we will model the propagation delay as a random variable with normal distribution. Additionally, in Chapter 4 we will consider the existence of observation noise which will prevent direct observation of a node's true infection time, and instead only observed infection times will be known. Observation noise will be modeled as a random variable with exponential or Laplace distribution.

Due to network size, limited resources and privacy issues, the infection times cannot be observed for all the nodes. We denote those nodes whose state can be observed and whose infection times are known as *observers*. We will denote with  $O = \{o_1, o_2, \dots, o_r\}$  the set of observers, with  $r$  typically being much smaller than the total number of nodes  $N$ . Infection times of observers are deterministic in Chapters 2 and 3, and in Chapter 4 they are stochastic.

*Note:* Vectors will be denoted in bold, matrices with bold capital letters,  $[M]_{ij}$  will denote the  $i, j$ -th entry of the matrix  $M$ , while  $\mathbf{v}^T$  will stand for the transpose of vector  $\mathbf{v}$ .

## 1.2 Related work

Due to many different events that can be modeled as spreading of epidemics in a network, this topic has been widely researched by many different communities. Initially, the focus has been on the dynamics of the diffusion process, for example, analyzing the effect of the rate of disease spreading on the final size of the

infected population, and investigating the conditions under which epidemics either die out or persist. Classic epidemiology models assume that the population is uniform and homogeneously mixing, i.e., an infected individual is equally likely to spread the disease to any other member of the population [12]. Later works removed this assumption and studied the effect of topology on the spreading of epidemics, for example [2, 13].

Another active line of research focuses on making predictions about the likelihood of an infectious disease outbreak. One type of prediction relates to the risk that a novel infection will appear in a given population, or given an infectious disease is present, what would be its impact on the population in terms of the number of infected individuals or which individuals are most likely to be infected next? Another type of prediction deals with the impact of possible intervention: how many and which individuals should be selected for treatment, vaccination or quarantine in order to contain the epidemic [14]. In order to predict the spatiotemporal patterns of epidemic spreading there has been a lot of work on developing realistic computational epidemic models. Generally, there have been two approaches to modeling: agent based - where the agents represent single individuals, and meta-population based - where the system is divided into regions [15]. Agent-based models provide a rich scenario, but with a high computation cost, while meta-population models are less detailed but more scalable. An example of an agent-based approach is presented in [16], where spreading of smallpox is simulated on large-scale graphs built using actual census, land-use, and population-mobility data. A general stochastic meta-population model that incorporates actual travel and census data from 220 countries was developed in [17] and validated on data from the global spread of SARS. A Global Epidemic and Mobility model, also based on meta-population scheme that incorporates railway and airline connections, presented in [15], allows for simulation of the spread of epidemics at the worldwide scale. When the contact network cannot be mapped fully as it changes in time, past contact data can also be used to infer the risk of infection. For example, in [18], a risk assessment analysis incorporating a measure of node's tendency to maintain contacts and knowledge of past structural and temporal pattern properties is shown to provide accurate predictions. The question of an optimal vaccination strategy has also been widely researched. For example, an optimal vaccination strategy for a foot-and-mouth outbreak is investigated in [19], and a radius of each infected farm around which vaccination should be performed is determined using a stochastic, farm-based, spatially-structured model. In [20], it is shown that the most efficient protocol for vaccination in the case of sexually-transmitted diseases consists of sampling people at random and vaccinating their latest contacts.

The study of identifying the source of diffusion started later, with the work of [4], where the most likely source of a rumor is located by observing which nodes have been infected at a certain time and knowing the underlying network structure. The standard Susceptible-Infected model for epidemics is assumed. The time taken for a node to infect its susceptible neighbor is modeled as a random variable. Across all edges, the random variables are independent and have an exponential distribution. A source estimator that depends on

a metric denoted as rumor centrality is proposed and it corresponds to the maximum-likelihood estimator for regular trees. Even with a single source and assuming that the neighbors of an infected node are all equally likely to be infected at each time step, it was shown in [4] that source localization is a #P-complete problem. Based on the estimator for trees, an efficient heuristic estimator for general graphs is proposed and its performance is verified through simulations.

Incorporating *a priori* knowledge of the set of suspect nodes with the snapshot observation of infected nodes, a maximum a posteriori (MAP) estimator for source identification is proposed in [21] and exact and asymptotic results on its performance on regular tree-type networks are presented.

The problem is extended to multiple sources in [22]. When the number of sources is unknown a priori, an estimator for sources and their infection regions (subsets of nodes infected by each source) is derived by approximating the rumor centrality metric of [4]. Theoretical performance measures are obtained for the class of geometric trees, and by simulation, for general networks.

In [23], the effect of multiple observations on the performance of the source estimator is analyzed, showing that sequential observations for a single instance of rumor spreading cannot improve detectability over the initial snapshot observation. On the other hand, multiple independent observations, which correspond to different spreading instances from the same source, lead to dramatic improvement in detectability.

Due to the size of the networks of interest and the cost of collecting data, it is often not feasible to know the status of all the nodes in the network. Assuming that each node reports its infection status with probability  $p > 0$ , the rumor centrality estimator is extended in [7]. It is shown that for regular trees, such an estimator achieves a probability of correct detection close to the optimal, where  $p = 1$ , as long as the sampling probability  $p$  is higher than a fixed threshold. On the other hand, for geometric trees, for any  $p > 0$ , the estimator achieves essentially the same performance as in the case of  $p = 1$ . Under the same assumptions, the problem is analyzed in [8] and it is shown that the source estimator associated with the most likely infection path in a tree is a Jordan center, i.e., the node with the minimum distance to the set of observed infected nodes.

Moving away from the Susceptible-Infected model, [24] investigates the single source estimation problem for the Susceptible-Infected- Recovered (SIR) model, where an infected node may recover and will not be infected again. Recovery can happen due to a number of reasons: an individual might heal and become immune, or anti-virus software can be installed on a computer. The maximum likelihood estimator, in this case, is hard to obtain even for regular trees, as there are many possible infection sample paths, and hence an estimator based on the most likely infection path is proposed. As in [8], the source estimator associated with the most likely infection path of infinite trees is a Jordan center of the network. Similar results are obtained for the Susceptible-Infected- Susceptible (SIS) model analyzed in [25]. In the SIS model, a recovered node is susceptible to be infected again, which can model certain diseases like tuberculosis, or change of opinion

under the influence of peers in social networks. In the independent cascade (IC) model, nodes are also in one of the two states: infected or susceptible and each infected node only attempts to activate each of its susceptible neighbors once with specified probability. In [26], it is proved that the Jordan infection center is also the MAP estimator of the source for tree networks under the IC model. Based on this estimator, an algorithm is developed for general networks with detection guarantees derived for Erdős-Rényi graphs.

For both SI and SIR models, in [27] many epidemic realizations are obtained by simulation for each suspected source node, and the node for which the realizations have highest similarity to the observed epidemics is identified as the source. Departing from maximum-likelihood estimation and its approximations, in [28], several different network centrality measures are applied to identify the source; The principle of Minimum Description Length and the smallest eigenvector of the Laplacian sub-matrix are used in [29] to localize multiple sources; a spectral technique which identifies the nodes whose removal leads to the highest reduction of the largest eigenvalue of the adjacency matrix is proposed in [30], while a greedy algorithm in [6] determines the minimal number of nodes needed to reach a subset of preselected nodes that reported the rumor. In [31], an inference algorithm based on Dynamic Message Passing is proposed to localize a source under the SIR model. In [32], a new metric, Rationality Observation Value, is defined for localizing a source in a tree graph and generalized for an arbitrary graph.

In all of the previously discussed works, observations based on which the source was localized comprised only a snapshot of the network at a certain time, i.e., knowledge of which nodes were infected at a certain time. However, in [5] additional information is available: the exact time of infection of a subset of nodes. In SI settings, the propagation time needed for a node to infect a neighbor is modeled as a Gaussian random variable, rather than an exponential one as in [4, 7, 21, 22, 23]. This is justified by the fact that in large networks observed infection times represent a sum of a large number of propagation times, hence, they can be approximated by Gaussian variables due to the central limit theorem. An optimal maximum-likelihood estimator is derived for tree networks, while its extension is applied to general networks and its effectiveness tested on a real data set from a cholera outbreak. As in other works [4, 21, 22, 23], the transition from a tree network to an arbitrary one is done by assuming that the diffusion occurred in a network through a breadth-first search (BFS) tree, motivated by intuition that the infection spreads from the source along minimum-distance paths. A modified breadth-first algorithm for constructing a spreading tree for each node is proposed in [33]. The nodes are then ranked according to either the cost of the tree or the timestamps, and the source is chosen as the top-ranked node. Simulation results in [33] show that using such construction of trees compared to BFS trees yields a higher accuracy of source localization. Table 1.1 summarizes related work that focuses on source localization.

In some of the above cited works [5, 6, 7, 8, 9, 10, 11], estimation involves only a subset of nodes in order to include the practical constraint that the status of all the nodes cannot be known in many real networks,

due to their size, resource constraints or privacy issues. In [7, 8] each node has a certain probability  $p$  of being observed, and the estimators achieve desirable performance conditioned on  $p$  being larger than a certain threshold. In [5, 6, 9, 10, 11], nodes whose status can be observed are selected in advance. Since the performance of the estimator depends on the number and choice of these preselected nodes, different selection techniques are investigated. In [5] two strategies are compared by simulations: random and the selection of high-degree nodes, while in [6] the proposed strategies involve not only random and high-degree nodes, but also nodes with the largest betweenness centrality and nodes at a specified distance away from each other. Similarly, in [10], several placement strategies of the observers based on centralities of nodes (high-degree, high-betweenness, high-clustering coefficient, high-eigenvector and high-closeness) are compared using simulations. In contrast to the probabilistic models, [34] studies the problem from a combinatorial optimization point of view: framing the problem of finding the smallest set of observed nodes that guarantees deterministic identification of the source as a graph theoretic problem of finding a minimum weighted doubly resolving set (DRS). As in [5], the infection times of a subset of nodes is known, while the time when the source became active is considered unknown. However, the propagation times are now assumed a constant. Using the concept of DRS, in [9], a polynomial-time dynamic programming algorithm is proposed for selecting an optimal number of observers in a tree that yields the lowest uncertainty in source localization, again for deterministic propagation times. A sufficient condition for source localization based on unique difference of distances to the observers is given in [11], without making a connection to the concept of DRS.

Another aspect of network diffusion that has increasingly received attention from the research communities is inference of the network topology over which diffusion takes place. The motivation for this line of investigation comes from certain types of propagation, where it is not always possible to know who has infected or informed whom, as in virus spreading when individuals become sick, without knowing from where the virus came from, or in viral marketing where people who purchase products or adopt particular behaviors do not explicitly acknowledge who was their influencer [35, 36, 37, 38].

The link prediction problem aims to extract missing or identify inaccurate diffusion links. This is useful, for example, in biological networks where costly field and/or laboratory experiments are needed to learn whether a link exists between two nodes. Then, instead of checking all possible links, researchers can focus on the most likely, predicted, links [35]. In addition, the data in constructing social networks may contain inaccurate information and link prediction algorithms can be applied to identify such links. The probability of a link between two nodes can depend solely on similarity of their network properties, or a certain underlying network structure can be assumed; the survey of different methods is found in [35]. Inference of both the missing edges and nodes is tackled in [36], where a Kronecker graph is used to model the underlying network, and the Expectation Maximization method is used to estimate both the model parameters, as well as the

edges in the missing part of the network.

In [37] the whole network structure is inferred based on infection times of nodes from multiple contagions (the idea, information, virus, disease), without any assumptions on the structure of the underlying network. The probability of an edge between any two nodes depends only on the time difference of their infection times, and the most likely propagation tree for each contagion is considered, as the number of possible diffusion trees is exponentially high. The final network is inferred by maximizing a log-likelihood function using the property of submodularity. The subsequent work [38], removes the assumption that all connected nodes in the network infect their neighbors with the same probability and estimates both the missing edges, as well as the edge transmission probabilities. The complete network structure is also inferred in [41], but now, the probability of an edge between two nodes does not depend on the difference of their infection times, but on the number of infected nodes between those times. In [39], the problem of source localization and the problem of learning the diffusion graph are tackled at the same time using compressed sensing. For the SIS model, an epidemic network is reconstructed observing the change in the state of the nodes and the source is localized as the node that never changes its infected state. In [40], the network is again reconstructed using the difference of infection times. The parameters of the Gaussian distribution that characterizes the propagation delays along the edges are learnt and then the source is localized by maximizing the log-likelihood, similarly to [5].

Our work most closely follows [5], as we also assume that we are able to observe the infection times of a subset of nodes and that a single contagion spreads according to the Susceptible-Infected model, with each infected node spreading the infection to its neighbors with probability equal to 1. In Chapter 4, we first study the problem in a purely deterministic scenario as done in [9, 34] in order to derive analytical results that would help in understanding a more practical framework. We assume the network structure to be completely known and we propose optimal, and efficient sub-optimal, both block and sequential, node selection strategies. Next, in Chapter 3, we relax the assumption of complete knowledge of the network and assume that some connections are not observed, with the same motivation as discussed for the link prediction and network completion problem [35, 36, 37, 38, 41]. Again for deterministic propagation times, we derive necessary and sufficient conditions for correct source localization in terms of selected observers, which has not been addressed previously. In Chapter 4, we present node selection strategies, again block and sequential, now for stochastic infection times, either assuming the propagation delay to be a random variable or by assuming some uncertainty in observing the infection times. Unlike in previous work [5, 6, 10, 11] that also assumes stochastic infection times, we go beyond comparing the performance of centrality based selection strategies through simulations. Specifically, we derive a theoretical framework based on which we propose new observer selection strategies. Table 1.2 summarizes and compares our work with related work that focuses on observer selection problem.

|                    | [4] | [8] | [21] | [22] | [23] | [7] | [24] | [25] | [27] | [28] | [29] | [30] | [32] | [39] | [31] | [40] | [33] |
|--------------------|-----|-----|------|------|------|-----|------|------|------|------|------|------|------|------|------|------|------|
| States available   | x   | x   | x    | x    | x    | x   | x    | x    | x    | x    | x    | x    | x    | x    | x    | x    | x    |
| All the nodes      |     |     |      |      |      |     |      |      |      |      |      |      |      |      |      |      |      |
| Some nodes         |     | x   |      |      |      | x   |      |      |      |      |      |      |      |      |      |      |      |
| Some timestamps    |     |     |      |      |      |     |      |      |      |      |      |      |      |      |      |      |      |
| No. of sources     | x   | x   | x    | x    | x    | x   | x    | x    | x    | x    | x    | x    | x    | x    | x    | x    | x    |
| one                |     |     |      |      |      |     |      |      |      |      |      |      |      |      |      |      |      |
| multiple           |     |     |      |      |      |     |      |      |      |      |      |      |      |      |      |      |      |
| Model of infection | x   | x   | x    | x    | x    | x   | x    | x    | x    | x    | x    | x    | x    | x    | x    | x    | x    |
| SI                 |     |     |      |      |      |     |      |      |      |      |      |      |      |      |      |      |      |
| SIR                |     |     |      |      |      |     |      |      |      |      |      |      |      |      |      |      |      |
| SIS                |     |     |      |      |      |     |      |      |      |      |      |      |      |      |      |      |      |
| Network structure  | x   | x   | x    | x    | x    | x   | x    | x    | x    | x    | x    | x    | x    | x    | x    | x    | x    |
| known              |     |     |      |      |      |     |      |      |      |      |      |      |      |      |      |      |      |
| unknown            |     |     |      |      |      |     |      |      |      |      |      |      |      |      |      |      |      |
| Node selection     | x   | x   | x    | x    | x    | x   | x    | x    | x    | x    | x    | x    | x    | x    | x    | x    | x    |
| block              |     |     |      |      |      |     |      |      |      |      |      |      |      |      |      |      |      |
| sequential         |     |     |      |      |      |     |      |      |      |      |      |      |      |      |      |      |      |
| Verification       | x   | x   | x    | x    | x    | x   | x    | x    | x    | x    | x    | x    | x    | x    | x    | x    | x    |
| synthetic data     |     |     |      |      |      |     |      |      |      |      |      |      |      |      |      |      |      |
| real networks,     |     |     |      |      |      |     |      |      |      |      |      |      |      |      |      |      |      |
| generated data     |     |     |      |      |      |     |      |      |      |      |      |      |      |      |      |      |      |
| real data          |     |     |      |      |      |     |      |      |      |      |      |      |      |      |      |      |      |

Table 1.1: Summary of related work with focus on source localization

|                                  | [5] | [6] | [9] | [10] | [11] | Chapter 2 | Chapter 3 | Chapter 4 |
|----------------------------------|-----|-----|-----|------|------|-----------|-----------|-----------|
| Information available            |     | X   |     | X    | X    | X         | X         | X         |
| State of some nodes              | X   |     | X   | X    | X    |           |           |           |
| Timestamps of some nodes         | X   | X   |     |      |      | X         |           |           |
| exponential variables            |     |     |     | X    | X    |           |           |           |
| Gaussian variables               | X   |     | X   |      | X    |           | X         | X         |
| deterministic                    |     |     |     |      | X    |           |           |           |
| deterministic, observation noise |     |     |     |      |      | X         |           | X         |
| No. of sources                   | X   | X   | X   | X    | X    | X         | X         | X         |
| Model of infection               | X   | X   | X   | X    | X    | X         | X         | X         |
| SI                               |     |     |     |      |      |           |           |           |
| Network structure                | X   | X   | X   | X    | X    | X         |           | X         |
| known                            |     |     |     |      |      |           |           |           |
| partially known                  |     |     |     |      |      |           | X         |           |
| Node selection                   | X   | X   | X   | X    | X    | X         | X         | X         |
| block                            |     |     |     |      |      |           |           |           |
| sequential                       |     |     |     |      |      | X         |           | X         |
| Verification                     |     |     |     | X    | X    |           | X         | X         |
| synthetic data                   | X   | X   |     |      |      | X         |           |           |
| real networks, generated data    |     |     |     | X    | X    |           |           |           |
| real data                        | X   |     |     |      |      |           |           | X         |

Table 1.2: Summary and comparison with related work with focus on observer selection

## 1.3 Thesis contributions

The main focus of this thesis is the analysis and design of node selection strategies for the purpose of source localization. We analyze the effect of partially available knowledge, both of the infection times and of the underlying topology over which diffusion takes place, on the source localization problem. Next, we list the thesis contributions chapter by chapter.

### **Chapter 2: Node selection for deterministic infection times**

- We define the concept of network observability that characterizes whether the infection times of observed nodes lead to correct source identification when the infection times are deterministic. We develop the model for describing diffusion dynamics similar to the model of the dynamics of a linear time-varying system. We present necessary and sufficient condition for network observability in the context of the proposed model, as well as in the context of graph theory. Leveraging on the approximate algorithms for the set cover problem, we develop algorithms for selecting the smallest number of observers for source localization and for achieving the lowest uncertainty for a specified number of observers, both with performance guarantees. Part of this work was published in [42].
- We analyze the problem of sequential selection of observed nodes from two perspectives: which nodes to observe such that the source is localized with the lowest cost, and for a pre-specified number of time-steps, which nodes to observe such that the resulting number of possible source candidates is lowest. We solve both problems optimally with a dynamic programming approach. Using the framework of adaptive submodularity, we also develop greedy algorithms with performance guarantees. This work was published in [43].

### **Chapter 3: Node selection for deterministic infection times and in the presence of uncertainty in the network topology**

- We extend the concept of network observability when the network structure is not completely known and the edges between different communities are hidden. We present necessary and sufficient conditions for network observability when the components are all trees, cycles, grids and complete graphs. We also give sufficient conditions when the components are of arbitrary structure. This work was published in [44] and [45].
- We show that the number of topologies consistent with the observed disconnected network scales exponentially with the number of unknown edges. We formulate the source localization problem in networks with unknown inter-components edges as a binary linear integer program. This work was published in [46].

#### **Chapter 4: Node selection for stochastic infection times**

- We define a metric based on error exponents for vanishing noise in order to compare the performance of different observer subsets in the context of source localization. We evaluate the error exponent for vanishing noise for three different diffusion scenarios; in each, the infection times are modeled as random variables with different distributions: Gaussian, Laplacian and exponential. This work has been submitted to IEEE Transactions on Signal Processing [47].
- We design an algorithm for sequential source localization when infection times are modeled as correlated Gaussian random variables. We apply a sequential multiple hypothesis test and an observer selection criterion inspired by adaptive submodularity. We validate the proposed algorithm with real data from a cholera outbreak.

## Chapter 2

# Node selection for deterministic infection times

Understanding how a particular selection of network nodes inherently affects the performance of any source estimator requires an analysis of a deterministic propagation model. Uncertainty in the observations or in the knowledge of the underlying network topology can additionally introduce ambiguity in the source localization. We would like to grasp the limitations of the observation model which are purely the result of node selection. Knowing the restrictions imposed by an observer subset on estimation of the source identity gives us a way to upper bound the performance of any source estimator under additional uncertainty. Considering a noiseless scenario to assess the limitations of the observation model is similar to the analysis of system observability. There, observation noise is not considered when characterizing whether the internal state of the system can be inferred from the system's output. Later in this chapter, we are going to use this analogy with the observability of linear systems to model the dynamics of deterministic diffusion and define our own concept of observability in regards to the inference of the source location.

Let us first describe a deterministic propagation model. Once a node  $u$  is infected at time  $t_u$ , it infects its neighbor  $v$  at time  $t_v = t_u + \mu$ . We are assuming the propagation delay along the edge  $u - v$  to be a constant  $\mu$ , for all  $u, v$  pairs of nodes connected by an edge. To simplify the notation, and without loss of generality, we assume  $\mu = 1$ , as we could easily normalize all relevant variables with the value of  $\mu$ . The time when the source node became active is denoted as  $t_0$ . Initially, we will assume  $t_0$  to be known, to model the cases when some external event influences the start of the diffusion. For example, after an earthquake or a public incident, rumors may start flooding the social media. Once the activation time is known, it can be subtracted from all infection times, and hence, we can set it to zero. In Subsections 2.1.3 and 2.2.4 we will analyze the case of unknown  $t_0$ . Assuming node  $s$  to be the source, the infection time of a node  $o_i$  equals the sum of

propagation delays along the edges on a shortest path from the source to node  $o_i$

$$t_{o_i} = t_0 + \sum_{u,v \in P(o_i,s)} \mu_{u,v} = t_0 + d(o_i, s), \quad (2.1)$$

where  $P(o_i, s)$  is the shortest path between  $o_i$  and  $s$  and  $d(o_i, s)$  is the graph distance, i.e., the number of edges in this path. Assuming  $t_0 = 0$ , we have that the infection time of each node in a deterministic model equals its graph distance to the source.

Since our ability to determine the source location based on the observed infection times heavily depends on the number and the choice of observed nodes, we are interested in finding a subset of nodes that would allow us to correctly localize the source. Given that usually resources for observing the nodes are limited and costly, in terms of time and effort required to learn the infection times, we would like to identify the source with the smallest number of observers. Another important issue that we analyze is how to choose a fixed number of observers, when our budget for observing is known and limited, to attain the lowest uncertainty in the source identity. In this Chapter we analyze these questions in two different settings: block and sequential. Sometimes, the choice of observers should be made before any diffusion has occurred, and hence all the observers are selected at the same time, in a block. Other times, however, the observers are selected dynamically, after the diffusion has already occurred. Then, previous observations can be used to decide which subsequent node should be selected in order to determine the source position, either with the smallest observation cost, or with the smallest uncertainty. For block selection strategies, in Section 2.1, we will analyze the problem using two different approaches, one based on linear systems, and the second based on graph theory, in order to gain intuition into the problem and leverage on the available results. For sequential observer selection, in Section 2.2, we also apply two different approaches, one optimal using dynamic programming, and another one, more efficient, applying the adaptive submodularity principle that gives a greedy approach, yet with performance guarantees.

## 2.1 Block selection

When the choice of observer nodes should be made in advance of any contagion spreading, block selection strategies need to be considered. In expectation of the arrival of an epidemic outbreak, due to epidemics spreading in nearby regions, medical teams can be placed in advance near certain communities to be able to quickly localize patient zero and quarantine an infection. By advance selection of appropriate individuals to follow on a social network, marketing companies can trace back trends to influential trendsetters. Since the source is determined using observers' infection times and these correspond to observers' distance to an unknown source node, we need to understand how graph distances affect the ability to localize the source.

In Subsection 2.1.1 we present a model for the dynamics of network diffusion similar to state update of a linear time-varying system. Based on this model we propose a concept of network observability which characterizes the ability to uniquely localize the source. We then provide a necessary and sufficient condition for unique localization. In Subsection 2.1.2, we reformulate the observer selection problem as an existing problem of finding a resolving set of a graph and leverage on existing results to design observer selection strategies. Subsection 2.1.3 discusses the results when the activation time,  $t_0$ , is not known.

### 2.1.1 Linear systems model

Since we are using the Susceptible-Infected (SI) model [12] for network diffusion, nodes can be in either one of two states: infected or not yet infected. Once a node is infected it remains in that state. Letting  $t$  denote a discrete time index, then in our deterministic model with known activation time, only the source node is infected at  $t = 0$ . A node infected at time  $t$  infects all its neighbors at time  $t + 1$ . Let us denote with  $x_i$  the state of node  $i$  at time  $t$ , such that

$$x_i(t) = \begin{cases} 0, & \text{node } i \text{ is still not infected at time } t \\ 1, & \text{otherwise} \end{cases} . \quad (2.2)$$

Stacking the states of all  $N$  nodes at time  $t$  into a vector, we obtain the vector of states  $\mathbf{x}(t)$ . Let  $\mathbf{e}_i$ , denote a column vector with all entries equal to 0 except for the  $i$ -th entry, which equals 1. Then, the initial state  $\mathbf{x}(0)$  equals  $\mathbf{e}_s$ , where  $s$  corresponds to the index of the source node. The infection time of node  $i$ ,  $t_i$ , corresponds to the time when the node became infected, i.e., the time when its state changed from  $x_i(t_i - 1) = 0$  to  $x_i(t_i) = 1$ . Let  $O = \{o_1, o_2, \dots, o_r\}$  denote the set of observers. Typically  $r$  is much smaller than the total number of nodes  $N$ , as not all the individuals report hearing a rumor, nor the infection times of all patients are available. The observers are the only nodes whose infection times are known and we denote the vector of their states as  $\mathbf{y}(t) \in \mathbb{R}^r$ . The states of observers are obtained from the full state vector through multiplication by  $r \times N$  matrix  $\mathbf{C} = [\mathbf{e}_{o_1}, \mathbf{e}_{o_2}, \dots, \mathbf{e}_{o_r}]^T$ . With  $\mathbf{A}$ , we represent an adjacency matrix of a graph. We will also be using the concept of a walk which is a sequence of vertices (possibly repeated) where each vertex is adjacent to the preceding vertex in the sequence. The length of a walk is the number of edges that it uses. Let us also denote by  $\overline{\mathbf{M}}$ , a binary matrix that has the same sparsity structure as matrix  $\mathbf{M}$ , but with all nonzero elements replaced with 1, as follows

$$[\overline{\mathbf{M}}]_{ij} = \begin{cases} 0, & [\mathbf{M}]_{ij} = 0 \\ 1, & [\mathbf{M}]_{ij} \neq 0 \end{cases} .$$

Now, we can state a theorem that characterizes the evolution of network diffusion under the above discussed assumptions.

**Theorem 1.** *The dynamics of network diffusion, under the deterministic SI propagation model, can be characterized as follows*

$$\mathbf{x}(t) = \mathbf{\Phi}(t, 0) \mathbf{x}(0) \quad (2.3a)$$

$$\mathbf{y}(t) = \mathbf{C} \mathbf{x}(t), \quad (2.3b)$$

where  $\mathbf{\Phi}(t, 0) = \overline{\mathbf{A}^t + \mathbf{A}^{t-1}}$ .

*Proof.* The state equation (2.3a) for node  $i$  can be rewritten as

$$x_i(t) = \sum_j [\mathbf{\Phi}]_{ij}(t, 0) x_j(0) = [\mathbf{\Phi}]_{is}(t, 0). \quad (2.4)$$

The last equality of (2.4) holds since  $\mathbf{x}(0)$  has a single nonzero entry for the source node. Now we refer to the specific properties of the powers of adjacency matrices [48], where the  $ij$ -th entry of  $A^t$  equals the number of walks of length  $t$  between nodes  $i$  and  $j$ . Based on this property, we have that if the distance of node  $i$  to the source is  $t_i$ , then  $[\mathbf{\Phi}]_{is}(t, 0) = 0$  for all  $t < t_i$ , which consequently gives  $x_i(t) = 0$  for all  $t < t_i$ . At  $t = t_i$ , both  $[\mathbf{\Phi}]_{is}(t, 0)$  and  $x_i(t)$  assume the value 1. If there exists a walk of length  $t_i$ , then there also exists at least one walk of length  $t_i + 2l$ , for  $l = 0, 1, \dots$ , as any edge included in the walk can be repeated (once in the forward and once in the backward direction) to add a cycle to the walk, increasing its length. Hence  $A^{t_i+2l} > 0$ , and subsequently  $[\mathbf{\Phi}]_{is}(t_i + 2l, 0) = 1$ . At times  $t = t_i + (2l + 1)$ ,  $[\mathbf{\Phi}]_{is}(t, 0)$  is equal to 1, at least due to the term  $A^{t-1}$ . Therefore, for all  $t \geq t_i$ ,  $[\mathbf{\Phi}]_{is}(t, 0) = 1$  and the state of the node is 1, reflecting the fact the node  $i$  became infected at time  $t_i$ .

The observation equation (2.3b) models that at each time  $t$ , only the state of the observers can be seen. Thus, the equations (2.3) describe the state evolution and available observations for the diffusion process in a general network.  $\square$

Presented model of dynamics of network diffusion corresponds to a space state representation of a linear time-varying system with a constant observation matrix. Stacking equations (2.3b) for times  $t = 0, \dots, N-1$ , we get the following matrix equation

$$\begin{bmatrix} \mathbf{y}(0) \\ \mathbf{y}(1) \\ \vdots \\ \mathbf{y}(N-1) \end{bmatrix} = \begin{bmatrix} \mathbf{C} \\ \mathbf{C}\Phi(1,0) \\ \vdots \\ \mathbf{C}\Phi(N-1,0) \end{bmatrix} \mathbf{x}(0),$$

or equivalently

$$\mathbf{Y}_{N-1} = \mathbf{O}_{N-1} \mathbf{x}(0). \quad (2.5)$$

We refer to  $Nr \times N$  matrix  $\mathbf{O}_{N-1}$  as a network *observability matrix*. Using the analogy with linear system we introduce the concept of *network observability* in the context of source localization.

**Definition 1.** For a subset of observers, we call a network observable, if and only if any source node can be unambiguously localized based on the observers' infection times in the deterministic propagation model.

Based on the proposed model of network diffusion 2.3 we present the necessary and sufficient conditions for network observability.

**Theorem 2.** *If the rank of the observability matrix  $\mathbf{O}_{N-1}$  is equal to  $N$  for a given subset of observers, then the network is observable. The source can be localized by recovering the initial condition as follows*

$$\mathbf{x}(0) = \left( \mathbf{O}_{N-1}^T \mathbf{O}_{N-1} \right)^{-1} \mathbf{O}_{N-1}^T \mathbf{Y}_{N-1}. \quad (2.6)$$

*The necessary condition for network observability is for the observability matrix  $\mathbf{O}_{N-1}$  to have  $N$  unique columns.*

*Proof.* In a network of  $N$  nodes, the largest distance between any pair of nodes is at most  $N-1$ , meaning that the states of all the observers will be 1, at most by time  $N-1$  and will remain the same for all  $t \geq N-1$ . Product  $\mathbf{C}\Phi(t,0)$  has an interesting structure; its  $ij$ -th entry is equal to 1, only if there is a path of length smaller or equal to  $t$  between observer  $o_i$  and node  $j$ , otherwise it is 0. Hence, all entries of  $\mathbf{C}\Phi(t,0)$  are equal to 1, for  $t \geq N-1$ . Therefore, stacking  $\mathbf{C}\Phi(t,0)$ , for  $t > N-1$  will not increase the rank of the observability matrix. This is parallel to the property of linear time-varying systems where, where if the initial state can be recovered, then it can be recovered from observations  $\mathbf{y}(0), \dots, \mathbf{y}(N-1)$ . From (2.5), if the observability matrix has a full column rank, we obtain (2.6), as a standard result from linear algebra.

In order to uniquely identify the source node based on the distances of observers to it, it is necessary that at least one observer has a different distance to the source node, compared to all the remaining nodes. If the observability matrix has  $N$  unique columns, looking at the structure of the product  $\mathbf{C}\Phi(t,0)$ , this is

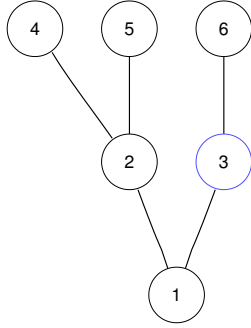


Figure 2.1: An example tree network with 6 nodes. Assuming that node 3 is the only observer, the observability matrix has only 4 unique columns and rank 4, and hence, the network is not observable. In this case, if the infection time of node 3 was  $t_3 = 3$ , then the source could be either node 4 or 5. However, if  $t_3 = 2$ , then we would be able to correctly identify the source as node 2, even though the network is not observable.

equivalent to the condition that there are no two nodes with the same distances to the observers, which is exactly what is needed for correct localization.  $\square$

Verifying the observability of a network using Theorem 2 does not require knowledge of infection times of the observers. Thus, it is a task that can be efficiently performed offline, before the actual source localization takes place. The observability of a network does not depend on the source node, meaning that in such a network, regardless of which node is the source, the information from the observers is sufficient to identify it. However, this condition is not necessary for a particular choice of the source node. As Figure 2.1 illustrates, a network might be generally unobservable given a particular choice of observers, but this does not imply that the information provided by the observers is insufficient to identify the source node in all the cases.

Since the infection times of the observers correspond to their graph distance to the source, localizing the source, other than with (2.6), can be performed directly using graph distances. Let us denote with  $\mathbf{D} \in \mathbb{R}^{r \times N}$  the distance matrix, whose elements  $[\mathbf{D}]_{ij}$  represent the distance between observer  $o_i$  and node  $j$ . Again, let  $\mathbf{y} \in \mathbb{R}^r$  be the vector of infection times of observers. Then the source localization problem can be stated as finding the column of matrix  $\mathbf{D}$  which exactly equals vector  $\mathbf{y}$ . The column number is then the identity of the source node. In case of unobservable network and multiple source suspects, there are multiple columns of  $\mathbf{D}$  equal to  $\mathbf{y}$ . Further analysis of the observer selection problem in the context of graph distance is presented in the next subsection.

### 2.1.2 Graph theoretic model

Network observability, other than through terminology from systems theory, can also be defined using the terms from graph theory as presented in the following Theorem.

**Theorem 3.** *For a given subset of nodes  $O$ , a network  $G$  is observable, if and only if the set  $O$  is a resolving set of  $G$ .*

*Proof.* The necessary condition for correct source localization from Theorem 2 implicitly states that the choice of observers needs to be such that all the nodes in a network have different distances to them. Let us denote with  $\mathbf{d}(i, O) = [d(i, o_1), \dots, d(i, o_k)]$  the  $r$ -vector of distances from node  $i$  to the set of observers  $O = \{o_1, \dots, o_r\}$ . Then, having the set of observers that will satisfy the necessary condition for correct node localization can be stated as  $\mathbf{d}(i, O) \neq \mathbf{d}(j, O)$  for all  $i, j$  pairs of nodes. Stated as such, finding the set of observers with this property corresponds to the problem of finding a resolving set of nodes  $O$  of the graph [49].  $\square$

The introduction of resolving sets by [50] was motivated by the application of placement of a minimum number of sonar detectors in a network and independently, also for describing the structure of chemical compounds in pharmaceutical chemistry [51]. In [52], resolving sets are analyzed in order to determine the minimum number of landmarks needed for robot navigation on a graph. A resolving set of the smallest cardinality is called a *metric basis* and the cardinality of the metric basis is called the *metric dimension* of a graph. We state the connection between the smallest set of observers and a metric basis in the following Corollary of Theorem 3.

**Corollary 4.** *The smallest set of nodes that makes a network  $G$  observable forms a metric basis of  $G$ .*

Due to the time and cost involved with monitoring the nodes, localizing the source using the minimum possible resources is certainly a problem of interest. By establishing a connecting between the minimum number of observers for network observability and a known problem of finding a metric basis, we can take advantage of known results from graph theory. Although finding a metric basis of an arbitrary graph is NP-hard problem [52], for some families of graphs it can be easily determined [53]. Table 2.1 summarizes some of these results. Specific results, among others, also exist for hypercubes and wheel graphs [53], as well as for random networks [54].

Table 2.1: A minimum number of nodes that achieves network observability for special graph classes

| Name              | path | cycle               | complete       | tree                 | d-dim grids     |
|-------------------|------|---------------------|----------------|----------------------|-----------------|
| Min no. of nodes  | 1    | 2                   | $n - 1$        | no. of leaves- $K^a$ | $d$             |
| An example subset | leaf | 2 consecutive nodes | all but 1 node | a subset of leaves   | corner vertices |

<sup>a</sup>  $K$  is the number of nodes of at least three degrees that are on the shortest path between at least two leaves.

The problem of finding the metric dimension of a graph can be cast as the set cover problem [52]. In the set cover problem there is a set  $U$  of  $n$  elements and a collection  $S = \{S_1, \dots, S_m\}$  of  $m$  subsets of  $U$  such that their union covers  $U$ . The goal is to select as few subsets as possible from  $S$  such that their union covers  $U$ . For the problem of finding the metric dimension, we have that the set  $U$  corresponds to the set of all node pairs  $i, j$  for  $i \neq j$ , and each  $S_i$  is a set of node pairs that node  $i$  distinguishes, for  $i = 1, \dots, N$ . A node  $i$  distinguishes two nodes  $u, v$  if it has different distances to them, i.e.,  $d(i, u) \neq d(i, v)$ . Hence, the goal

is to select as few nodes as possible in order to distinguish all node pairs. Set cover problem is known to be NP-Hard, but there exist approximation algorithms for it. Greedy cover algorithm that selects one by one the node that distinguishes the highest number of node pairs is a  $(\log N + 1)$  approximation [52, 55]. Then the same greedy approach with performance guarantees can be applied in order to select the minimum number of observers that achieve network observability. Algorithm 1 shows the pseudocode for the greedy cover.

---

**Algorithm 1** Greedy algorithm for selecting the minimum number of observers needed for network observability

---

```

1:  $O \leftarrow \emptyset$  //  $O$  is the current observer set
2:  $U \leftarrow \{\text{all } i, j \text{ pairs of nodes, for } i \neq j\}$  //  $U$  is the current set of indistinguishable pairs
3: while  $U \neq \emptyset$  do
4:   select a node  $i$  that distinguishes the most node pairs
5:    $O \leftarrow O \cup i$ 
6:    $U \leftarrow U \setminus \{\text{node pairs distinguished by node } i\}$ 
7: end while

```

---

Other than finding the smallest set that achieves observability, we are also interested in selecting a given number of observers that achieves the smallest uncertainty in source identity. One way to look at this problem is to frame it as a maximum coverage problem. Maximum coverage is another known NP-hard problem where there is a set  $U$  of  $n$  elements and a collection  $S = \{S_1, \dots, S_m\}$  of  $m$  subsets of  $U$  such that their union covers  $U$ . Also, an integer  $r \leq m$  is specified, and the goal is to select  $r$  subsets from  $S$  such that their union has the maximum cardinality. Greedy cover is now a  $1 - \frac{1}{e}$  approximation algorithm for the maximum coverage problem [55]. Again, the same greedy approach with performance guarantees can be applied in order to select  $r$  observers that distinguish between the most node pairs. Here, we measure the ambiguity in the source identity with the number of indistinguishable node pairs. If there are  $p$  nodes that cannot be mutually distinguished, that means  $\binom{p}{2}$  pairs that are not distinguishable. Algorithm 2 shows the pseudocode for the greedy cover.

---

**Algorithm 2** Greedy algorithm for selecting  $r$  observers that lead to the smallest ambiguity in the source identity

---

```

1:  $O \leftarrow \emptyset$  //  $O$  is the current observer set
2:  $U \leftarrow \{\text{all } i, j \text{ pairs of nodes, for } i \neq j\}$  //  $U$  is the current set of indistinguishable pairs
3: for  $k = 1$  to  $r$  do
4:   select a node  $i$  that distinguishes the most node pairs
5:    $O \leftarrow O \cup i$ 
6:    $U \leftarrow U \setminus \{\text{node pairs distinguished by node } i\}$ 
7: end for

```

---

The performance of Algorithm 1 is illustrated with the following simulation example. We generated 500 Erdős-Rényi graphs, each with with 20 nodes and a randomly chosen probability of an edge,  $p \in (0, 1)$ . Erdős-

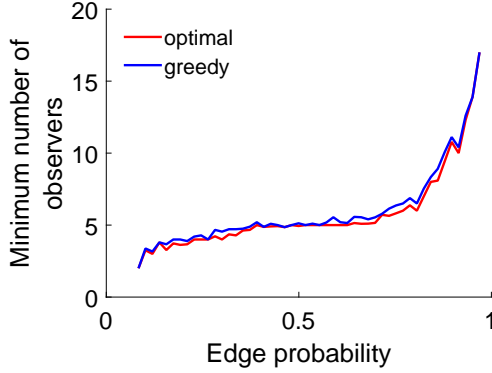


Figure 2.2: Performance of the Algorithm 1 for 500 Erdős-Rényi graphs with 20 nodes and different edge probabilities.

Rényi is a random graph model where each pair of nodes is connected with equal probability, independently of other pairs. For each graph, we found the smallest set of observers, by checking all the possible combinations. Since finding the smallest set is a combinatorial problem, it is computationally very intensive and hence we use only a 20 node graph. Also, for each graph, we use Algorithm 1 to find an approximation of the smallest set. We binned the edge probabilities in 50 evenly sized bins, and for each bin, we averaged the true smallest number of observers, as well as the number of observers found by the greedy algorithm. As Figure 2.2 shows, the approximation algorithm closely follows the optimal solution, and in around 70% of cases, the two quantities actually coincide. The greedy approach chooses at most two observers more than the minimum needed, and this occurred in less than 2% of realizations. Also, the example illustrates that as the edge probability increases and the graph becomes more dense, more observers are needed to correctly distinguish between the nodes. For very sparse graphs, the number of needed observers is small, but as the graph increasingly resembles a complete one, the minimum number of observers tends to  $n - 1$ .

### 2.1.3 A note on unknown activation time

When the activation time of the source is not known, then the infection times of the observers are not used to directly estimate the source location [5, 9, 34, 40]. Instead, one of the observers is chosen as a reference point, and relative observed times are defined. Let us select  $o_1$  as the reference observer, and denote with  $x_{o_i}$  the relative infection time of observer  $o_i$ . Assuming the source to be node  $s$ , from the expression for observers' infection time (2.1) we have

$$x_{o_i} = t_{o_i} - t_{o_1} = d(o_i, s) - d(o_1, s). \quad (2.7)$$

Now, the new observations for source localization are no longer observers' distances to the source, but the difference of distances. In [34] it was shown that the source can be unambiguously localized using the difference of distances if the observers form a *doubly resolving set*. Let  $u, v, i, j$  be four distinct nodes of  $G$ .

Nodes  $\{u, v\}$  doubly resolves  $\{i, j\}$ , or  $\{u, v\}$  doubly resolves  $i$  and  $j$ , if [56]

$$d(u, i) - d(u, j) \neq d(v, i) - d(v, j).$$

Every doubly resolving set is also a resolving set, while the reverse does not hold [56]. Finding the smallest set of the observers that achieves network observability corresponds to another known problem in graph theory: finding a minimum doubly resolving set, which is an *NP*-hard problem. Polynomial time approximation algorithm exist for this problem that achieves an approximation ratio of  $(1 + o(1)) \log N$  [34]. Hence, this algorithm can also be applied to find a minimum number of observers needed for network observability. The result from [34] shows that if  $S$  is a doubly resolving set, and  $s$  is any node from  $S$ , then every pair of nodes is distinguished by at least one element of  $\{\{s, v\} : v \in S \setminus \{s\}\}$ . As a consequence of this result, the definition of resolved and unresolved set does not depend on the particular choice of a reference point [9], which is a fact that we will make use of in Subsection 2.2.4.

## 2.2 Sequential selection

In the previous section, we proposed selection strategies where all observers were selected at the same time. Now, we analyze the selection strategy when nodes are chosen dynamically, and the current observer is selected based on the infection times of the previous observers. This might be useful, for example, when a person who initiated a certain trend over a social network should be identified. Then the choice of which blog or site should be examined to help track this person is made after reading the previous site, as the newly acquired information is used to narrow down the search. Similarly, after an outbreak, mobile teams of doctors can be dispatched one by one to track down the zero patient and each new team can benefit from the observations of the previous teams in order to decide which is the most informative site to observe next. We examine the dynamic selection problem from two perspectives. First, we wish to find a selection strategy such that the source can be unambiguously localized with the smallest cost. Here, we consider that nodes might have different cost of observing, where cost is associated with resources, like time and effort, required to learn the node's infection time. The second problem we analyze is when the number of nodes that can be observed is predefined and we look at the strategy that would result with the smallest number of source candidates.

Now, we formulate the problem of finding a selection strategy that leads to source localization with the lowest cost. As shown in Theorem 3, a source  $s$  can be unambiguously identified by an observer set  $O$  if and only if  $\mathbf{d}(s, O) \neq \mathbf{d}(i, O)$ , for all nodes  $i \in V, i \neq s$ . However, as the identity of node  $s$  is unknown, the goal is to find a strategy  $\pi$  that minimizes the expected cost, for all possible sources  $s \in V$ . Let us denote with

$c(i)$  the cost of observing node  $i$ . Then finding the optimal strategy can be formulated as follows

$$\begin{aligned} & \min_{\pi} \mathbb{E}_s [c(O(\pi))] \\ & \text{subject to } \mathbf{d}(O(\pi), s) \neq \mathbf{d}(O(\pi), i), \forall s \in V, s \neq i, \end{aligned} \quad (2.8)$$

where  $O(\pi)$  is the set of observers selected according to strategy  $\pi$  and  $c(O(\pi))$  is the sum of costs of all nodes in the set  $O(\pi)$ , i.e.,  $c(O(\pi)) = \sum_{i \in O(\pi)} c(i)$ . Let  $\mathbf{t}$  be a vector of observed infection times. We denote with  $S(O) = \{s_1, \dots, s_l\}$  a set of source candidates after a set  $O$  of nodes has been observed, i.e.,  $S(O) = \{s' : \mathbf{d}(O, s') = \mathbf{t}\}$ . It is important to note that the members of set  $O$  are selected one at a time, and the selection stops when  $S(O) = \{s\}$ , i.e., there is only a single source candidate. The order by which the nodes are selected influences the total cost  $c(O)$ , as for different sequences of observers the stopping criterion might be met at different times, thereby incurring different total cost.

Next, we formulate the problem of finding a strategy of selecting a number of observers  $r$  such that the ambiguity in the source identity is the lowest. Here, we consider all nodes have cost equal to 1, as the cost here denotes a time-step. Then the goal is to find a strategy  $\pi$  for observer selection, such that the expected ambiguity is the lowest, i.e., the expected number of source candidates is the smallest for  $r$  selected observers. The problem can be stated as follows

$$\begin{aligned} & \min_{\pi} \mathbb{E}_s |S(O(\pi))| \\ & \text{subject to } |O(\pi)| \leq r, \end{aligned} \quad (2.9)$$

where again the expectation refers to all the possible sources.

In Subsection 2.2.1 we show that both of these problems can be optimally solved using dynamic programming with imperfect state knowledge. However, since most networks of interest are very large, the computation cost of the optimal approach is prohibitive. Hence, in Subsection 2.2.2, we propose efficient approximation strategies. The performance of the proposed selection strategies is illustrated in Section 2.2.3. Initially, we assume that the time when the source became active is known, and in the Subsection 2.2.4, we relax that assumption and extend the results.

## 2.2.1 Optimal strategy

Stochastic dynamic programming is an optimization methodology for problems where information becomes available sequentially, and each time after new information becomes available, a certain action is selected and executed [57]. In order to optimally solve (2.8) and (2.9), we apply dynamic programming for imperfect state

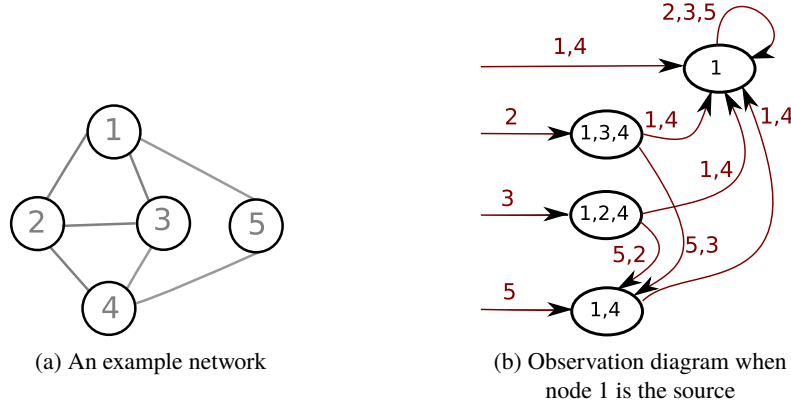


Figure 2.3: Analysis of source candidates (b) for a network shown in (a). The source candidates are shown given that the true source is node 1. Red arrows and numbers on (b) represent the nodes selected for observation, while the ovals show the resulting source candidates, with some self-loops omitted. For example, if node 4 is selected as the first observer, the source is exactly determined, as  $S(\{4\}) = \{1\}$ , while selecting the sequence of observers 5, 2, 3 results in source candidates 1, 4, since  $S(\{5, 2, 3\}) = \{1, 4\}$ . The metric dimension of the network is 2, while the resolving number is 4.

information, i.e., when the exact state of the system is not known, and the decisions are based on partially available information about the state. In our settings, the state of the system corresponds to the identity of the source. Each node has a certain probability of being the source, encoded as the prior distribution over the nodes. When prior is not available, initial probabilities are set to  $1/N$ . The identity of the source cannot be directly observed, and instead the distances to it are known through the infection times of the observers. In the first part, for simplified presentation, we will assume the activation time to be known. Later, we will extend the results to accommodate unknown activation time.

For  $t_0 = 0$ , although what is directly observed are the infection times of the observers, which are equal to their distance to the source, for more intuitive presentation, we will model the information that becomes available as the identity of the current source candidates, i.e., nodes whose distance vector to the observers equals observed infection times. We denote as  $S_k = \{s_1, \dots, s_l\}$  the source candidates after  $k$  nodes have been observed, i.e., after  $k$ -th time step. Figure 2.3b shows an analysis of resulting source candidates for all possible observer sequences, when the source is node 1 and the network is as shown on 2.3a. At the beginning of each time-step  $k$ , the information vector based on which the subsequent action is taken is  $I_k = (o_1, \dots, o_{k-1}, S_{k-1})$ . Hence, the selection of a new observer is based on the knowledge of previously selected observers and the current source candidates.

In order to apply dynamic programming, we analyze all the possible sequences backwards, starting from the selection of the last observer, to the first, one step at a time. However, since different sequences of selected observers result in localizing the source at different time steps, the last step occurs at different times

for different sequences. Therefore, we propose to do the following. We set the final time step equal to the *resolving number* of the graph,  $\rho$ . The resolving number is the minimum number  $p$  such that every  $p$ -subset of  $V$  is a resolving set of  $G$  [58]. Hence, after  $\rho$  time-steps, every observer sequence results in a single source candidate, and there is no need to analyze longer sequences. Unlike metric dimension, it can be determined in polynomial time. Now, we set the terminal cost, i.e., the cost after time step  $\rho$ , to 0 for all sequences. Next, we address the issue that some observer sequences resulted in source localization at times earlier than  $\rho$ . Let  $g_l$  denote the cost at step  $l$ , specifically let  $g_l(i)$  denote the cost of selecting node  $i$  as the  $l$ -th observer at time step  $l$ . Then, if the source is identified at the end of time-step  $k$ , i.e.,  $|S_k| = 1$ , we set the cost  $g_l$  of each subsequent action to 0, i.e.,  $g_l(i) = 0$ , for  $l > k$  and  $\forall i \in V$ . Until the source is identified, the cost of selecting each node  $i$  is its cost  $c(i)$ , i.e.,  $g_l(i) = c(i)$ , for  $l \leq k$ , if the source is identified in the  $k$ -th step. In this way, we can analyze all the sequences from the same ending point, while accommodating that some sequences reach the goal at an earlier time, hence the cost of each subsequent step after source localization has already been done should be 0. Now, applying the dynamic programming cost calculation [57], we have that the tail cost  $J_\rho(I_\rho)$  for the last step  $\rho$  is

$$J_\rho(I_\rho) = \min_{o \in V} \left[ \mathbb{E}_s \left\{ g_\rho(o) | I_\rho, o \right\} \right], \quad (2.10)$$

where the expectation is taken over all the possible sources  $s \in V$ . Hence, the tail cost examines the cost for each possible information vector  $I_\rho$ , which contains all preceding sequences of  $\rho - 1$  observers and the resulting source candidates of each sequence. The cost of action at time step  $\rho$  is conditioned on the new observer selected, as well as on the existing information vector. This models that the cost of selecting an observer might be 0, even though the cost of the nodes is non-zero, if the source has already been localized, i.e.,  $|S_{\rho-1}| = 1$ . For each information vector, the optimal cost (2.10) is evaluated, and the observer that achieves this cost is selected as the optimal observer for a given  $I_\rho$ .

$$o_\rho^*(I_\rho) = \arg \min_{o \in V} \mathbb{E}_s \left\{ g_\rho(o) | I_\rho, o \right\}.$$

For the preceding observers  $k = 1, \dots, \rho - 1$ , the tail cost is given as the solution of the optimization problem

$$J_k(I_k) = \min_{o \in V} \left[ \mathbb{E}_s \left\{ g_k(o) + J_{k+1}(I_{k+1}) | I_k, o \right\} \right]. \quad (2.11)$$

Now the tail cost at time  $k$  not only includes the cost of selecting a node  $o$  as the observer, but also the remaining cost-to-go  $J_{k+1}$ , which depends on all the previous, and the newly selected observer, as well as the updated source candidates, obtained after observing the  $k$ -th observer. Again, for each possible information

vector, a node that minimizes the cost at step  $k$  is chosen as the optimal observer for a given  $I_k$ .

$$o_k^*(I_k) = \arg \min_{o \in V} \mathbb{E}_s \{g_k(o) + J_{k+1}(I_{k+1})|I_k, o\}.$$

The information vector  $I_1$  is empty, as there is no previous observation available for the selection of the first observer. The obtained optimal sequences are of length  $\rho$ , but only the  $k$  first nodes are of interest, where  $k$  is the first step for which  $|S_k| = 1$ . The calculations (2.10) and (2.11) are done off-line, before the observer selection starts. Then, the optimal  $o_1^*$  is the first selected node, and based on its observation which results in  $I_2$ , the second observer is selected, and so on.

The value of the optimal cost  $J_1$  represents the total optimal cost, an expected amount of resources that are spent to identify the source without any uncertainty. If the cost of all the nodes equals 1, the optimal cost is upper bounded by the metric dimension. The reasoning is as follows: one selection strategy could be observing the nodes that form a resolving set. With this strategy, it is guaranteed that regardless of the source, there would be no ambiguity after selection of such a set. Now, equations (2.10) and (2.11) give an optimal solution which cannot be larger than the solution produced by any other strategy. The additional information available during the selection process can contribute to the reduction of the expected cost, compared to the off-line strategy.

Next, in order to apply dynamic programming to optimally solve optimization problem (2.9), we slightly modify the previously described setup. Since a sequence of  $r$  nodes should be selected, the horizon is set to  $r$  time-steps, and different sequences of the same length have different terminal cost, as they result in different number of source candidates. The terminal cost is associated with the cardinality of the set of candidates; the larger the set is, the larger the uncertainty. Now, we have the cost of the last step for an information vector  $I_r$  is determined as

$$J_r(I_r) = \min_{o \in V} [\mathbb{E}_s \{|S_r||I_r, o\}]. \quad (2.12)$$

Again, for each information vector, an optimal observer is selected as the node that achieves the minimal cost.

The remaining steps,  $k = 1, \dots, r - 1$  do not add any additional cost, as we assume all nodes have the same cost and the goal is to have the smallest ambiguity possible within a given time frame. Hence the preceding tail-costs only average over possible sources as follows

$$J_k(I_k) = \min_{o \in V} [\mathbb{E}_s \{J_{k+1}(I_{k+1})|I_k, o\}], \quad (2.13)$$

and at each time step, for a given  $I_k$ , an optimal observer is selected as the node that achieves the minimal cost. As mentioned before, there is no previous observation available for the selection of the first observer.

Again, these calculations are completed before the selection process starts. After selection of the first node, based on its infection time, the subsequent observer is chosen as the node that minimizes the cost  $J_2$ , for the given information vector. From (2.13) the obtained optimal cost,  $J_1$  represents an expected number of node suspects after observing  $T$  observers. The results of applying (2.11) and (2.13) to a network depicted in Figure 2.3a is shown in Table 2.2.

Table 2.2: The expected cost calculated for each node of the network shown in Figure 2.3a of being selected as  $o_1$ . For problem(2.8), the cost is evaluated with (2.11), while for problem (2.9), it is evaluated with (2.13). All nodes are assumed to have cost equal to 1 and for problem (2.9),  $r = 1$ . Optimal  $J_1$  is calculated as the smallest such cost. We have, then, for problem (2.8), that the expected cost is calculated as  $\mathbb{E}_s \{1 + J_2(o, S_1)|o\}$ , with  $J_1 = 8/5$  and any one of the nodes 1, 2, 3 or 4 as an optimal first observer. As for the problem (2.9) when only one can be selected for observation, the expected cost is  $\mathbb{E}_s \{|S_1||o\}$ , the optimal node is node 5, and  $J_1 = 9/5$ , i.e., on average there will be  $9/5$  source candidates after observing the infection time of node 5.

| Expected cost of $o_1$ for | Node |      |      |      |     |
|----------------------------|------|------|------|------|-----|
|                            | 1    | 2    | 3    | 4    | 5   |
| Problem (2.8) from (2.11)  | 8/5  | 8/5  | 8/5  | 8/5  | 9/5 |
| Problem (2.9) from (2.13)  | 11/5 | 11/5 | 11/5 | 11/5 | 9/5 |

## 2.2.2 Greedy strategies

Even though dynamic programming leads to optimal solutions, it is not a feasible strategy for larger networks. Problems (2.8) and (2.9) are of combinatorial nature and there is an exponential growth of computational and storage requirements as the network size increases. Hence, we need to resort to sub-optimal, yet more efficient, selection strategies. We will take advantage of adaptive submodularity, as for the problems with this property, a simple adaptive greedy algorithm is guaranteed to be competitive with the optimal policy [59]. Before we apply the adaptive submodular framework, we explain the necessary concepts [59].

Adaptive submodular functions are a generalization of submodular set functions to adaptive policies [59]. Submodular functions are functions with diminishing return property, where the benefit of an item when added to a set will not be increase when that item is added to a larger set. Whereas submodular functions deal with sets, adaptive submodular functions handle sequences. Additional difference is the presence of uncertainty in the state of the items, whose true state is learned only when the item is selected. Let  $E$  be a finite set of items, and each item  $i \in I$  is in unknown state from a set  $T$  of possible states. The item states are represented by a function  $\phi : I \rightarrow T$  which is called a *realization*. Prior probability over realization,  $p(\phi)$  is known. After selection of each item, its state is observed, and observations are represented using partial realization  $\psi$ , a function that maps the items that we already picked into their states. A *partial realization*

$\psi$  is consistent with a realization  $\phi$ ,  $\psi \sim \phi$ , if they are equal everywhere in the set of observed items. Let  $f$  denote a *utility* function that depends on which items we pick and which state each item. Then, given a partial realization  $\phi$  and an item  $i$ , the *conditional expected marginal benefit* of  $i$  conditioned on having observed  $\psi$ , is

$$\Delta(i|\psi) = \mathbb{E} [f(\psi \cup i, \phi) - f(\psi, \phi) | \phi \sim \psi],$$

where the expectation is computed with respect to the posterior belief about the state of all items  $i$  not yet selected,  $p(\phi|\psi)$ . Hence, the conditional expected marginal benefit of a function quantifies the expected benefit of selecting an item, given previously observed items, where the expectation is taken with respect to the posterior probability distribution of the unknown state. A function  $f$  is *adaptive monotone* if

$$\Delta(i|\psi) \geq 0, \forall i \in I. \quad (2.14)$$

A function  $f$  is *adaptive submodular* if

$$\Delta(i|\psi) \geq \Delta(i|\psi'), \text{ for } \psi \subseteq \psi', \quad (2.15)$$

and  $i$  is an action not included in  $\psi'$ . It is important to note that when comparing the two expected marginal benefits, there is a difference in both the set of items previously selected and the expectation is taken with respect to two different posterior distributions,  $p(\phi|\psi)$  vs.  $p(\phi|\psi')$ .

Now, that we have introduced the known concepts of adaptive submodularity framework, we need to apply it for problems 2.8 and 2.9. We define our utility function as the number of discarded source candidates after observing a set of observers  $O$ , i.e.,  $f(O, s) = N - |S(O)|$ . In the following theorem we state its interesting properties.

**Theorem 5.** *Function  $f(O, s) = N - |S(O)|$  is adaptive monotone and submodular for a uniform source prior.*

*Proof.* The set of nodes that can be selected as the observers represent the set of items. The unknown state of the item is the node's infection time, i.e., its distance to the source, which is learnt only after a node is observed. A realization is the identity of the source node, while a partial realization is the identity of the current source candidates. For a uniform source prior, all nodes are equally likely to be the source and  $P(\mathfrak{s} = s)$ , for  $s = 1, \dots, N$ . After observing a set of observers  $O$ , and obtaining a set of source candidates  $S(O) = \{s_1, s_2, \dots, s_l, s_{l+1}, \dots, s_m\}$ , the posterior probability of each node being the source is updated. Now  $P(\mathfrak{s} = s) = \frac{1}{|S(O)|}$ , for  $s \in S(O)$ , and  $P(\mathfrak{s} = s) = 0$ , for  $s \notin S(O)$ . The conditional expected marginal benefit

of observing a node  $o$  equals

$$\Delta(o|S(O)) = \mathbb{E}[N - S(O \cup o) - N + S(O)|S(O)] = \mathbb{E}[|S(O)| - |S(O \cup o)||S(O)], \quad (2.16)$$

where the expectation is taken with respect to the posterior probability of the source given the current source candidates. Let us fix source  $s$ . All the nodes that are source candidates after observing the set  $O$  cannot be mutually distinguished, and for any node  $s' \in S(O)$  and  $s'' \in S(O \cup o)$  we have that

$$d(s', O) = d(s'', O) = d(s, O). \quad (2.17)$$

For all the nodes that remain source candidates after additionally observing node  $o$ ,  $s' \in S(O \cup o)$ , it also holds  $d(s', o) = d(s, o)$ . Hence,  $S(O) \supseteq S(O \cup o)$  holds for any source  $s$ , and thus for the expected value as well. Therefore,  $\Delta(o|S(O)) \geq 0$ , and hence the condition for adaptive submodularity (2.14) holds.

Let  $h_s(O, o) = |S(O)| - |S(O \cup o)|$  denote the number of source candidates from  $S(O)$  that are discarded after observing  $o$ , given that the source was  $s$ . A source candidate  $s'$  is discarded if its distance to the observer  $o$  is not equal to  $d(s, o)$ , where  $s$  is the true source. Hence  $h_s(O, o)$  equals the number of source candidates  $s' \in S(O)$  that have  $d(s', o) \neq d(s, o)$ .

In order to establish the condition for submodularity (2.15), we need to show that

$$\frac{1}{|S(O)|} \sum_{s \in S(O)} h_s(O, o) \geq \frac{1}{|S(O')|} \sum_{s \in S(O')} h_s(O', o) \quad (2.18)$$

holds for any set  $O' \supseteq O$  and any new observer  $o \notin O'$ .

Let  $S(O') = \{s_1, s_2, \dots, s_l\}$  denote the set of source candidates after a set of  $O'$  observers is selected. Since  $O' \supseteq O$ , we have that  $S(O') \subseteq S(O)$ . Let  $X = S(O) \setminus S(O')$  denote a set of candidates which are discarded after  $O' \setminus O$  observers were additionally selected after the initial set  $O$ . Set  $X$  can also be empty, if newly selected observers have the same distance to all the source candidates. Now we can split the sum that runs over  $s \in S(O)$  into  $s \in S(O')$  and  $s \in X$  to obtain a new expression for the LHS of (2.18)

$$\frac{1}{|S(O)|} \sum_{s \in S(O)} h_s(O, o) = \frac{1}{|S(O)|} \sum_{s \in S(O')} h_s(O, o) + \frac{1}{|S(O)|} \sum_{s \in X} h_s(O, o). \quad (2.19)$$

Let us denote with  $R_s(T) = \{i : i \in T, d(i, o) \neq d(s, o)\}$  a subset of nodes from  $T$  that are no longer considered source candidates after observing  $o$ . Now we can further split the sum  $\sum_{s \in S(O')} h_s(O, o)$  into two sums, one referring to discarded source candidates from  $S(O')$  and the other including the discarded source candidates

from  $X$ , after a new observer  $o$  is selected

$$\sum_{s \in S(O')} h_s(O, o) = \sum_{s \in S(O')} h_s(O', o) + \sum_{s \in S(O')} |R_s(X)|. \quad (2.20)$$

Plugging back (2.19) and (2.20) into (2.18) we obtain

$$\frac{1}{|S(O)|} \left( \sum_{s \in X} h_s(O, o) + \sum_{s \in S(O')} |R_s(X)| \right) \geq \left( \frac{1}{|S(O')}| - \frac{1}{|S(O)|} \right) \sum_{s \in S(O')} h_s(O', o). \quad (2.21)$$

After a little simplification of (2.21) we obtain

$$\sum_{s \in X} h_s(O, o) + \sum_{s \in S(O')} |R_s(X)| \geq \frac{|X|}{|S(O')}| \sum_{s \in S(O')} h_s(O', o). \quad (2.22)$$

Now, we analyze the RHS of (2.22). For  $s = s_1$ , the value of  $h_s(O', o)$  equals the number of nodes from  $S(O') = \{s_1, s_2, \dots, s_l\}$  that have distance to the observer  $o$  different from  $d(s_1, o)$ . The sum on the RHS of (2.22) runs over all values of  $s \in \{s_1, s_2, \dots, s_l\}$ . Therefore,  $\sum_{s \in S(O')} h_s(O', o)$  counts the number of node pairs that have different distance to  $o$  (and equals twice this number) as shown in Table 2.3. Now, let  $k$  be the number of different values that  $d(s', o)$ , for  $s' \in S(O')$  can take. Denoting each of the possible values as  $a_i$ , for  $i = 1, \dots, k$ , let  $p_i$  be a number of nodes  $s' \in S(O')$  that have  $d(s', o) = a_i$ . Then we can rewrite  $\sum_{s \in S(O')} h_s(O', o)$  as

$$\sum_{s \in S(O')} h_s(O', o) = |S(O')|(|S(O')| - 1) - \sum_{i=1}^k p_i(p_i - 1), \quad (2.23)$$

as  $|S(O')|(|S(O')| - 1) -$  is the value the sum can take if all  $d(s', o)$  for  $s' \in S(O')$  have different values from each other and each term  $p_i(p_i - 1)$  subtracts those pairs that have the same value of the distance to the observer. This subtraction only takes place if there are at least two nodes with the same value  $a_i$ .

|                              |             | $g_s(O', o)$ |             |         |             |
|------------------------------|-------------|--------------|-------------|---------|-------------|
|                              |             | $d(s_1, o)$  | $d(s_2, o)$ | $\dots$ | $d(s_l, o)$ |
| running values<br>of the sum | $d(s_1, o)$ |              |             |         |             |
|                              | $d(s_2, o)$ |              |             |         |             |
|                              | $\dots$     |              |             |         |             |
|                              | $d(s_l, o)$ |              |             |         |             |

Table 2.3: RHS of (2.22):  $\sum_{s \in S(O')} h_s(O', o)$

Let  $p = \max_i p_i$  be the cardinality of the largest set of source candidates with the same value  $d(s', o)$ ,  $s' \in S(U)$ . Now we can bound the RHS of (2.22) as

$$\frac{|X|}{|S(O')|} \sum_{s \in S(O')} h_s(O', o) \leq \frac{|X|}{|S(O')|} (|S(O')|(|S(O')| - 1) - p(p - 1)). \quad (2.24)$$

Next, we analyze the LHS of (2.22). Similarly, as above, we notice that for  $s = s_{l+1}$ , the value of  $g_s(O, o)$  equals the number of nodes from  $\{s_1, s_2, \dots, s_l, s_{l+1}, \dots, s_m\}$  which have the distance to  $o$  different from  $d(s_{l+1}, o)$ . The sum  $\sum_{s \in X} g_s(O, o)$  runs for values  $s \in \{s_{l+1}, \dots, s_m\}$ . The second term on the LHS of (2.22) is  $\sum_{s \in S(O')} |R_s(X)|$ . For  $s = s_1$ , the value of  $|R_s(X)|$  equals to the number of nodes from  $\{s_{l+1}, \dots, s_m\}$  which have the distance to  $o$  different from  $d(s_1, o)$ . The sum  $\sum_{s \in S(O')} |R_s(X)|$  runs for values  $s \in \{s_1, \dots, s_l\}$ . Now, we notice that both terms of the LHS of (2.22) count the number of different values of the distance to the observer  $o$  for sets of nodes  $\{s_1, \dots, s_l\}$  and  $\{s_{l+1}, \dots, s_m\}$ . Additionally, the first term of the LHS of (2.22) also counts the number of node pairs that have different values of distances to the new observer  $o$  from the set of nodes  $\{s_{l+1}, \dots, s_m\}$ .

Let us analyze the smallest number of nodes from the set of  $S(O') = \{s_1, \dots, s_l\}$  that have the distance to observer different from  $d(s_{l+1}, o)$ . We have already grouped the values of these distances into groups of  $p_1, \dots, p_k$  nodes, with  $p$  denoting the cardinality of the largest group. Then, the number of nodes with the different distance from  $d(s_{l+1}, o)$  is at least  $|S(O')| - p$ . The same reasoning holds also for  $d(s_{l+2}, o), \dots, d(s_m, o)$ . Therefore the LHS of (2.22) is at least  $2|X|(|S(O')| - p)$ . Now applying these bounds to (2.22), we need to show that

$$2|X|(|S(O')| - p) \geq \frac{|X|}{|S(O')|} (|S(O')|(|S(O')| - 1) - p(p - 1)). \quad (2.25)$$

Since  $|S(O')| \geq 1$ , we can rearrange (2.25) to obtain

$$(p - |S(O')|)(p - |S(O')| - 1) \geq 0. \quad (2.26)$$

As  $1 \leq p \leq |S(O')|$ , we can see that (2.26) always holds, which implies that (2.18) also always holds, which, in turn, proves the submodularity claim.  $\square$

Now, applying the results of Theorem 5, we can reformulate (2.8) and (2.9) with a uniform prior as an adaptive stochastic optimization problem, in order to take advantage of the guarantees available for its greedy approximate algorithms. Problem (2.8) can be cast as an *Adaptive Stochastic Minimum Cost Cover* problem

as follows

$$\begin{aligned} & \min_{\pi} \mathbb{E}_s [c(O(\pi))] \\ & \text{subject to } N - S(O(\pi)) \geq N - 1, \forall s \in V, s \neq i, \end{aligned} \quad (2.27)$$

while (2.9) can be stated as *Adaptive Stochastic Maximization*

$$\begin{aligned} & \max_{\pi} \mathbb{E}_s [N - |S(O(\pi))|] \\ & \text{subject to } |O(\pi)| \leq r. \end{aligned} \quad (2.28)$$

Greedy algorithm, at each iteration, myopically increases the expected objective value, given currently available observations. Hence, at each time step, a node  $o$  is selected, such that it maximizes the expected marginal benefit  $\Delta(o|S(O))$  given by (2.16), knowing the current source candidates  $S(O)$ . Basically, a node  $o$  is selected as the next observers if its expected decrease in the number of current source candidates is the highest. Algorithm 3 shows the pseudocode for the greedy approach applied to problem (2.27).

---

**Algorithm 3** Greedy algorithm for sequential selection of observers for source localization with the smallest cost based on adaptive submodularity

---

```

1:  $O \leftarrow \emptyset$  //  $O$  is the current observer set
2:  $S(O) \leftarrow \{1, \dots, N\}$  //  $S(O)$  is the set of current source candidates
3: while  $|S(O)| > 1$  do
4:   foreach  $o \in V \setminus O$  do  $\Delta(o|S(O)) = \mathbb{E}_{s \in S(O)} [|S(O)| - |S(O \cup o)| | S(O)]$ 
5:   Select  $o^* \in \arg \max_o \frac{\Delta(o|S(O))}{c(o)}$ 
6:    $O \leftarrow O \cup \{o^*\}$ 
7:   Observe  $o^*$  and determine new source candidates  $S(O)$ 
8: end while

```

---

Let  $c(\pi^{opt})$  denote the optimal cost of (2.27), and  $c(\pi^g)$  represent the expected cost achieved by Algorithm 3. Then  $c(\pi^g) \leq c(\pi^{opt}) (\log(N(N-1)) + 1)$  is guaranteed to hold [59].

Greedy approach can also be applied to problem (2.28). Again, node  $o$  is chosen such that it maximizes the expected decrease in the number of source candidates. Algorithm 4 shows the pseudocode for the greedy approach applied to problem (2.27). Let  $f(\pi_r^{opt})$  denote the optimal expected number of source candidates after  $r$  steps, and  $f(\pi_r^g)$  represents the expected value of candidates obtained by Algorithm 4. Then the results in [59] guarantee that  $f(\pi_k^g) \leq (1 - e^{-1})f(\pi_k^{opt}) + \frac{N}{e}$ .

We additionally propose a second approximation strategy for observer selection. In the adaptive Algorithms 3 and 4, an observer is selected that minimizes the weighted *expected* number of source candidates. In this approach, an observer is selected based on the worst case scenario, by minimizing the weighted *highest*

---

**Algorithm 4** Greedy algorithm for sequential selection of  $r$  observers that lead to the smallest ambiguity in the source identity based on adaptive submodularity

---

```

1:  $O \leftarrow \emptyset$  //  $O$  is the current observer set
2:  $S(O) \leftarrow \{1, \dots, N\}$  //  $S(O)$  is the set of current source candidates
3: for  $k = 1$  to  $r$  do
4:   foreach  $o \in V \setminus O$  do  $\Delta(o|S(O)) = \mathbb{E}_{s \in S(O)} [|S(O)| - |S(O \cup o)| | S(O)]$ 
5:   Select  $o^* \in \arg \max_o \frac{\Delta(o|S(O))}{c(o)}$ 
6:    $O \leftarrow O \cup \{o^*\}$ 
7:   Observe  $o^*$  and determine new source candidates  $S(O)$ 
8: end for

```

---

possible number of source candidates. We denote as  $T_S^p(o)$  the nodes of the set  $S$  which are at distance  $p$  to node  $o$ , where  $p = 1, \dots, l_S(o)$ , and  $l_S(o)$  is the maximum such distance, i.e.  $T_S^p(o) = \{t : t \in S, d(o, t) = p\}$  and  $l_S(o) = \max_{i \in S} d(o, i)$ . Then  $|T_{S(O)}^p(o)|$  represents the number of current source candidates that are at the same distance from the node  $o$ , i.e., they cannot be distinguished by node  $o$ , and will remain as the source candidates. Hence,  $\delta(o, S(O)) = \max_p |T_{S(O)}^p(o)|$  is the number of the largest, mutually indistinguishable, group of source candidates. In this approach that minimizes the worst case ambiguity, a node  $o$  is chosen such that this largest group is the smallest. The pseudocode for the greedy approach that myopically minimizes the highest ambiguity in order to localize the source with the smallest cost is given by Algorithm 5.

---

**Algorithm 5** Greedy algorithm for sequential selection of observers for source localization with the smallest cost based on minimizing the worst case

---

```

1:  $O \leftarrow \emptyset$  //  $O$  is the current observer set
2:  $S(O) \leftarrow \{1, \dots, N\}$  //  $S(O)$  is the set of current source candidates
3: while  $|S(O)| > 1$  do
4:   foreach  $o \in V \setminus O$  do  $\delta(o, S(O)) = \max_p |T_{S(O)}^p(o)|$ 
5:   Select  $o^* \in \arg \min_o c(o)\delta(o, S(O))$ 
6:    $O \leftarrow O \cup \{o^*\}$ 
7:   Observe  $o^*$  and determine new source candidates  $S(O)$ 
8: end while

```

---

The same approach can be used to approximate the problem (2.28), and the resulting pseudocode is shown in Algorithm 6.

### 2.2.3 Simulation results

Now, we illustrate the performance of the approaches proposed in Sections 2.2.1 and 2.2.2. We will compare the performance of both the optimal and the greedy algorithms with a weighted random selection which we will use as a benchmark. Specifically, this random selection at each step randomly selects a node  $i$  with a normalized probability  $p(i)$  inversely proportional to its cost, i.e.,  $p(i) = \frac{1}{c(i)} / \sum_j \frac{1}{c(j)}$ , thereby selecting

**Algorithm 6** Greedy algorithm for sequential selection of  $r$  observers that lead to the smallest ambiguity in the source identity based on minimizing the worst case

---

```

1:  $O \leftarrow \emptyset$  //  $O$  is the current observer set
2:  $S(O) \leftarrow \{1, \dots, N\}$  //  $S(O)$  is the set of current source candidates
3: for  $k = 1$  to  $r$  do
4:   foreach  $o \in V \setminus O$  do  $\delta(o, S(O)) = \max_p |T_{S(O)}^p(o)|$ 
5:   Select  $o^* \in \arg \min_o c(o)\delta(o, S(O))$ 
6:    $O \leftarrow O \cup \{o^*\}$ 
7:   Observe  $o^*$  and determine new source candidates  $S(O)$ 
8: end for

```

---

more costly nodes with less probability.

We applied the algorithms for observer selection to randomly generated small world networks of various sizes. Small world networks are used to model many real-world phenomena and systems, such as power grids, social influence networks and even the collaboration graph of film actors [60]. The small world model starts from a ring lattice, where each edge is rewired at random with a certain probability  $p$ . This construction interpolates between a regular graph ( $p = 0$ ) and a completely random one ( $p = 1$ ). We generated a lattice, with each node being connected with an edge to all the nodes within distance 2 in a lattice. Then, all the edges were rewired randomly with  $p = 0.3$ . For each network size, 100 random networks were considered, and the result of each algorithm was averaged for these 100 realizations. A uniform source prior was used, and node costs were chosen randomly in the range  $(0, 1)$ .

The cost incurred by the optimal and greedy approaches for localizing the source, i.e., for problem (2.8), is shown in Figure 2.4. As Figure 2.4a clearly demonstrates, both the optimal and the two greedy

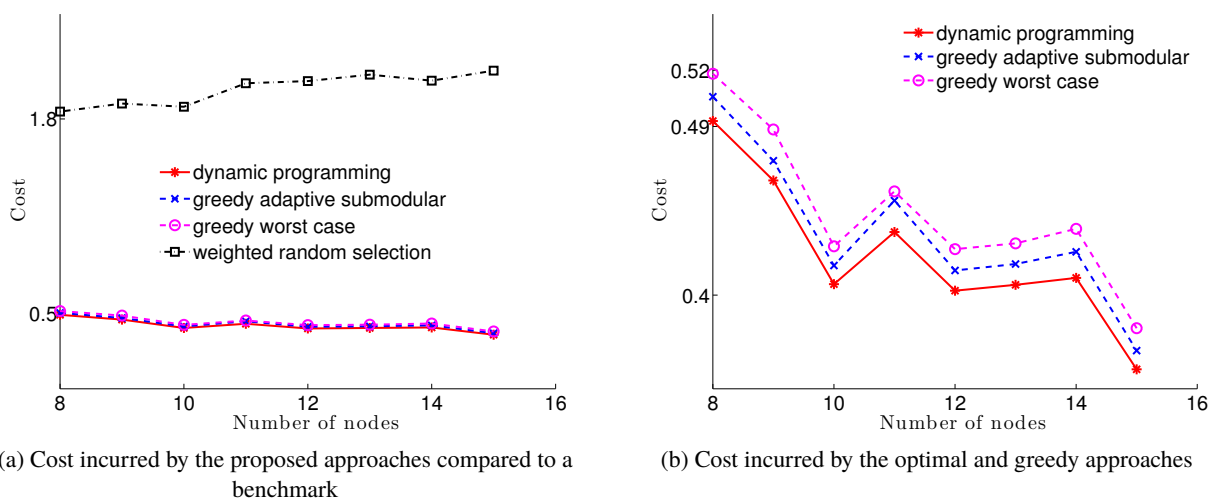


Figure 2.4: The performance of dynamic programming and greedy approaches for solving the problem (2.8)

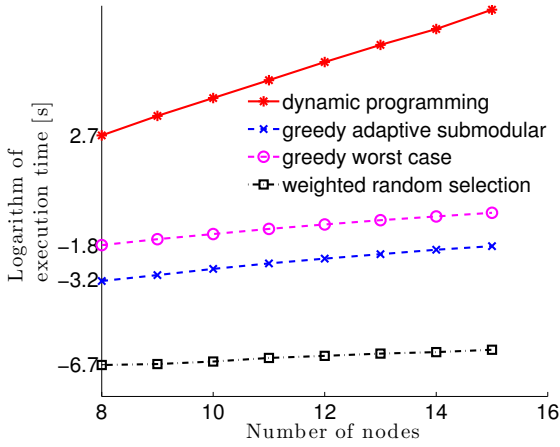


Figure 2.5: Time required by dynamic programming and the greedy approaches for solving the problem (2.8)

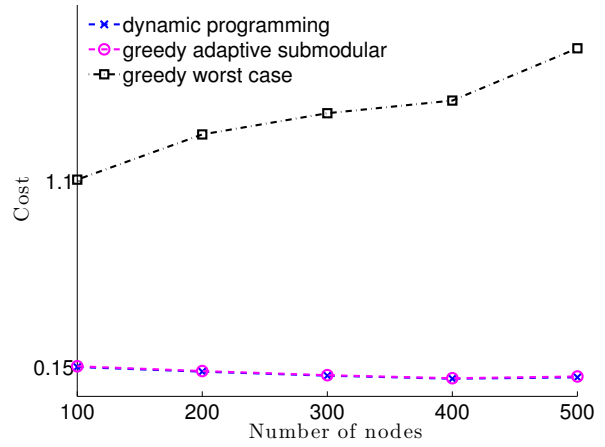


Figure 2.6: The performance of Algorithms 3 and 5 for larger sized networks

approaches, Algorithms 3 and 5, incur significantly lower cost than the benchmark random selection. In order to compare the proposed approaches, their costs are shown in Figure 2.4b, without the benchmark. Both greedy algorithms result in only slightly higher cost than the one incurred by the optimal strategy, with Algorithm 3 performing slightly better than the Algorithm 5. The cost of source localization counter intuitively decreases with the network size, which is just an artifact of the way that the node cost is generated, and not normalized by the sum of all the node costs. In a network with higher number of nodes, since node costs are generated randomly, there is a wider range of values available, and a higher number of less expensive nodes, resulting in a lower total cost, even though the number of the observed nodes increases.

Figure 2.5 shows the corresponding average execution time, which is, as expected, much higher for the

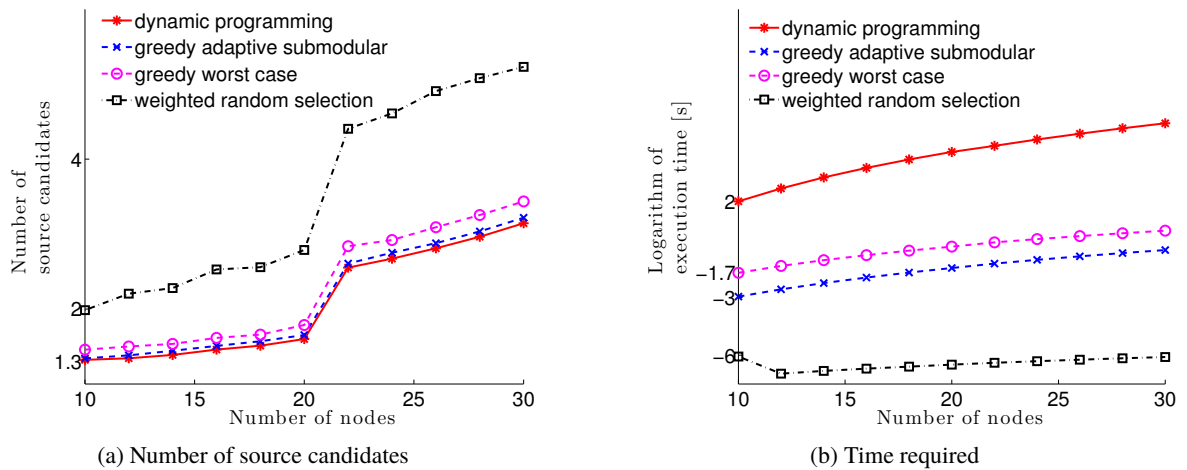


Figure 2.7: The performance of dynamic programming and greedy approaches for solving the problem (2.9)

optimal solution, and the lowest for the random selection. Due to the high computation cost of dynamic programming, we compared only the performance of the approximation algorithms for larger networks, sized 100 – 500 nodes. Figure 2.6 shows that both the greedy approaches, Algorithms 3 and 5, achieve source localization with a cost much lower than the benchmark random selection, on the average 13 times lower. The gap between greedy and random selection increases as the number of nodes increases.

Similar conclusions can be made regarding the algorithms' performance for localizing the source with the smallest ambiguity, given that only 2 observers can be selected. In this case, all the nodes have the same cost that equals 1. The performance of the dynamic programming and greedy approaches for solving the problem (2.9) is shown in Figure 2.7, now for networks with 10 – 30 nodes. Again, both the optimal approach and the Algorithms 4 and 6 yield much lower number of source candidates than the random selection, especially as the number of nodes in the network increases. Algorithm 4 achieves near optimal performance. The time required for all of the approaches is shown in Figure 2.7b. The dynamic programming is much more computationally intensive than the other algorithms, requiring around 700 times more execution time than the Algorithm 4 for the network of 30 nodes, for comparable performance.

## 2.2.4 Extending the results to unknown activation time

As discussed in Subsection 2.1.3, when the activation time is not known, instead of infection times, the relative infection times are used, defined by (2.7). Since the source can be unambiguously identified only if the set of observers forms a doubly resolving set, we can reformulate the problem of finding a strategy for observer selection that achieves source localization with the smallest cost as follows

$$\begin{aligned} & \min_{\pi} \mathbb{E}_s [c(O(\pi))] \\ & \text{subject to } d(o_i(\pi), s) - d(o_j(\pi), s) \neq d(o_i(\pi), s') - d(o_j(\pi), s'), \\ & \quad \forall s, s' \in V, s \neq s', \text{ for some } o_i(\pi), o_j(\pi) \in O(\pi). \end{aligned} \quad (2.29)$$

Here  $o_i(\pi)$  and  $o_j(\pi)$  denote a pair of observers selected by the strategy  $\pi$ , and it can be a different observer pair that differentiates between different pairs of nodes  $s$  and  $s'$ , for  $s, s' \in V$ . Next, let us fix the source to be node  $s$  and stack relative infection times of  $r$  observers into a vector  $\mathbf{x} = [d(o_2, s) - d(o_1, s), \dots, d(o_r, s) - d(o_1, s)]^T$ . Now, the source candidates are all the nodes that have their relative infection time equal to that of the source, i.e.,

$$S(O) = \{s' : [d(o_2, s') - d(o_1, s'), \dots, d(o_r, s') - d(o_1, s')]^T = \mathbf{x}\}. \quad (2.30)$$

With this modified definition of the source candidates, the formulation of the problem of finding a strategy of selecting  $r$  observers, such that the ambiguity in the source identity is the lowest, is equivalent to (2.9). Since relative times are used, at least two observers are needed, hence,  $|O(\pi)| \geq 2$ .

the dynamic programming approach can again be applied to solve the problems (2.29) and (2.9) with the updated definition of  $S(O)$ . Only a few more adjustments are necessary for the method given in the Subsection 2.2.1. An important result from [34], stated in the Subsection 2.1.3, shows that for a doubly resolving set, a choice of the reference point is not important; it can be any node from the set. Hence, when analyzing sequences of observers, we can arbitrarily choose a reference observer, and easily determine source candidates. The horizon for analysis of observer sequences of the problem (2.29) is set to  $N - 1$ , instead of the resolving number,  $\rho$ , of the graph. Now, any  $N - 1$  subset of nodes is a doubly resolving set, and, therefore, any sequence of  $N - 1$  observers will result in an unambiguous source localization. For both problems, the selection of the first and the second observer, which was the penultimate and the ultimate step in the backward analysis in the Subsection 2.2.1, are performed at the same time. As selecting a single observer is not meaningful, initially, a pair of observers should be selected. Then, instead of determining costs-to-go,  $J_1$  and  $J_2$ , for example, for the first problem (2.29), there is only a single stage

$$J_{1,2} = \min_{o_1, o_2 \in V} [\mathbb{E}_s \{g_{1,2}(o_1) + g_{1,2}(o_2) + J_3(I_3)|o_1, o_2\}],$$

and, analogously, for the second problem. In this step, there are no previous observations available and information vector  $I_{1,2}$  is empty, as was previously  $I_1$ . Again, all the analysis is performed before the selection takes place, then, the first two observers are selected as the ones that achieve  $J_{1,2}$ . Based on their infection times, their relative infection time is determined, and the next observer is selected. Hence, the results from the Subsection 2.2.1 can also be used when the activation time is not known.

Again, we are also interested in the approximation algorithms due to the combinatorial nature of the problems. Next, we show that the results from Subsection 2.2.2 also apply.

**Theorem 6.** *Function  $f(O, s) = N - |S(O)|$  is adaptive monotone and submodular for a uniform source prior and when  $S(O)$  represents a set of source candidates with the relative infection times equal to the source.*

*Proof.* The conditional expected marginal benefit is again given by (2.16), except that  $S(O)$  is now defined as (2.30). Let us fix the source to be node  $s$ . All the nodes that are source candidates after observing the set  $O = \{o_1, \dots, o_r\}$  cannot be mutually distinguished, and for any node  $s' \in S(O)$  and  $s'' \in S(O \cup o)$  we have

that

$$\begin{aligned} [d(s', o_2) - d(s', o_1), \dots, d(s', o_r) - d(s', o_1)]^T &= [d(s'', o_2) - d(s'', o_1), \dots, d(s'', o_r) - d(s'', o_1)]^T \\ &= [d(s, o_2) - d(s, o_1), \dots, d(s, o_r) - d(s, o_1)]^T. \end{aligned}$$

For all the nodes that remain source candidates after additionally observing node  $o$ ,  $s' \in S(O \cup o)$ , it also holds  $d(s', o) - d(s', o_i) = d(s, o) - d(s, o_i)$ , for all  $i = 1, \dots, r$ . Hence,  $S(O) \supseteq S(O \cup o)$  again holds for any source  $s$ , and thus for the expected value as well. Therefore, we once more have  $\Delta(o|S(O)) \geq 0$ , and the condition for adaptive submodularity (2.14) holds.

Again, let  $h_s(O, o) = |S(O)| - |S(O \cup o)|$  denote the number of source candidates from  $S(O)$  that are discarded after observing  $o$ , given that the source was  $s$ . A source candidate  $s'$  is discarded if

$$d(s', o) - d(s', o_i) \neq d(s, o) - d(s, o_i). \quad (2.31)$$

The choice of observer  $o_i \in O$  is arbitrary, as if (2.31) holds for one  $o_i$ , it holds for all the other observers, as well. We prove this by contradiction. We assume (2.31) holds for some  $o_i \in O$ , but not for  $o_j \in O$ ,  $j \neq i$ , i.e.,

$$d(s', o) - d(s', o_j) = d(s, o) - d(s, o_j). \quad (2.32)$$

Since  $s' \in S(O)$ , it means it cannot be doubly resolved from  $s$  by  $o_i, o_j$ , and

$$d(s', o_i) - d(s', o_j) = d(s, o_i) - d(s, o_j) \quad (2.33)$$

holds. Combining (2.32) and (2.33) we have

$$d(s', o_i) - d(s, o_i) = d(s', o_j) - d(s, o_j) = d(s', o) - d(s, o),$$

which is a contradiction with the assumption (2.31). Hence, if a node  $o$  doubly resolves  $s'$  and  $s$ , the choice of the reference node is again arbitrary. Then,  $h_{s'}(O, o)$  equals the number of source candidates  $s' \in S(O)$  for which (2.31) holds. To show that the function is adaptive submodular, we need to show that the condition (2.18) holds. Now we fix  $o_i$  and denote  $q(s) = d(s, o) - d(s, o_i)$ . Then, for  $s = s_1$ , the value of  $h_s(O', o)$  equals the number of nodes  $s'$  from  $S(O') = \{s_1, \dots, s_l\}$  that have  $q(s') \neq q(s_1)$ , and  $\sum_{s \in S(O')} h_s(O', o)$  counts the number of node pairs that have different values of  $q(s)$  (and equals twice this number). This is similar to the Table 2.3, except  $d(s', o)$  is replaced with  $q(s')$ , for  $s' = s_1, \dots, s_l$ . Using the same reasoning as in the Theorem 5, we can once more bound  $\sum_{s \in S(O')} h_s(O', o)$  with (2.23). The rest of the proof also

follows the proof of Theorem 5, with  $q(s')$  taking the role of  $d(s', o)$ .  $\square$

Applying the results of the Theorem 6, we can again use the formulations (2.27) and (2.27) and solve them using greedy approaches that has performance guarantees. Hence, Algorithm 3 can be applied to perform sequential selection of observers for source localization with the smallest cost based on adaptive submodularity and Algorithm 4 for sequential selection of  $r$  observers that lead to the smallest ambiguity in the source identity based on adaptive submodularity, even when the activation time is not known.

## 2.3 Summary

In this Chapter, we have analyzed the observer selection problem assuming there was no uncertainty in the nodes' infection times. This enabled us to isolate the effect of the choice of observers on the ability to uniquely localize the source, ignoring (for now) the additional ambiguity introduced by noise. We have tackled two specific problems: determining a set of nodes that would lead to source localization with the smallest cost, and determining a set of nodes with a given cardinality that would lead to the smallest uncertainty in the source identity. These two problems were analyzed in two different settings: block and sequential.

For the block selection that assumes all the nodes are selected at the same time, in Subsection 2.1.1, we have modeled the dynamics of diffusion as a linear time-varying system. This allowed us to define a concept of network observability which characterizes the ability to localize a diffusion source given the observations of a subset of nodes. We presented a sufficient and necessary condition for network observability. In Subsection 2.1.2 we have related the problem of observer selection to a known problem of finding a resolving set of a graph. We have shown that the network is observable only if the set of observers forms a resolving set. We leveraged on existing results from graph theory to determine the smallest set of nodes needed for network observability for special graph classes, whereas for general graphs this is an NP-hard problem. Using the connection with resolving sets and the set cover problem, we presented approximation algorithms with performance guarantees. These results were established under the assumption that the time when the source became active is known, while in Subsection 2.1.3 we presented available results when that time is unknown.

In Section 2.2, we have analyzed the dynamic observer selection strategies, i.e., when the observations of the previous observer are used to select the subsequent one. Using dynamic programming with imperfect state knowledge, in Subsection 2.2.1, we determined the optimal strategy for both problems. As the optimal approach is computationally very intensive, in Subsection 2.2.2, we developed efficient approximation algorithms. Using the adaptive submodularity framework, we obtained performance guarantees for a greedy approach. In Subsection 2.2.3, we illustrated the near optimal performance of the greedy algorithms. Once more, these results were established under the assumption that the time when the source became active is

known, while in Subsection 2.2.4 we omitted this assumption and extended the results. We showed that the presented algorithms can also be applied in this case.

## Chapter 3

# Node selection for deterministic infection times and in the presence of uncertainty in the network topology

In the previous chapter, we have assumed that the network topology, the underlying graph over which contagion spreads, is completely known. However, in many cases, this assumption does not hold. Individuals may not be willing to disclose all their social connections, and not all information is propagated through monitored social network sites. Often, local connections within communities are well known, while the connections between them are not always fully observed. This may happen when diseases spread from one community to another through random contact, rather than a known friendship connection, or when novel information is spread through weak, rather than strong, social ties [61]. In this chapter, we relax the assumption of complete knowledge of network topology and instead assume that the structure of local network components is available, while inter-component edges are the ones that are not observed. We, once more, assume deterministic propagation, in order to specifically analyze the effect of the choice of observers on the ability to disambiguate the source, now in the presence of uncertainty in the network topology. We will assume the activation time to be known.

Since we assume to have the knowledge of the structure of local communities, but not of the connections between them, the observed network is a disconnected graph  $F$  that comprises  $k \geq 2$  connected components,  $C_i$ , for  $i = 1, \dots, k$ . As we are interested only in the first time that a node gets informed or infected, we assume the number of unobserved inter-component edges is  $k - 1$ , making the graph connected, yet there are no

cycles between the components. We denote as  $\mathcal{F}(k)$  the class of such observed graphs with  $k$  components and  $k - 1$  missing edges. Then, with  $\mathcal{H}(F)$ , we denote the class of all the possible graphs that can be constructed by adding  $k - 1$  edges between the components of the observed graph such that the resulting graph is connected. If the observed graph is  $F \in \mathcal{F}(k)$ , then the true network structure can be any graph from the class  $\mathcal{H}(F)$ . One straightforward idea in handling the network uncertainty would be to analyze separately all possible graphs from the class  $\mathcal{H}(F)$  from the perspective of network observability. The following Theorem shows why the explicit enumeration of all such topologies is not a feasible option.

**Theorem 7.** *For a disconnected graph  $F \in \mathcal{F}(k)$  of  $k$  components, each comprising  $|C_i|$  nodes,  $i = 1 \dots k$ , the cardinality of the class  $\mathcal{H}(F)$  is*

$$|\mathcal{H}(F)| = \sum_{p=1}^{k^{k-2}} \prod_{(i,j) \in T_p} |C_i||C_j|, \quad (3.1)$$

where  $T_p \in \mathcal{T}(k)$  and  $\mathcal{T}(k)$  denotes a class of trees with  $k$  nodes.

*Proof.* Given  $k$  nodes, there are  $k^{k-2}$  spanning trees that can be constructed [62]. Considering components as isolated supernodes, we denote with  $T_p \in \mathcal{T}(k)$ , for  $p = 1, \dots, k^{k-2}$ , all the possible trees that can be formed by joining supernodes in a tree, by adding  $k-1$  edges between them. Since an edge between two components can connect any two nodes on each component, there is a total of  $|C_i||C_j|$  ways in which components  $i$  and  $j$  can be linked. Therefore, as each edge between components  $i$  and  $j$  in a tree  $T_p$  can be realized in  $|C_i||C_j|$  ways, each tree of supernodes,  $T_p$ , can be realized as  $\prod_{(i,j) \in T_p} |C_i||C_j|$  different trees on the set of nodes, from which (3.1) follows.  $\square$

Arranging the component sizes in ascending order,  $|C_1| \leq \dots \leq |C_k|$ , the number of possible topologies,  $|\mathcal{H}(F)|$ , can be bounded as

$$k^{k-2}|C_1|^{k-1} \prod_{j=2}^k |C_j| \leq |\mathcal{H}(F)| \leq k^{k-2}|C_k|^{k-1} \prod_{j=1}^{k-1} |C_j|. \quad (3.2)$$

From Theorem 7 and (3.2), it follows that the number of possible topologies scales exponentially with the number of connected components, and also grows with the components' sizes. Hence, analyzing each possible topology separately is computationally very challenging even for small networks with only a few missing edges. Again, we are interested in unambiguous source localization and determining the smallest set of nodes that would achieve it, despite the lack of complete knowledge of the diffusion graph. Hence, in Section 3.1, we extend the concept of network observability to accommodate incomplete network topology. Then, we determine the smallest set of observers needed to achieve observability for certain graph classes,

and establish an upper bound for an arbitrary graph. In Section 3.2, we address the problem of source localization in a partially known graph using binary linear integer programming.

### 3.1 Block selection

When the network topology is completely known, the concept of network observability is given by Definition 1. When the edges between different components are unknown, we extend the concept in the following Definition.

**Definition 2.** For a subset of observers, we call a partially known network  $F \in \mathcal{F}(k)$  observable, if and only if any source node can be unambiguously localized based on the observers' infection times in the deterministic propagation model, even without knowing which graph from  $\mathcal{H}(F)$  is the true underlying diffusion graph.

Now, in an observable network, observers' infection times are sufficient to disambiguate the source without knowing exactly how local components are connected. Once more, due to the limited resources, and the cost associated with node observation, a question of interest would be finding the smallest set of nodes that would lead to observability. Previously, in Theorem 3, it was shown that the set of nodes that makes a network observable, forms a resolving set of a graph. The smallest set needed for observability actually corresponds to a resolving set of the smallest cardinality: a metric basis of the graph. In order to accommodate for the uncertainty in network topology, we extend the concept of resolving sets. Now, let  $\mathbf{d}_{H_1}(u, O)$  be the distance vector of  $u$  to the set  $O = \{o_1, \dots, o_r\}$  in the graph  $H_1$ , that is,  $d_{H_1}(u, o_i)$  is the length of the shortest path between nodes  $u$  and  $o_i$  in the graph  $H_1$ , for  $i = 1, \dots, r$ . Then, we introduce the following concept.

**Definition 3.** For a graph  $F \in \mathcal{F}(k)$ , we call a set  $O \subseteq V$  an extended resolving set, if for any two different vertices  $u$  and  $v$ , and any two graphs  $H_1, H_2 \in \mathcal{H}(F)$ , we have  $\mathbf{d}_{H_1}(u, O) \neq \mathbf{d}_{H_2}(v, O)$ .

The cardinality of the smallest extended resolving set of a graph  $F$ , denoted by  $\gamma(F)$ , we call the *extended metric dimension* of  $F$ . Denoting a metric dimension of a graph with  $\text{md}$ , we have that  $\max_{H_i \in \mathcal{H}(F)} \text{md}(H_i) \leq \gamma(F) \leq n - 1$ . Note that while a resolving set is determined for one fixed graph, a generalized resolving set concerns a whole class of graphs. In the next Theorem, we relate the concepts of observability and an extended resolving set.

**Theorem 8.** For a given subset of nodes  $O$ , a partially known network  $F \in \mathcal{F}(k)$  is observable, if and only if the set  $O$  is an extended resolving set of  $F$ .

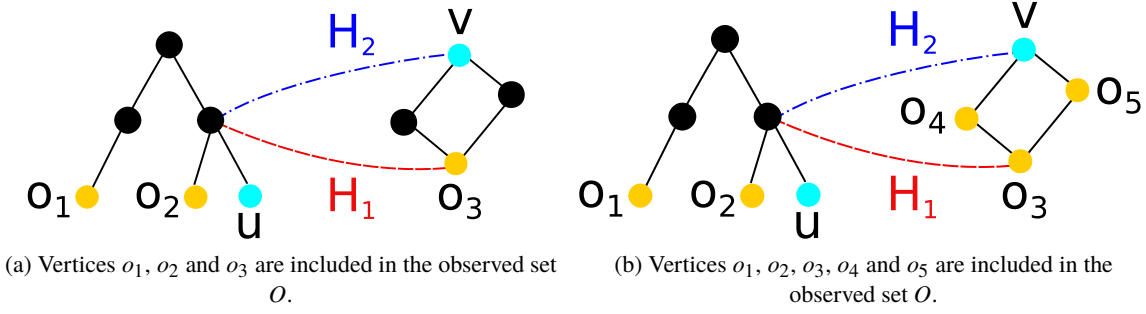


Figure 3.1: An example of a partially known network with two components. A missing edge is the one connecting the two components. In (a) distances of a vertex  $u$  from the set  $O$  in the graph  $H_1$  are the same as the distances of a vertex  $v$  to the set  $O$  in the graph  $H_2$ :  $d_{H_1}(u, o_1) = 4 = d_{H_2}(v, o_1)$ ,  $d_{H_1}(u, o_2) = 2 = d_{H_2}(v, o_2)$  and  $d_{H_1}(u, o_3) = 2 = d_{H_2}(v, o_3)$ . Without knowing if the true graph is  $H_1$  or  $H_2$  the source cannot be correctly identified, as it can be either vertex  $u$  or  $v$ . In (b), two more vertices are included in set  $O$ . It can be checked that  $O$  is now a minimum cardinality extended resolving set. Now, the distances of the vertices  $u$  and  $v$  to the set  $O$  are different, as  $d_{H_1}(u, o_4) = 3 \neq 1 = d_{H_2}(v, o_4)$  and  $d_{H_1}(u, o_5) = 3 \neq 1 = d_{H_2}(v, o_5)$ . Hence, the vertices  $u$  and  $v$  can be distinguished and the source can be unambiguously localized, even if it is not known exactly how the two components are connected.

*Proof.* The infection times of the observers correspond to their distance to the source. These node distances might be different for different topologies from the class of  $\mathcal{H}(F)$ . Whereas, previously, for one fixed graph, unambiguous source localization was possible given that all nodes had distinct distances to the set of observers, now these distances should be distinct, in and across, all possible graphs. Then, even without knowing the exact identity of the graph from  $\mathcal{H}(F)$ , the uniqueness of distances is both necessary and sufficient to identify any possible source based on the observed distances.  $\square$

An example that illustrates network observability for a partially known network is shown in Figure 3.1. In Subsection 3.1.1 we determine the smallest set of nodes that is both necessary and sufficient for unambiguous source localization when components have a specific structure, while in Subsection 3.1.2 we present a sufficient condition when components have an arbitrary structure.

### 3.1.1 Results for special graph classes

For uninterrupted flow, we first state all the results, and then give the proofs at the end of the Subsection. First, we set up the notation. For a connected graph  $G$ ,  $i, j \in V$ , denote an  $i - j$ -path to be a sequence of all different vertices  $v_0 = i, v_1, \dots, v_\ell = j$ , such that for  $i = 0, \dots, \ell - 1$ ,  $\{v_i, v_{i+1}\} \in E$ . Let  $V(C_i)$  denote the set of all vertices of component  $C_i$ . Let  $L(C_i)$  denote the set of all leaves of component  $C_i$ . Let  $K(C_i)$  be the set of vertices of component  $C_i$  that have degree greater than two, and that are connected by paths of degree-two vertices to one or more leaves in  $C_i$  (when considering  $C_i$  as a separate graph and ignoring edges to other

components). For a given vertex  $c \in K(C_i)$ , call the leaves connected to  $c$  via such degree-two-paths to be the *associated leaves* of  $c$ . Note that for a tree that is not a path each leaf is associated to exactly one vertex  $c \in K(C_i)$ . For a fixed component  $C_i$  of  $F \in \mathcal{F}(k)$ , denote by  $S_i$  a minimum cardinality resolving set of  $C_i$  (so that  $\text{md}(C_i) = |S_i|$ .) The  $M \times N$ -grid with  $M, N \geq 2$ , is the graph whose vertices correspond to the points in the plane with integer coordinates,  $x$ -coordinates being in the range  $0, \dots, M - 1$ ,  $y$ -coordinates in the range  $0, \dots, N - 1$ , and two vertices are connected by an edge whenever the corresponding points are at Euclidean distance 1. The four vertices of degree two are called corner vertices.

**Theorem 9.** *Let  $F \in \mathcal{F}(k)$  be a graph of  $k$  components, where each component is a tree. Then for  $F$  to be observable, the necessary and sufficient number of observers is  $\min_j \sum_{i=1, i \neq j}^k |L(C_i)| + |S_j|$ , unless all components are isolated vertices, in which case  $k - 1$  nodes are needed. In the first case, we may assume without loss of generality, that the minimum is attained for  $j = k$ . Then the set consisting of all leaves from components  $1, \dots, k - 1$  together with a minimum cardinality resolving set of the  $k$ -th component is a minimum cardinality extended resolving set of the graph  $F$ .*

**Theorem 10.** *Let  $F \in \mathcal{F}(k)$  be a graph of  $k$  components, where each component is a complete graph. Let  $\mathcal{I}_1$  denote the set of indices of components that are isolated vertices,  $\mathcal{I}_2$  the set of indices of components that have only 2 vertices, and  $\mathcal{I}_3$  the set of indices of components that contain at least 3 vertices. If  $\mathcal{I}_1$  and  $\mathcal{I}_2$  are empty, then, for  $F$  to be observable the necessary and sufficient number of observers is  $n - k$  and the set consisting of all but one vertex of each component is a minimum cardinality extended resolving set of the graph  $F$ . Otherwise,  $\sum_{i \in \mathcal{I}_3} (|C_i| - 1) + 2|\mathcal{I}_2| + |\mathcal{I}_1| - 1$  nodes are needed (note that  $\mathcal{I}_3$  might be empty, in which case the contribution of the preceding sum over  $\mathcal{I}_3$  is zero). The set consisting of all but one vertex from each component of at least size 3 and all but one vertex from the components of sizes 1 or 2 is a minimum cardinality extended resolving set of the graph  $F$ .*

**Theorem 11.** *Let  $F \in \mathcal{F}(k)$  be a graph of  $k$  components, where each component is a grid. Then, for  $F$  to be observable the necessary and sufficient number of observers is  $3k - 1$ . Let  $O_i = \{r_1^i, r_2^i, r_3^i\}$  denote a set of three corner vertices from component  $C_i$ . Then  $O = \cup_{i=1}^{k-1} O_i \cup S_k$  is a minimum cardinality extended resolving set of  $F$ .*

**Theorem 12.** *Let  $F \in \mathcal{F}(k)$  be a graph of  $k$  components, where each component is a cycle of size greater than 3. Let  $k_e$  denote the number of components with an even number of vertices. Then, for  $F$  to be observable the necessary and sufficient number of observers is  $2k + k_e - 1$ , if  $k_e > 0$ , and  $\gamma(F) = 2k$ , otherwise. For a component  $C_i$  with an even number of vertices  $n_i$ , define  $O_i = \{r_1^i, r_2^i, r_3^i\}$ , where  $r_1^i, r_2^i$  are two neighboring vertices in  $C_i$  and  $r_3^i$  is a vertex at distance at least  $\frac{n_i-2}{2}$  from both of them, also in  $C_i$ . For a component  $C_i$  with an odd number of vertices  $n_i$ , define  $O_i = \{r_1^i, r_2^i\}$ , where  $r_1^i$  and  $r_2^i$  are two vertices of  $C_i$  that are at distance  $\frac{n_i-1}{2}$  from each other. If  $k_e = 0$ ,  $O = \cup_{i=1}^k O_i$  is a minimum cardinality extended*

resolving set of  $F$ . If  $k_e > 0$ , assume without loss of generality that  $C_k$  is a component with an even number of vertices. Then  $O = \cup_{i=1}^{k-1} O_i \cup S_k$  is a minimum cardinality extended resolving set of  $F$ .

*Proof of Theorem 9.*

Let  $u, v \in V$  be any two different vertices, and let  $H_1, H_2$  be any two graphs from the set of possible graphs  $\mathcal{H}(F)$ . We need to show that the set  $O = \cup_{i=1}^{k-1} L(C_i) \cup S_k$  is a set of smallest cardinality for which  $\mathbf{d}_{H_1}(u, O) \neq \mathbf{d}_{H_2}(v, O)$  holds when all the components are trees, unless all components are isolated vertices, in which case  $O = \cup_{i=1}^{k-1} C_i$ .

We first prove the claim of sufficiency. If both  $u$  and  $v$  are any two vertices in the same component, then  $u$  and  $v$  are distinguishable as the set of all the leaves of a tree is a resolving set. Hence we may assume  $u \in V(C_i)$  and  $v \in V(C_j)$  for  $i \neq j$ . We may also assume without loss of generality that  $i < k$ . Let  $p$  be the vertex in  $C_i$  and  $q$  the vertex in  $C_j$ , such that any path from a vertex in  $C_i$  to any vertex in  $C_j$  in  $H_2$  contains a subpath  $p - q$ . Note that  $d_{H_2}(p, q) \geq 1$ . If  $u$  is a leaf, as it is contained in  $L(C_i)$ , it is distinguishable from  $v$ , since  $0 = d_{H_1}(u, u) < d_{H_2}(u, v)$ . If  $u$  is not a leaf, and  $u = p$ , then for any leaf  $r \in L(C_i)$ ,  $d_{H_2}(r, v) = d_{H_2}(r, p) + d_{H_2}(p, q) + d_{H_2}(q, v) \geq d_{H_1}(r, p) + d_{H_2}(p, q) > d_{H_1}(r, p)$ . Thus, the two distance vectors are not equal either. Otherwise, if  $u$  is not a leaf, and  $u \neq p$ , let  $r$  be a leaf in  $L(C_i)$  such that  $u$  is on the path from  $r$  to  $p$ . Such a leaf clearly exists, as  $u$  is not a leaf, it has at least two neighbors and, hence, it has a descendant leaf  $r$  on the path that does not include  $p$ . Then  $d_{H_2}(r, v) = d_{H_2}(r, u) + d_{H_2}(u, p) + d_{H_2}(p, q) + d_{H_2}(q, v) > d_{H_1}(r, u) + d_{H_1}(u, p) > d_{H_1}(r, u)$ . Thus, the two distance vectors also in this case are not equal, which completes the proof of sufficiency.

Now, we prove the claim of necessity. Let  $O$  be an arbitrary extended resolving set. We will show that  $O$  has to be at least of the size given by the sufficient condition.

Case I: Let  $C_i$  and  $C_j$  be two components with at least 2 vertices, such that both have a leaf which is not included in  $O$ . Let  $u$  be such a leaf in component  $C_i$  with neighbor  $u'$  and  $v$  be a leaf in  $C_j$  with neighbor  $v'$ , such that  $u, v \notin O$ . We claim that  $u$  and  $v$  are indistinguishable, as illustrated in Figure 3.2a. We can construct  $H_1$  by connecting  $u$  with  $v'$ , and  $u$  with some vertex  $z_\ell$  of every other component  $C_\ell$  (if there are more than 2 components).  $H_2$  is then constructed by connecting  $v$  with  $u'$  and  $v$  with the same vertex  $z_\ell$  for any  $C_\ell$  with  $\ell \notin \{i, j\}$  as in  $H_1$ ; the other newly added edges are the same in  $H_1$  and  $H_2$  (and not involving either  $C_i$  nor  $C_j$ ). Now, we have  $\mathbf{d}_{H_1}(u, O) = \mathbf{d}_{H_2}(v, O)$ , as follows. For any vertex  $r \in C_i \setminus \{u\}$ , we have  $d_{H_1}(u, r) = 1 + d_{H_1}(u', r)$ , and  $d_{H_2}(v, r) = d_{H_2}(u', r) + 1 = d_{H_1}(u', r) + 1$ . For any vertex  $r \in C_j \setminus \{v\}$ , we have  $d_{H_1}(u, r) = d_{H_1}(v', r) + 1$ , and  $d_{H_2}(v, r) = d_{H_2}(v', r) + 1 = d_{H_1}(v', r) + 1$ . Finally, for a vertex  $r \in C_\ell$ ,  $\ell \neq i, j$ , we have  $d_{H_1}(u, r) = 1 + d_{H_1}(z_\ell, r) = 1 + d_{H_2}(z_\ell, r) = d_{H_2}(v, r)$ . Thus the vertices  $u$  and  $v$

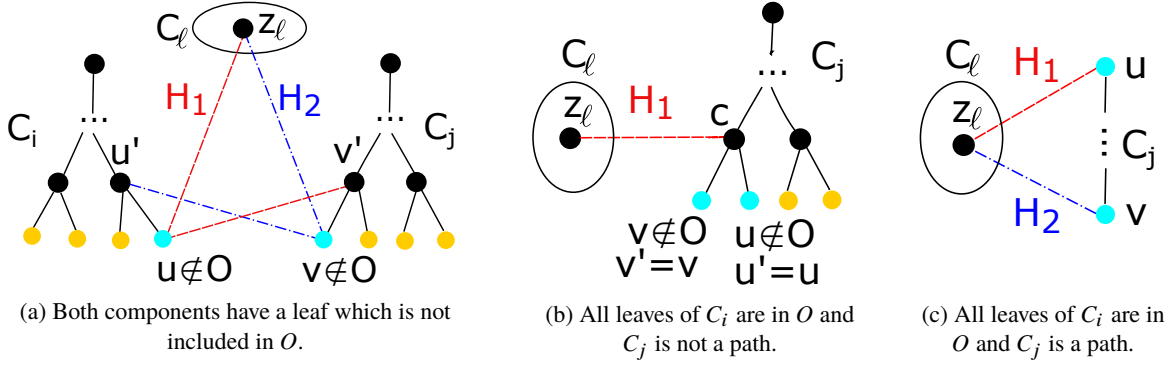


Figure 3.2: Case I in the Proof of Theorem 9: Constructing trees  $H_1$  and  $H_2$  when both components  $C_i$  and  $C_j$  have at least two vertices.

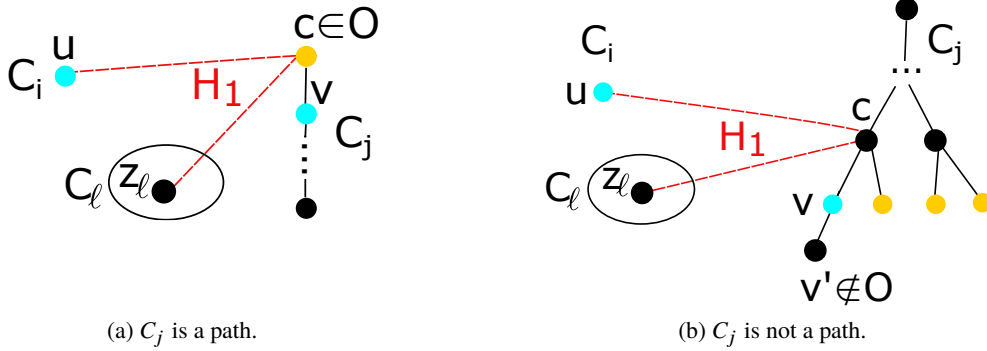


Figure 3.3: Case II in the Proof of Theorem 9: Constructing trees  $H_1$  and  $H_2$  when component  $C_i$  has only one vertex.

are indistinguishable, and the claim holds. Hence, either all the leaves of component  $C_i$  or component  $C_j$  have to be included in  $O$ . Without loss of generality, let us assume that all the leaves of  $C_i$  are included in  $O$ . Now we assume that only  $|S_j| - 1$  vertices are selected from the component  $C_j$ . In the first sub-case, when  $C_j$  is not a path, from [49], we have  $|S_j| = |L(C_j)| - |K(C_j)|$ . If only  $|S_j| - 1$  vertices were taken from  $C_j$ , then there exists a vertex  $c$  in  $K(C_j)$  with two associated leaves  $u$  and  $v$ , such that no vertex from the paths  $c - u$  nor  $c - v$  is included in  $O$ . But then there exist a vertex  $u'$  on the path  $c - u$ , and a vertex  $v'$  on the path  $c - v$ , such that  $d_{C_j}(u', c) = d_{C_j}(v', c)$ . Note that  $u'$  might coincide with  $u$ , and  $v'$  might coincide with  $v$ . The vertices  $u'$  and  $v'$  are indistinguishable from each other in  $C_j$ . Constructing a tree  $H_1$  by connecting any vertex  $z_\ell$  from every other component  $C_\ell$ ,  $\ell \neq j$ , with any fixed vertex in  $K(C_j)$ , we see that  $u'$  and  $v'$  still are indistinguishable by vertices in  $O$ , as shown in Figure 3.2b. In the second sub-case, when  $C_j$  is a path with leaves  $u$  and  $v$ ,  $S_j$  comprises only one leaf. If no vertex from  $C_j$  is in  $O$ ,  $H_1$  can be constructed by connecting one of its leaves  $u$  with some vertex  $z_\ell$  of every other component  $C_\ell$ , while  $H_2$  is constructed by connecting  $z_\ell$  to the other leaf  $v$ , and vertices  $u$  and  $v$  are indistinguishable, as Figure 3.2c shows. Thus, at

least  $|S_j|$  vertices have to be taken from  $C_j$ .

Case II:  $C_i$  consists of only one vertex,  $u$ , and  $C_j$  has at least 2 vertices. By the same arguments as in Case I, it can be seen that at least  $|S_j|$  vertices from component  $C_j$  have to be included in  $O$ . We will show now that  $u$  has to be included in  $O$  as well. In the first sub-case, when  $C_j$  is a path,  $H_1$  can be constructed by connecting  $u$  with the leaf  $c$  of  $C_j$  where  $c \in O$ , and then connecting  $c$  to a vertex  $z_\ell$  of every other component  $C_\ell$ ,  $\ell \neq i, j$ . Let  $v$  be the vertex in  $C_j$  which is the neighbor of  $c$ . If  $u$  is not chosen,  $u$  is indistinguishable within  $H_1$  from  $v$ , as can be seen in Figure 3.3a. As for the second sub-case, when  $C_j$  is not a path, let  $c$  be a vertex in  $K(C_j)$  such that the path to its associated leaf  $v'$  contains no vertices from  $O$ . Then  $H_1$  is constructed by connecting  $u$  with  $c$ , and then connecting  $c$  to a vertex  $z_\ell$  of every other component  $C_\ell$ ,  $\ell \neq i, j$ . Let  $v$  be the neighbor of  $c$  in  $C_j$  which lies on the path  $c - v'$ . Note that  $v$  can coincide with  $v'$ . Then  $u$  is indistinguishable within  $H_1$  from  $v$ , as shown in Figure 3.3b. Hence,  $u$  must also be included in  $O$ .

Case III: Both  $C_i$  and  $C_j$  contain only one vertex. Call these  $u$  and  $v$ , respectively. At least one of them has to be included in  $O$ : otherwise, we can construct  $H_1$  by connecting both  $u$  and  $v$  to some vertex  $z_\ell$  from every other component  $C_\ell$ ,  $\ell \neq i, j$ , and then  $u$  and  $v$  are indistinguishable within  $H_1$ . If there are only two components, each with one vertex,  $H_1$  is constructed by connecting them. Clearly, if neither vertex is included in  $O$ , the set  $O$  is empty, and the two vertices are indistinguishable within  $H_1$ .

Therefore, for any pair of components  $C_i$  and  $C_j$ , an extended resolving set  $O$  has to include all leaves from one component and a resolving set from the other, unless both have size 1, in which case only 1 vertex is enough. Hence, if there exists at least one component which has 2 or more vertices, from all but one component all the leaves have to be taken, and from the remaining component, at least a resolving set. If all  $k$  components have only one vertex, the set  $O$  has to contain  $k - 1$  vertices.  $\square$

### *Proof of Theorem 10.*

Let  $u, v \in V$  be any two different vertices, and let  $H_1, H_2$  be any two graphs from the set of possible graphs  $\mathcal{H}(F)$ . First we need to show that the set  $O$  consisting of all but one vertex from each component is a set of smallest cardinality for which  $d_{H_1}(u, O) \neq d_{H_2}(v, O)$  holds when all the components are complete graphs with at least 3 vertices.

First, we prove the claim of sufficiency. Let us denote the set of all but one vertex on component  $C_i$  by  $O_i$ . If  $u$  and  $v$  are in the same component, they are distinguishable, since each  $O_i$  is a resolving set of component  $C_i$  [52]. Hence, let us assume that vertex  $u \in V(C_i)$  is not included in  $O_i$ , and that vertex  $v \in V(C_j)$  is not included in  $O_j$ , and  $i \neq j$ . Let  $p \in V(C_i)$  and  $q \in V(C_j)$ , such that  $p - q$  is contained in every shortest path between vertices of components  $C_i$  and  $C_j$  in  $H_2$ . Note again that  $d_{H_2}(p, q) \geq 1$ . We prove the claim by

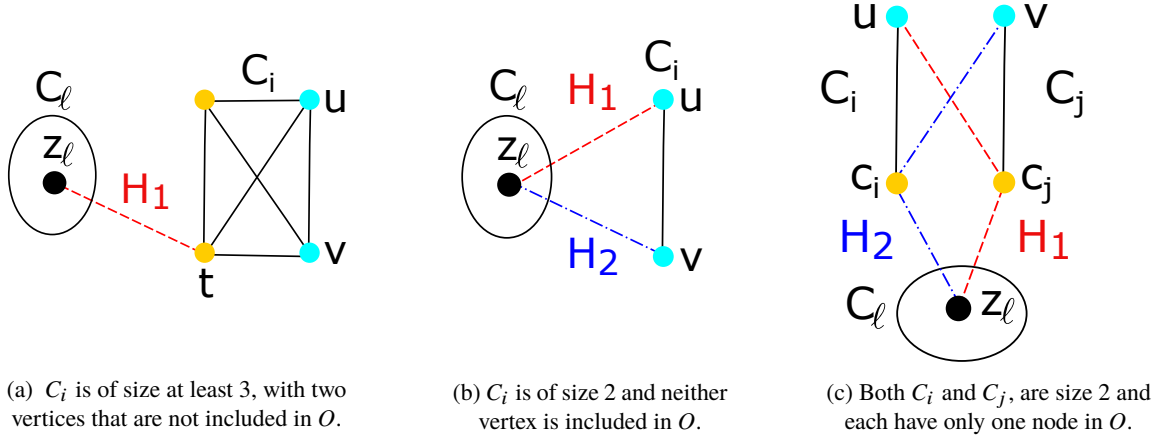


Figure 3.4: Proof of Theorem 10: Constructing trees  $H_1$  and  $H_2$  when both components  $C_i$  and  $C_j$  are complete graphs.

contradiction and assume that the following relations hold:

$$d_{H_1}(u, r) = 1 = d_{H_2}(v, r) = d_{H_2}(v, q) + d_{H_2}(q, p) + d_{H_2}(p, r), \quad (3.3)$$

for every  $r \in O_i$ . Then for  $d_{H_2}(p, q) = 1$ , the condition  $d_{H_2}(p, r) = 0$  would have to hold, while for  $d_{H_2}(p, q) > 1$ , the condition  $d_{H_2}(p, r) < 0$  would have to hold for all  $r \in O_i$ . In either case, this is not possible, and the claim is proved.

To prove the claim of necessity, let  $O$  be an arbitrary extended resolving set. Assume that in one component  $C_i$  there are two vertices,  $u$  and  $v$ , that are not included in  $O$ . We construct  $H_1$  by adding the edges between a fixed vertex  $t \in V(C_i) \setminus \{u, v\}$  and some fixed vertex  $z_\ell$  of some other component  $C_\ell$ . Then we have  $d_{H_1}(u, r) = d_{H_1}(v, r)$  for all  $r \in O$ , and this completes the proof.

Now, we consider the case when there is at least one component of size 1 or 2. We need to show that a minimum cardinality extended resolving set  $O$  should contain all but one vertex of each component of size at least 3 and all but one vertex from the components of sizes 1 or 2. First, we prove the claim of sufficiency. If either  $u$  or  $v$  is included in  $O$ , w.l.o.g. say  $u$ , then  $u$  and  $v$  are clearly distinguishable, as,  $d_{H_1}(u, u) = 0 \neq d_{H_2}(u, v)$ , for any  $H_1, H_2 \in (F)$ . Therefore, let  $u \notin O$  be a vertex belonging to component  $C_i$ , and let  $v \notin O$  be a vertex belonging to component  $C_j$ . Let  $p \in V(C_i)$  and  $q \in V(C_j)$ , such that the path  $p - q$  is contained in every shortest path between vertices from  $C_i$  and  $C_j$  in  $H_2$ . Note that  $d_{H_2}(p, q) \geq 1$ . Since only one vertex from a component of sizes 1 or 2 is not included in  $O$ , let us assume  $u$  is in a component of size at least 3. Then by the same argument as in (3.3) and the following discussion, we must have  $d_{H_1}(u, r) \neq d_{H_2}(v, r)$  for some  $r \in O$ .

To prove the claim of necessity, let  $O$  be an arbitrary extended resolving set. We will show that  $O$  has to

be at least of the size given by the sufficient condition.

Case I: Let  $C_i$  be a component of size at least 3, with two vertices,  $u$  and  $v$ , that are not included in  $O$ . This is exactly the case discussed when there are only components of size at least 3 and it is shown in Figure 3.4a. Thus, all but one vertex from each component of size at least 3 has to be included in  $O$ .

Case II: Let  $C_i$  be a component of size 2, where neither vertex is included in  $O$ . Let  $u, v$  be the two vertices from the component  $C_i$ . We can construct  $H_1$  by connecting  $u$  with any vertex  $z_\ell \in V(C_\ell)$ , and  $H_2$  by connecting  $v$  again to the same vertex  $z_\ell \in V(C_\ell)$ , for any  $\ell \neq i$ . In both  $H_1$  and  $H_2$  all other connections between components are the same and not including  $C_i$ . Then, we have that  $u$  and  $v$  cannot be distinguished, as illustrated in Figure 3.4b. Hence at least one vertex from a component of size 2 has to be included in  $O$ .

Case III: Let  $C_i$  be a component of size 2 with one vertex,  $u$ , that is not included in  $O$ . First, let us consider the sub-case when  $C_j$  is a component of size 2, and vertex  $v \in V(C_j)$  is a vertex not included in  $O$ . Then,  $H_1$  can be constructed by connecting  $u$  with the vertex  $c_j \in C_j$ , where  $c_j \in O$ , and then connecting  $c_j$  to some vertex  $z_\ell$  of every other component  $C_\ell$ .  $H_2$  can be constructed by connecting  $v$  with the vertex  $c_i \in C_i$ , where  $c_i \in O$ , and then connecting  $c_i$  to the same vertex  $z_\ell$  of every other component  $C_\ell$ . All the other connections in  $H_1$  and  $H_2$  are the same and not including either  $C_i$  or  $C_j$ . Now we have that  $d_{H_1}(u, r) = d_{H_2}(v, r)$  for all  $r \in O$ , and  $u$  and  $v$  are indistinguishable, as Figure 3.4c shows. Next, we consider the sub-case when  $C_j$  is an isolated vertex, not included in  $O$ . We can construct  $H_1$  by connecting  $c_i \in V(C_i)$ , where  $c_i \in O$  to the isolated vertex from  $C_j$ . Then,  $u$  and the vertex from  $C_j$  are indistinguishable. Hence, all but one vertex from the components of size 2 have to be included in  $O$ .

Case IV: Let both  $C_i$  and  $C_j$  be isolated vertices. Note that this is equivalent to Case III of the Proof of Theorem 9. Now all but one vertex from the components of sizes 1 have to be included in  $O$ .

Hence, the set  $O$  should contain all but one vertex on each component of at least size 3 and all but one vertex from the components of sizes 1 or 2.  $\square$

### *Proof of Theorem 11.*

Let  $u, v \in V$  be any two different vertices, and let  $H_1, H_2$  be any two graphs from the set of possible graphs  $\mathcal{H}(F)$ . We need to show that the set  $O$  comprising three corner vertices from  $k - 1$  components and a resolving set of the  $k$ -th component is a set of smallest cardinality for which  $\mathbf{d}_{H_1}(u, O) \neq \mathbf{d}_{H_2}(v, O)$  holds when all the components are grids.

Let us denote the size of the grid  $C_i$  as  $x_i \times y_i$ . We assume that each vertex  $l \in V(C_i)$  has assigned to it a position vector  $(x_l, y_l)$  which represents its location on the integer lattice  $C_i$ , with the first selected corner vertex  $r_1^i$  at position  $(0, 0)$ ,  $r_2^i$  at  $(x_i, 0)$  and  $r_3^i$  at  $(0, y_i)$ . First, let us prove the claim of sufficiency. If  $u$  and  $v$  are in the same component, they are distinguishable, since any two corner vertices having the same value in one coordinate form a resolving set of a grid [52]. Hence, let us assume that  $u \in V(C_i)$  and

$v \in V(C_j)$ , for  $i \neq j$  and  $i < k$ . Let  $p$  be the vertex in  $C_i$  and  $q$  the vertex in  $C_j$ , such that any path from a vertex in  $C_i$  to any vertex in  $C_j$  in  $H_2$  contains a subpath  $p - q$ , with  $d_{H_2}(p, q) \geq 1$ . If  $u = p$ , then for all  $r \in O_i$  we have  $d_{H_2}(v, r) = d_{H_2}(r, p) + d_{H_2}(p, q) + d_{H_2}(q, v) > d_{H_2}(r, p) = d_{H_1}(r, u)$ . Therefore  $u$  and  $v$  are distinguishable. For  $u \neq p$ , let us prove the claim by contradiction. Assuming  $d_{H_1}(u, O_i) = d_{H_2}(v, O_i)$ , we obtain the following equations:

$$\begin{aligned}
d_{H_1}(u, r_1^i) &= x_u + y_u \\
&= d_{H_2}(v, r_1^i) = x_p + y_p + d_{H_2}(p, q) + d_{H_2}(q, v) \\
d_{H_1}(u, r_2^i) &= x_i - x_u + y_u \\
&= d_{H_2}(v, r_2^i) = x_i - x_p + y_p + d_{H_2}(p, q) + d_{H_2}(q, v) \\
d_{H_1}(u, r_3^i) &= x_u + y_i - y_u \\
&= d_{H_2}(v, r_3^i) = x_p + y_i - y_p + d_{H_2}(p, q) + d_{H_2}(q, v).
\end{aligned} \tag{3.4}$$

The system of equations (3.4) can be rewritten in matrix form

$$\mathbf{A}\boldsymbol{\alpha} = \mathbf{b},$$

where

$$\mathbf{A} = \begin{bmatrix} 1 & 1 & -1 \\ -1 & 1 & -1 \\ 1 & -1 & -1 \end{bmatrix}, \quad \boldsymbol{\alpha} = \begin{bmatrix} x_u \\ y_u \\ d_{H_2}(p, q) + d_{H_2}(q, v) \end{bmatrix}, \quad \mathbf{b} = \begin{bmatrix} x_p + y_p \\ -x_p + y_p \\ x_p - y_p \end{bmatrix}.$$

$\mathbf{A}$  is a matrix of full rank, implying that the system of equations (3.4) has a unique solution, given by  $\mathbf{A}^{-1}\mathbf{b}$ . The only solution is  $x_u = x_p$ ,  $y_u = y_p$ , and  $d_{H_2}(p, q) + d_{H_2}(q, v) = 0$ , contradicting  $d_{H_2}(p, q) \geq 1$ . The set  $\cup_{i=1}^{k-1} O_i \cup S_k$  is a set of cardinality  $3k - 1$ , and this completes the sufficiency claim.

For the claim of necessity, let us assume that there exist two components  $C_i$  and  $C_j$ , such that from each of them, only two vertices are chosen. Let  $\{r_1^i, r_2^i\}$  be the set of two vertices from  $C_i$  and let  $\{r_1^j, r_2^j\}$  be the set of two vertices from  $C_j$  that are included in  $O$ .

Case I: In at least one component, the vertices included in  $O$  are not two corner vertices with one identical coordinate. Let us assume that this is the case with  $C_i$ . We claim that there exist two vertices  $u$  and  $v$  in  $C_i$  which are indistinguishable by  $r_1^i$  and  $r_2^i$ . Denote by  $(x_{r_1^i}, y_{r_1^i})$  and by  $(x_{r_2^i}, y_{r_2^i})$  the positions at which  $r_1^i$  and  $r_2^i$  are located in the grid.

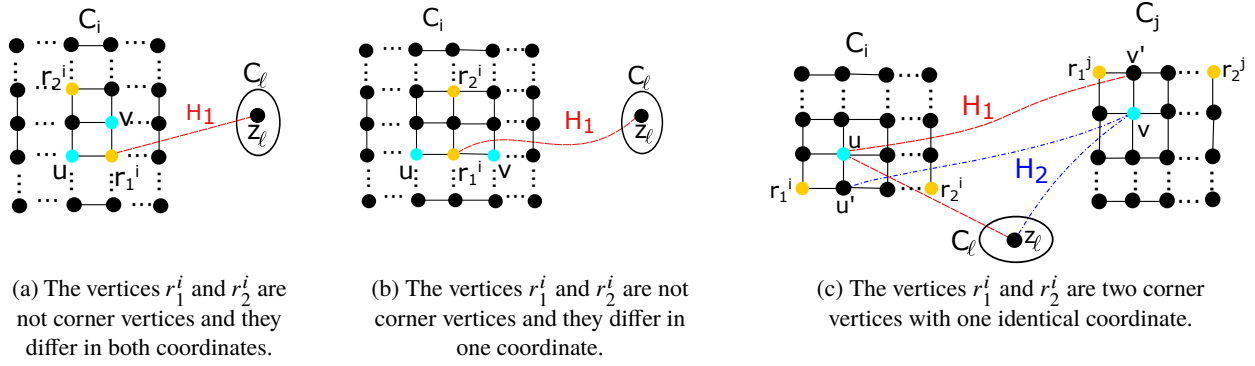


Figure 3.5: Proof of Theorem 11: Constructing  $H_1$  and  $H_2$  when the components are grids.

First, let us consider the sub-case, when  $r_1^i$  and  $r_2^i$  differ in both coordinates, as shown in Figure 3.5a. Without loss of generality, let us assume that  $y_{r_1^i} < y_{r_2^i}$ . Let  $\Delta_x = |x_{r_2^i} - x_{r_1^i}|$  and  $\Delta_y = y_{r_2^i} - y_{r_1^i}$ . Let  $u$  be the vertex at  $(x_{r_2^i}, y_{r_1^i})$ . For  $\Delta_x \leq \Delta_y$ , let  $v$  be the vertex at  $(x_{r_1^i}, y_{r_1^i} + \Delta_x)$ , while for  $\Delta_x > \Delta_y$ , we consider two possible cases. For  $x_{r_1^i} < x_{r_2^i}$ , let  $v$  be the vertex at  $(x_{r_1^i} + \Delta_x - \Delta_y, y_{r_2^i})$ , and for  $x_{r_1^i} > x_{r_2^i}$ , let  $v$  be the vertex at  $(x_{r_2^i} + \Delta_y, y_{r_2^i})$ . Constructing a tree  $H_1$  by connecting some vertex  $z_\ell$  from every other component  $C_\ell$ ,  $\ell \neq i$ , with either  $r_1^i$  or  $r_2^i$ , we have  $d_{H_1}(u, r_1^i) = \Delta_x = d_{H_1}(v, r_1^i)$  and  $d_{H_1}(u, r_2^i) = \Delta_y = d_{H_1}(v, r_2^i)$ . Hence the vertices  $u$  and  $v$  are indistinguishable by any vertex in  $O$ .

In the second sub-case,  $r_1^i$  and  $r_2^i$  differ in only one coordinate, as Figure 3.5b illustrates. Then, let  $u$  and  $v$  be two neighbors of  $r_1^i$ , which are not on the shortest path  $r_1^i - r_2^i$ . These two vertices exist, as all vertices on the grid, except the corner vertices, have at least 3 neighbors. Now, we have  $d_{C_i}(u, r_1^i) = 1 = d_{C_i}(v, r_1^i)$  and  $d_{C_i}(u, r_2^i) = 1 + d_{C_i}(r_1^i, r_2^i) = d_{C_i}(v, r_2^i)$ . Therefore, there always exist two vertices  $u$  and  $v$ , such that they are not distinguishable by any two vertices of  $C_i$  which are not two corner vertices with one identical coordinate. Constructing a tree  $H_1$  by connecting some vertex  $z_\ell$  from every other component  $C_\ell$ ,  $\ell \neq i$ , with either  $r_1^i$  or  $r_2^i$ , we see that  $u$  and  $v$  still are indistinguishable by any vertex in  $O$ .

Case II: From both components  $C_i$  and  $C_j$ , two corner vertices with one identical coordinate are included in  $O$ . Let  $u'$  be a vertex on  $C_i$  that is a neighbor of  $r_1^i$  such that it shares one coordinate with both  $r_1^i$  and  $r_2^i$ . Then let  $u$  be a neighbor of  $u'$  such that it does not share any coordinates with  $r_1^i$ . Similarly, let  $v'$  be a vertex in  $C_j$  that is a neighbor of  $r_1^j$  such that it shares one coordinate with both  $r_1^j$  and  $r_2^j$ . Then let  $v$  be a neighbor of  $v'$  such that it does not share any coordinates with  $r_1^j$ . We can construct  $H_1$  by connecting  $u$  with  $v'$  and  $u$  with some vertex  $z_\ell$  of every other component  $C_\ell$  (if there are more than 2 components). Then  $H_2$  is constructed by connecting  $v$  with  $u'$  and  $v$  with the same vertex  $z_\ell$  as in  $H_1$ , as shown in Figure 3.5c.

The distances of  $u$  and  $v$  from the vertices in  $O$  are

$$\begin{aligned}
d_{H_1}(u, r_1^i) &= d_{H_2}(v, r_1^i) = 2 \\
d_{H_1}(u, r_2^i) &= d_{H_2}(v, r_2^i) = 1 + d_{H_1}(u', r_2^i) \\
d_{H_1}(u, r_1^j) &= d_{H_2}(v, r_1^j) = 2 \\
d_{H_1}(u, r_2^j) &= d_{H_2}(v, r_2^j) = 1 + d_{H_2}(v', r_2^j) \\
d_{H_1}(u, r) &= d_{H_2}(v, r) = 1 + d_{H_1}(z_\ell, r),
\end{aligned}$$

for  $r \in C_\ell$ ,  $\ell \neq i, \ell \neq j$ . Hence the vertices  $u$  and  $v$  are indistinguishable.

Therefore, at least 3 vertices of component  $C_i$  or component  $C_j$  have to be included in  $O$ . Without loss of generality, let us assume that 3 vertices in  $C_i$  are included in  $O$ . Now we assume that only  $|S_j| - 1 = 1$  vertex is selected from  $C_j$ . Then there exist two vertices  $u$  and  $v$  in component  $C_j$ , which are at the same distance from the only vertex  $r$  included from  $S_j$ . We construct  $H_1$  by connecting some vertex  $z_\ell$  from every other component  $C_\ell$  to vertex  $r$  in component  $C_j$ . Observe that the vertices  $u$  and  $v$  are still not distinguishable within  $H_1$ , and hence at least  $|S_j| = 2$  vertices have to be included from component  $C_j$ . In conclusion, for any two components, at least 3 vertices from one and 2 vertices from the other one have to be included in  $O$ , and thus  $|O| \geq 3(k - 1) + 2 = 3k - 1$ .  $\square$

*Proof of Theorem 12.*

Let  $u, v \in V$  be any two different vertices, and let  $H_1, H_2$  be any two graphs from the set of possible graphs  $\mathcal{H}(F)$ . We need to show that the set  $O$  as defined in the statement of the theorem with cardinality equal to  $2k + k_e - 1$  if the number of components with an even number of vertices,  $k_e$  is non-zero, or  $2k$ , otherwise, is a set of smallest cardinality for which  $d_{H_1}(u, O) \neq d_{H_2}(v, O)$  holds when all components are cycles.

First, let us prove the claim of sufficiency. As in Theorem 11, let us assume that vertex  $u$  is located in component  $C_i$  and vertex  $v$  is in component  $C_j$  (when  $u$  and  $v$  belong to the same component, they are clearly distinguishable, as any two neighboring vertices of an even cycle and any two vertices at distance  $(n_i - 1)/2$  in the case of an odd cycle  $C_i$  form a resolving set of a cycle). Let  $u \in V(C_i)$ ,  $v \in V(C_j)$ , with  $i \neq j$  and  $i < k$ . Let  $p$  be the vertex in  $C_i$  and  $q$  the vertex in  $C_j$ , such that any path from a vertex in  $C_i$  to any vertex in  $C_j$  in  $H_2$  contains a subpath  $p - q$ , with  $d_{H_2}(p, q) \geq 1$ . If the vertices  $u$  and  $v$  are not distinguishable by  $O_i$ , then  $d_{H_1}(u, r) = d_{H_2}(v, r) = d_{H_1}(p, r) + d_{H_2}(p, q) + d_{H_2}(q, v)$  holds for some  $H_1$  and  $H_2$  and all  $r \in O_i$ .

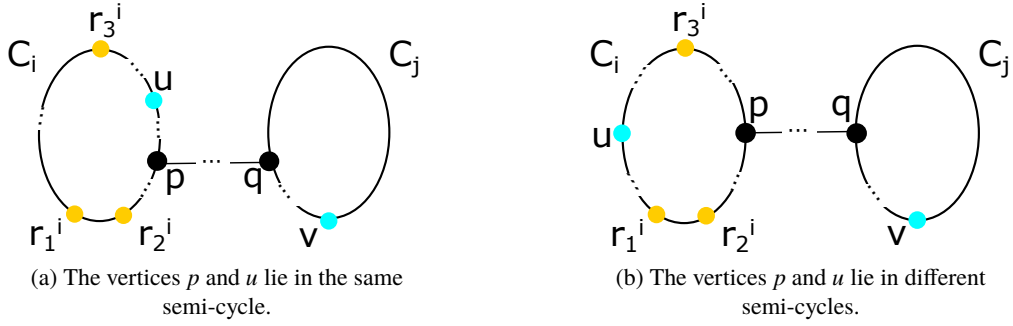


Figure 3.6: Case I in the Proof of Theorem 12: Both cycle components have an even number of vertices.

Therefore, the following must hold

$$d_{H_1}(u, r) > d_{H_1}(p, r). \quad (3.5)$$

Case I: Both components  $C_i$  and  $C_j$  have an even number of vertices. For a component  $C_i$ , due to the placement of  $r_3^i$ , the distance  $d_H(r_1^i, r_3^i) \in \left\{ \frac{n_i-2}{2}, \frac{n_i}{2} \right\}$ , for any  $H \in \mathcal{H}(F)$ . The same holds for  $d_H(r_2^i, r_3^i)$ . Let us first consider the sub-case where both  $p$  and  $u$  lie in the same half of the cycle, i.e., both lie either on the shorter path  $r_2^i - r_3^i$  or on the shorter path  $r_1^i - r_3^i$ , as shown in Figure 3.6a. Suppose without loss of generality that they both lie on the shorter path  $r_2^i - r_3^i$ . As one of the vertices out of  $\{u, p\}$  is closer to  $r_3^i$  and the other one is closer to  $r_2^i$ , (3.5) cannot hold simultaneously for both  $r_2^i$  and  $r_3^i$ . The other sub-case that needs to be considered is when  $u$  and  $p$  lie in different semi-cycles, one on the shorter path  $r_2^i - r_3^i$ , and the other on the shorter path  $r_1^i - r_3^i$ , as illustrated in Figure 3.6b. Notice that for any vertex  $w$  that is on the shorter path  $r_1^i - r_3^i$ , the distance  $d_H(w, r_2^i) = \min\{d_H(w, r_1^i) + 1, d_H(w, r_3^i) + d_H(r_3^i, r_2^i)\}$ . We have  $d_H(w, r_1^i) + 1 \leq \frac{n_i}{2} - 1 + 1 = \frac{n_i}{2}$ , and also  $d_H(w, r_3^i) + d_H(r_3^i, r_2^i) \geq 1 + \frac{n_i-2}{2} = \frac{n_i}{2}$ . Therefore, the first term of the minimum can never be larger than the second term, hence we can write  $d_H(w, r_2^i) = d_H(w, r_1^i) + 1$ . The same reasoning holds when  $w$  is on the shorter path  $r_2^i - r_3^i$ , and then we can write  $d_H(w, r_1^i) = d_H(w, r_2^i) + 1$ .

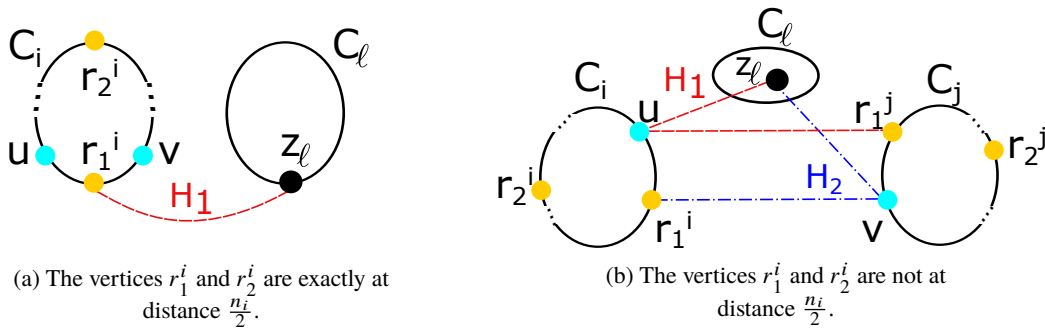


Figure 3.7: Proof of Theorem 12: Constructing  $H_1$  and  $H_2$  when the components are cycles.

Now, for vertices  $u$  and  $p$  that lie in different semi-cycles, we either have  $d_{H_1}(u, r_1^i) = d_{H_1}(u, r_2^i) + 1$  and  $d_{H_1}(p, r_1^i) = d_{H_1}(p, r_2^i) - 1$ , or  $d_{H_1}(u, r_1^i) = d_{H_1}(u, r_2^i) - 1$  and  $d_{H_1}(p, r_1^i) = d_{H_1}(p, r_2^i) + 1$ . If now (3.5) holds and  $u$  and  $v$  are indistinguishable by  $r_1^i$  and  $r_2^i$ , then we would have to have

$$d_{H_2}(p, q) + d_{H_2}(q, v) = d_{H_1}(u, r_1^i) - d_{H_1}(p, r_1^i) = d_{H_1}(u, r_2^i) - d_{H_1}(p, r_2^i).$$

If now  $d_{H_1}(u, r_1^i) = d_{H_1}(u, r_2^i) + 1$  and  $d_{H_1}(p, r_1^i) = d_{H_1}(p, r_2^i) - 1$  holds, then we would have to have

$$d_{H_1}(u, r_1^i) - d_{H_1}(p, r_1^i) = d_{H_1}(u, r_2^i) - 1 - d_{H_1}(p, r_2^i) - 1,$$

which is clearly not possible. If  $d_{H_1}(u, r_1^i) = d_{H_1}(u, r_2^i) - 1$  and  $d_{H_1}(p, r_1^i) = d_{H_1}(p, r_2^i) + 1$  holds, the analogous contradiction appears, and hence in both cases (3.5) cannot hold.

Case II: At least one of the components  $C_i$  or  $C_j$  has an odd number of vertices. Let us assume that this is the case with  $C_i$ . Similarly, as in Case I, let us first consider the sub-case where both  $p$  and  $u$  lie in the same half of the cycle, i.e., both on the shorter path  $r_1^i - r_2^i$  or both on the longer path  $r_1^i - r_2^i$ . As before, one of the vertices out of  $\{u, p\}$  is closer to  $r_1^i$ , and the other is closer to  $r_2^i$ , and thus (3.5) cannot hold simultaneously for both  $r_1^i$  and  $r_2^i$ . The other sub-case that needs to be considered is when  $u$  and  $p$  lie in different semi-cycles, one on the shorter path  $r_1^i - r_2^i$ , of length  $\frac{n_i-1}{2}$ , and the other on the longer path  $r_1^i - r_2^i$ , of length  $\frac{n_i+1}{2}$ . Then either we have  $d_{H_1}(u, r_2^i) = \frac{n_i-1}{2} - d_{H_1}(u, r_1^i)$  and  $d_{H_1}(p, r_2^i) = \frac{n_i+1}{2} - d_{H_1}(p, r_1^i)$ , or  $d_{H_1}(u, r_2^i) = \frac{n_i+1}{2} - d_{H_1}(u, r_1^i)$  and  $d_{H_1}(p, r_2^i) = \frac{n_i-1}{2} - d_{H_1}(p, r_1^i)$ . From  $d_{H_1}(u, r_2^i) > d_{H_1}(p, r_2^i)$  as given by Condition (3.5), we obtain  $d_{H_1}(p, r_1^i) > d_{H_1}(u, r_1^i) + 1$  or  $d_{H_1}(p, r_1^i) > d_{H_1}(u, r_1^i) - 1$ . In either case, we get that (3.5) cannot hold for both  $r = r_1^i$  and  $r = r_2^i$ .

Note that when comparing components  $C_i$  and  $C_j$  with  $i \neq j$ , only vertices of the extended resolving set coming from component  $C_i$  were used to distinguish between any two vertices from components  $C_i$  and  $C_j$ . Hence, for one component, say,  $C_k$ , it is enough to choose a resolving set, that is, a set that distinguishes all vertices within  $C_k$  (a minimum cardinality resolving set is always of size 2). Hence, if  $k_e > 0$ , we may assume that  $C_k$  is an even cycle. Thus only 2 vertices are chosen from  $C_k$ , and from all other even cycles 3 vertices are chosen. Thus, in this case  $2k + k_e - 1$  vertices are enough. If  $k_e = 0$ , then 2 vertices are chosen from each component, giving the bound  $2k$  in this case.

Now, we prove the claim of necessity. Observe first that clearly at least 2 vertices of each cycle have to be chosen, as otherwise the two neighbors of the chosen vertex  $r$  cannot be distinguished; one can construct a graph  $H_1$  by connecting  $r$  with one fixed vertex of each other component, and the two neighbors of  $r$  are indistinguishable.

Let us first assume that there exist two components  $C_i$  and  $C_j$  both containing an even number of vertices, and from each component, only two vertices are included in  $O$ . Denote by  $r_1^i, r_2^i$  the vertices chosen from  $C_i$

and by  $r_1^j, r_2^j$  the vertices chosen from  $C_j$ . If in at least one component, say  $C_i$ , the two selected vertices  $r_1^i$  and  $r_2^i$  are at distance exactly  $\frac{n_i}{2}$  from each other, let  $u$  and  $v$  be two neighbors of  $r_1^i$ . Note that  $u$  and  $v$  are equidistant from both  $r_1^i$  and  $r_2^i$ . Constructing  $H_1$  by connecting some vertex  $z_\ell$  from every other component  $C_\ell$  to  $r_1^i$ , the vertices  $u$  and  $v$  are still not distinguishable within  $H_1$ , as shown in Figure 3.7a. Otherwise, let us assume that in both components  $C_i$  and  $C_j$  the vertices selected in  $O$  are not at distance exactly  $\frac{n_i}{2}$  ( $\frac{n_j}{2}$ , respectively) from each other. Let  $u$  then be a neighbor of  $r_1^i$  in  $C_i$  that is on the longer path  $r_1^i - r_2^i$ , and let  $v$  be a neighbor of  $r_1^j$  in  $C_j$  that is on the longer path  $r_1^j - r_2^j$ . We can construct  $H_1$  by connecting  $u$  with  $r_1^j$  and  $u$  with some vertex  $z_\ell$  of every other component  $C_\ell$  (if there are more than 2 components).  $H_2$  is constructed by connecting  $v$  with  $r_1^i$  and  $v$  with the same vertex  $z_\ell$  (for every other component  $C_\ell$ ) as in  $H_1$ , as shown in Figure 3.7b. The distances of the vertices  $u, v$  from the vertices in  $O$  are

$$\begin{aligned}
d_{H_1}(u, r_1^i) &= d_{H_2}(v, r_1^i) = 1 \\
d_{H_1}(u, r_2^i) &= d_{H_2}(v, r_2^i) = 1 + d_{H_1}(r_1^i, r_2^i) \\
d_{H_1}(u, r_1^j) &= d_{H_2}(v, r_1^j) = 1 \\
d_{H_1}(u, r_2^j) &= d_{H_2}(v, r_2^j) = 1 + d_{H_2}(r_1^j, r_2^j) \\
d_{H_1}(u, r) &= d_{H_2}(v, r) = 1 + d_{H_1}(z_\ell, r),
\end{aligned}$$

for  $r \in O_l, l \neq i, j$ . Hence the vertices  $u$  and  $v$  are indistinguishable.

Therefore, if both  $C_i$  and  $C_j$  have an even number of vertices, at least 3 vertices of component  $C_i$  or 3 vertices of component  $C_j$  have to be included in  $O$ . Hence, from all but one component with an even number of vertices, 3 vertices have to be chosen, and from the remaining ones, at least 2. This completes the proof.  $\square$

### 3.1.2 Results for general graph classes

Next, we determine a set of nodes that achieves network observability when components are of arbitrary structure. In order to clearly present the results, we review the concept of boundary of a graph. For a connected graph  $G$ , a vertex  $v$  is a *boundary vertex* of  $u$  if  $d_G(w, u) \leq d_G(v, u)$ , for all  $w$  that are neighbors of  $v$  [63]. A vertex  $v$  is a boundary vertex of  $G$  if it is a boundary vertex of some vertex of  $G$ . The set of all boundary vertices of a vertex  $u$  is denoted as  $\partial(u)$ . The boundary of a vertex set  $S \subseteq V$  is the set of vertices in  $G$  that are boundary vertices for some vertex  $u \in S$ . The *boundary* of graph  $G$ ,  $\partial(G)$ , is the set of all boundary vertices of  $G$ . It is well known that the boundary is a resolving set, see [64]. For example, the boundary of a tree is the set of its leaves, whereas the boundary of a grid is the set of its 4 corner vertices,

and the boundary of a cycle is the whole vertex set [64]. We start with the following easy observation.

**Observation 1.** Let  $G$  be a connected graph. Consider any two vertices  $r$  and  $u$  of  $G$ , and consider a shortest path  $r - u$ . Either  $u$  is a boundary vertex for  $r$ , or there exists some vertex  $u'$  such that the shortest path  $r - u$  can be extended to a shortest path  $r - u'$ , with  $u'$  being a boundary vertex for  $r$ .

*Proof.* If  $u$  is not a boundary vertex for  $r$ , then by definition there exists a neighbor  $w$  of  $u$  such that  $d_G(w, r) > d_G(u, r)$ . Thus,  $d_G(w, r) \geq d_G(u, r) + 1$ , and in particular, a shortest path  $r - u$  can be extended to  $w$  such that along this extended path, the lower bound can be attained, and thus  $d_G(w, r) = d_G(u, r) + 1$ . Hence, the path  $r - w$  going through  $u$  is also a shortest path  $r - w$ . If  $w$  is then a boundary vertex for  $r$ , we are done, and otherwise we iteratively apply the same argument with  $w$  playing the role of  $u$ . The claim follows.  $\square$

We are now ready to show our results in terms of boundary vertices.

For general graph classes we have the following results, the second one tightening the first one, as the boundary of a graph can be very large.

**Theorem 13.** For any arbitrary graph  $F \in \mathcal{F}(k)$  with  $k$  connected components, the observer set  $O = \cup_{i=1}^{k-1} \partial(C_i) \cup S_k$  achieves network observability.

**Theorem 14.** Let  $F \in \mathcal{F}(k)$  be an arbitrary graph with  $k$  connected components, let  $S_i$  be a resolving set of  $C_i$ , and let  $O_i = S_i \cup \partial(S_i)$ . Then the observer set  $O = \cup_{i=1}^{k-1} O_i \cup S_k$  achieves network observability.

*Proof of Theorem 13.*

Let  $u, v \in V$  be any two different vertices, and let  $H_1, H_2$  be any two graphs from the set of possible graphs  $\mathcal{H}(F)$ . We need to show that for the set  $O = \cup_{i=1}^{k-1} \partial(C_i) \cup S_k$  the condition  $\mathbf{d}_{H_1}(u, O) \neq \mathbf{d}_{H_2}(v, O)$  holds for an arbitrary graph.

Since the boundary is a resolving set, any two vertices belonging to the same component are distinguishable by a set that contains the boundaries of  $k - 1$  components and a resolving set of the  $k$ -th component. As before, let  $u \in V(C_i), v \in V(C_j)$ , let  $p \in V(C_i)$  and  $q \in V(C_j)$  such that any path from a vertex in  $C_i$  to any vertex in  $C_j$  in  $H_2$  contains a subpath  $p - q$ , and let  $i < k$ . If  $u$  is a boundary vertex, it is distinguishable from  $v$ , since  $0 = d_{H_1}(u, u) < d_{H_2}(u, v)$ . If  $u$  is not a boundary vertex, and  $u = p$ , then for any boundary vertex  $r \in \partial(C_i)$ ,  $d_{H_2}(r, v) = d_{H_2}(r, p) + d_{H_2}(p, q) + d_{H_2}(q, v) \geq d_{H_1}(r, p) + d_{H_2}(p, q) > d_{H_1}(r, p)$ . Thus, the two distance vectors are not equal either. Now, we consider the case when  $u \neq p$ . If  $u$  is a boundary vertex for  $p$ , let  $u' = u$ . Otherwise, the shortest path between  $p$  and  $u$  in component  $C_i$  can be extended to a shortest path  $p - u'$  by Observation 1, such that  $u'$  is a boundary vertex of  $p$ . For a fixed shortest path  $p - u'$  we have  $d_{H_2}(u', v) = d_{H_2}(u', p) + d_{H_2}(p, q) + d_{H_2}(q, v) = d_{H_1}(u', u) + d_{H_1}(u, p) + d_{H_2}(p, q) + d_{H_2}(q, v) > d_{H_1}(u', u)$ , which completes the proof.  $\square$

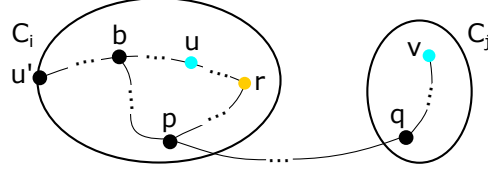


Figure 3.8: Proof of Theorem 14: Extending the shortest path  $r - u$  to a shortest path  $r - u'$ .

*Proof of Theorem 14.*

Let  $u, v \in V$  be any two different vertices, and let  $H_1, H_2$  be any two graphs from the set of possible graphs  $\mathcal{H}(F)$ . We need to show that for the set  $O = \cup_{i=1}^{k-1} O_i \cup S_k$ , where  $O_i = S_i \cup \partial(S_i)$ , the condition  $d_{H_1}(u, O) \neq d_{H_2}(v, O)$  holds for an arbitrary graph.

Let  $r \in S_i$  be a vertex from a resolving set of a component  $C_i$ . Once more, let  $u \in V(C_i), v \in V(C_j)$ , with  $i < k$ . Let  $p$  be the vertex in  $C_i$  and  $q$  the vertex in  $C_j$ , such that any path from a vertex in  $C_i$  to any vertex in  $C_j$  in  $H_2$  contains a subpath  $p - q$ , with  $d_{H_2}(p, q) \geq 1$ . As in the proof of Theorem 13, if  $u$  is a boundary vertex for  $r$ , let  $u = u'$ . Otherwise, by Observation 1, the shortest path between  $r$  and  $u$  in component  $C_i$  can be extended to a shortest path  $r - u'$ , with  $u'$  being a boundary vertex for  $r$ . We need to show that  $d_{H_1}(u, u') \neq d_{H_2}(v, u')$ , for any vertex  $v$  belonging to some other component  $C_j$  (as in the previous theorems, if  $u$  and  $v$  are in the same component, they are distinguishable by the resolving set of that component). If  $u$  is a boundary vertex itself, then we clearly have  $d_{H_1}(u, u') = 0 \neq d_{H_2}(v, u')$ , so we may assume  $u \neq u'$ . If  $r$  does not distinguish  $u$  and  $v$ , then  $d_{H_1}(u, r) = d_{H_2}(v, r) = d_{H_1}(p, r) + d_{H_2}(p, q) + d_{H_2}(q, v)$  and

$$d_{H_1}(u, r) > d_{H_1}(p, r), \quad (3.6)$$

holds, since  $d_{H_2}(p, q) \geq 1$ .

Case I: There exists a shortest path from  $u'$  to  $p$  in component  $C_i$  that passes through  $u$ . Hence there exists a shortest path from  $u'$  to  $v$  in  $H_2$  that passes through  $u$ . Then we have  $d_{H_2}(u', v) = d_{H_1}(u', u) + d_{H_1}(u, p) + d_{H_2}(p, v) > d_{H_1}(u', u)$ . Thus  $u$  and  $v$  have different distances to  $u'$ , and they are distinguishable.

Case II: All shortest paths from  $u'$  to  $p$  in component  $C_i$  do not pass through  $u$ . Hence no shortest path from  $u'$  to  $v$  in  $H_2$  passes through  $u$ . Let  $b$  be the vertex closest to  $u$  on this path, such that the path  $b - u'$  is common to both shortest paths  $p - u'$  and  $r - u'$ , as illustrated in Figure 3.8. Note that  $b$  might coincide with  $u'$ , but not with  $u$ . Also observe that since  $b$  is on the extension of a shortest path  $r - u$  to a shortest path  $r - u'$ , at least one shortest path  $r - b$  passes through  $u$ . Therefore, we have

$$d_{H_1}(r, u) + d_{H_1}(u, b) \leq d_{H_1}(r, p) + d_{H_1}(p, b). \quad (3.7)$$

Since (3.6) holds, from (3.7) it follows that

$$d_{H_1}(u, b) < d_{H_1}(p, b). \quad (3.8)$$

Now, from (3.8) and the fact that  $d_{H_2}(v, p) = d_{H_2}(v, q) + d_{H_2}(q, p) \geq 1$  we obtain

$$\begin{aligned} d_{H_2}(v, u') &= d_{H_2}(v, p) + d_{H_2}(p, b) + d_{H_2}(b, u') \\ &> d_{H_2}(v, p) + d_{H_2}(u, b) + d_{H_2}(b, u') \\ &> d_{H_1}(u, u'). \end{aligned}$$

Therefore,  $u$  and  $v$  have different distances to the boundary vertex  $u'$ , and they are thus distinguishable by a boundary vertex of a vertex belonging to the resolving set. The theorem follows.  $\square$

Inspecting the proofs of Theorems 9, 11, 12, we see that when comparing two vertices from  $C_i$  and  $C_j$ , in fact only the structure of  $C_i$  and its resolving set matters. Therefore, whenever one of the components of the observed disconnected graph  $F$  is a tree (cycle, or grid, respectively), then instead of including a resolving set and its boundary vertices, it is sufficient to choose all leaves in the case the component is a tree (two neighboring vertices together with a vertex at distance at least  $\frac{n-2}{2}$  from both of them in the case of the even cycle on  $n$  vertices, two vertices at distance  $\frac{n-1}{2}$  from each other in the case of an odd cycle on  $n$  vertices, and three corner vertices in the case of the grid, respectively). Note that this might be better than the bound claimed by Theorem 14, which for example in the case of the grid requires all four corner points to be chosen. Also, note that applying Theorem 14 to the case when all components are trees can yield exactly the results of Theorem 9. When a subset of leaves is selected as a resolving set of a tree component, then the resolving set and its boundary is precisely the set of all the leaves, hence Theorem 14 constructs a minimum cardinality extended resolving set.

In order to illustrate the tightness of the bound given by Theorem 14 on the cardinality of the smallest set that achieves unambiguous source localization in a partially known network, we performed the following simulations. Since the calculation of the true smallest set is computationally intensive even for modest network sizes, we have adapted Algorithm 1 as follows. For a partially known graph  $F \in \mathcal{F}(2)$ , we constructed all the possible graphs from the class of  $\mathcal{H}(F)$ . Then the set of pairs that need to be distinguished was set to the set of all possible pairs  $(i, j)$ , for  $i \neq j$ , across all possible graphs, i.e., node  $i$  in any graph  $H_1$  should be distinguishable from node  $j$  in any graph  $H_2$ , for  $H_1, H_2 \in \mathcal{H}(F)$ . Even this approximation algorithm has high memory and computation requirements. Then, such modified Algorithm 1 selects one by one a node that distinguishes the most node pairs across all possible topologies that can be constructed by adding an edge between two components of the graph. We have generated 200 graphs, where each graph

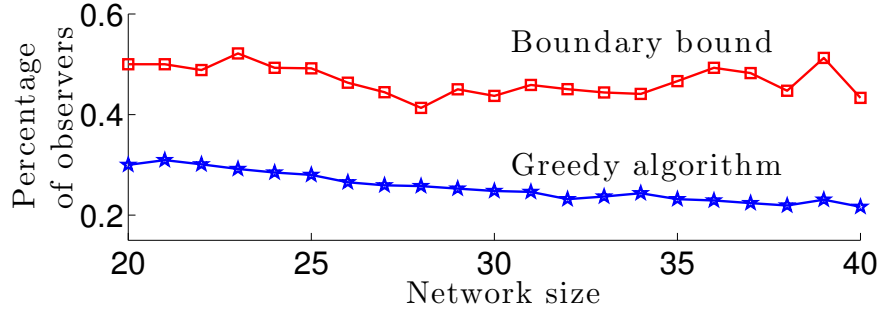


Figure 3.9: Performance of the boundary bound

comprises two Erdős-Rényi components, of random size  $n_i \in [10, 20]$  nodes, and with  $n_i p = 4$ , where  $p$  is the edge probability. For each graph, we found the observer set given by Theorem 14, where the boundary was determined of a (not necessarily the smallest) resolving set of each component, found by Algorithm 1, as, again, determining the exact metric basis was computationally too intensive. Also, for each graph, adapted Algorithm 1 was used to find an observer set that achieves network observability and we have averaged all the results for the same size networks. Figure 3.9 shows that the average percentage of observers selected by the bound is higher than by the greedy algorithm. However, unlike the latter, Theorem 14 does not require comparison of distance vectors through an exponential number of enumerated topologies, but can be applied in polynomial time.

### 3.2 Source localization using observed infection times

Source localization in a deterministic diffusion model without any additional uncertainties is a straightforward process of identifying a node whose distances to the observers match the infection times, as shown in Subsection 2.1.1. Once, the assumption of complete knowledge of network edges is relaxed, localizing the source becomes a challenging problem. Now, the number of possible topologies that are consistent with the partially known network can be very high as shown in Theorem 7. Source localization should be performed in each of one of those topologies in order to find the source node and topology consistent with the observed infection times. If a network is observable, as defined by Definition 2, then, the source localization would result in a single source candidate, otherwise, more than one node may fit the observed infection time. Next, we formulate the localization of a source in a partially known network  $F \in \mathcal{F}(k)$  as a binary integer linear program. Although the proposed approach is computationally very intensive, it does not require explicit enumeration of all the possible topologies from  $\mathcal{H}(F)$ , and source localization need not be performed for each topology individually. In our formulation, for each node  $s \in V$ , a multicommodity flow problem with side constraints [65] is formulated, assuming node  $s$  is the source, and the feasibility of the problem is

checked. If the problem is feasible, then a node  $s$  is a viable source candidate. A feasible solution implies that there exists a topology consistent with the known disconnected network, such that the distances from the assumed source to the observers are equal to the observed infection times. Assuming the optimization problem is feasible for a certain node, by solving it, we recover the topology. For some source candidates, there might exist more than one possible topology where the distances match the infection times. Solving the optimization problem gives us the structure of at most one such graph, as the main goal is to verify the possibility of a node being the source, and for this, the existence of a single topology is sufficient. Before stating the optimization problem, we introduce concepts and notation.

The incidence matrix  $\mathbf{B}$  of a graph with  $m$  edges and  $N$  nodes is an  $N \times m$  matrix defined as

$$[\mathbf{B}]_{ij} = \begin{cases} 1, & \text{node } i \text{ is the head of the edge } j \\ -1, & \text{node } i \text{ is the tail of the edge } j \\ 0, & \text{otherwise} \end{cases} .$$

As we are considering undirected graphs, the direction of the edges can be set arbitrarily, as later we will consider each edge twice, once in each direction, as it is typically done for similar network optimization problems [65]. Let us denote with  $E^p$  a set of all possible missing edges, those between nodes of different components. With  $\mathbf{B}_{ext}$  we denote an extended incidence matrix, where the edges are from the set of known edges  $E$ , as well as from the set of possible missing edges  $E^p$ . With  $\tilde{\mathbf{B}} = [\mathbf{B}_{ext}, -\mathbf{B}_{ext}]$  we denote an incidence matrix, where we consider all the edges of  $\mathbf{B}_{ext}$  in both directions. The set  $E_j$  is a set of edges that are incident with the observer  $j$ , and similarly, the set  $E_s$  is a set of edges that are incident with the assumed source  $s$ . The set of edges that connect components  $C_a$  and  $C_b$  is denoted as  $E_{a,b}$ , for  $a, b = 1, \dots, k$  and  $a \neq b$ . An optimization variable in our formulation is a binary vector,  $\mathbf{x} \in \mathbb{R}^m$ , whose  $i$ -th entry is set to 1 if edge  $i$ , from the matrix  $\mathbf{B}_{ext}$ , is selected to be a part of the final constructed topology. For each observer node  $j$ , an auxiliary binary optimization variable  $\mathbf{x}_j \in \mathbb{R}^{2m}$  is used to construct a path between the observer  $j$  and an assumed source  $s$ . If  $i$ -th entry of  $\mathbf{x}_j$  equals 1, then this implies that edge  $i$  from matrix  $\tilde{\mathbf{B}}$  is a part of the constructed path. The infection time of the observer node  $j$  is denoted as  $t_j$ . With  $\mathbf{1}$  we denote a vector where all entries are equal to 1, while  $\mathbf{e}_i$  denotes a column vector where all entries are equal to 0 except for the  $i$ -th entry, which equals 1. The matrix  $\mathbf{J}$  has the structure  $[\mathbf{I}_m, \mathbf{I}_m]$ , where  $\mathbf{I}_m$  is an identity matrix of size  $m$ . Finally, we state a binary integer program that verifies whether a node  $s$  could be the source of diffusion for the observed infection times.

$$\min \mathbf{1}^T \mathbf{x} \tag{3.9}$$

subject to

$$\tilde{\mathbf{B}}\mathbf{x}_j = \mathbf{e}_j - \mathbf{e}_s \quad (3.10)$$

$$\mathbf{1}^T \mathbf{x}_j = t_j \quad (3.11)$$

$$\mathbf{J}\mathbf{x}_j \leq \mathbf{1} \quad (3.12)$$

$$\sum_{p \in E_j} \mathbf{e}_p^T \mathbf{J}\mathbf{x}_j \leq 1 \quad (3.13)$$

$$\sum_{p \in E_s} \mathbf{e}_p^T \mathbf{J}\mathbf{x}_j \leq 1 \quad (3.14)$$

$$\mathbf{J}\mathbf{x}_j \leq \mathbf{x} \quad (3.15)$$

$$\sum_{o \in O} \mathbf{J}\mathbf{x}_o \geq \mathbf{x} \quad (3.16)$$

$$\mathbf{x} \leq \mathbf{1} \quad (3.17)$$

$$\sum_{p \in E_{a,b}} \mathbf{x}^T \mathbf{e}_p \leq 1 \quad (3.18)$$

$$\sum_{p \in E^p} \mathbf{x}^T \mathbf{e}_p \leq k - 1 \quad (3.19)$$

$$\mathbf{x}_j \in \{0, 1\}^{2m} \quad (3.20)$$

$$\forall j = 1, \dots, r$$

$$\forall a, b = 1, \dots, k, a \neq b.$$

With the constraint (3.10), a path between each observer node  $j$  and the assumed source  $s$  is constructed, by selecting the edges from the incidence matrix which includes all the existing and all additional possible edges in both directions [65]. The constraint (3.11) makes the length of such path exactly equal to the infection time. Each observer - source path should not include the same edge in two different directions, as we are looking for the shortest path between two nodes, and this is set by (3.12). For the same reason, the observer  $j$  and the source  $s$  should only be the terminal points of the path, which is constrained by (3.13) and (3.14), respectively. The paths are directed from the observers to the source, and therefore constructed from the edges of matrix  $\tilde{\mathbf{B}}$ , which includes each edge in both directions. However, the goal is to construct an undirected topology from the union of these paths, hence, a direction of the edge should be disregarded. By (3.15)–(3.17), an edge is used in the final topology if it is in at least one observer-source path, regardless of the direction in which it was used. Thus, the dimension of  $\mathbf{x}$ , a variable that represents edges in the final topology is only half of the dimension of the variables  $\mathbf{x}_j$  that represent the paths. Constraint (3.18) ensures

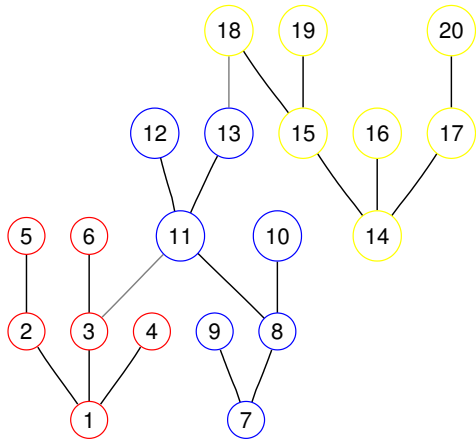
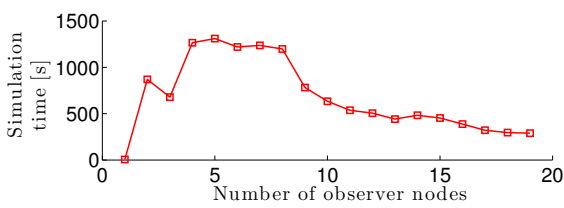


Figure 3.10: A tree network of 20 nodes with two unobserved edges. The edge between nodes 3 and 11, and the edge between nodes 13 and 18 are not known, hence, the observed graph is disconnected, with 3 components. Each component is labeled with a different color.

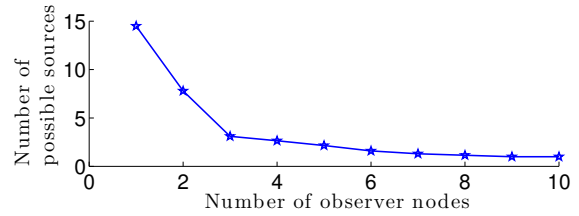
that the constructed union of paths contains at most one edge that connects two components, in order to avoid inter-component loops. Since there are  $k$  components, at most  $k-1$  edges can be added from the set of all the possible edges, and this is the role of the constraint (3.19). Finally, (3.20) constrains the variables  $x_j$  to be binary. Explicit enforcement for the binary structure of  $x$  is not necessary, as it is formed through constraints (3.15)–(3.17) on binary variables  $x_j$ .

The number of nodes and topologies that match the observed times and network structure depend on the number of missing edges, the placement of observers and the source. If a network is not observable, the proposed program (3.9) will be feasible for more than one node, and this is not related to the proposed approach. However, the proposed approach itself can also contribute to the number of false candidates. Although constraints (3.13) and (3.14) prevent loops around terminal points in the observer-source paths and constraint (3.18) limits the number of inter-component edges, still paths could include some loops, for example in the case where there are components with no observers. In such a case a node might be falsely classified as feasible.

We illustrate the effect of the number of observers on the source localization problem for a tree network of 20 nodes with only 2 unobserved edges shown in Figure 3.10. From this partially known tree, 5,880 trees can be constructed by adding 2 edges. We have used GNU Linear Programming Kit (GLPK) package, that is intended for solving large-scale programming, to solve the proposed optimization program (3.9). The total time needed to verify the feasibility of the linear binary program (3.9) for each node in a network was recorded, as well as the number of nodes for which the problem was feasible. These results were averaged over all possible sources and simulations were repeated for different numbers of observers, selected from each of the 3 components sized 6, 7 and 7 nodes. During selection, priority was given to 11 leaves. Figure 3.11a shows that initially the time needed to solve (3.9) dramatically grows with the number of observers, while Figure 3.11b shows an opposite trend in the number of possible solutions. Initially, with almost no constraints, a tree consistent with the observations can quickly be constructed for many nodes. Including



(a) Time required to solve (3.9)



(b) Number of possible solutions to (3.9)

Figure 3.11: The effect of the number of observers on the optimization problem (3.9) for a 20 node tree with two unobserved edges.

more observers increases the number of constraints and more time is needed to find such a tree or to conclude that the problem is unfeasible. The rate by which the number of suspects decreases with the number of observed leaves dramatically drops after including, at least, one node from each component. When the number of observers reaches 9, the network becomes observable. Around that point, correspondingly, the solving time starts to decrease with the number of observers. Now, only one node can be the source suspect, and for all the other nodes, the problem can relatively quickly be classified as unfeasible due to an increasing number of constraints.

### 3.3 Summary

In this Chapter, we have analyzed the observer selection problem, again for a deterministic diffusion model, but this time allowing partial knowledge of network topology. Often, the structure of local communities is well known, while the connections between different communities are unknown, as it may be a weak connection or a random contact. Hence, we have studied source localization problem in a graph, where the edges in each connected components are known, but not the edges that connect different components. We have extended the concept of network observability in this context to denote the ability to disambiguate the source based on the infection times of the observers, even without knowing the full diffusion graph. We have shown that the number of connected graphs that can be constructed by connecting  $k$  components with  $k - 1$  edges scales exponentially with the number of components. Therefore, we did not analyze the observability problem in each of these topologies separately.

In Subsection 3.1.1, we have presented necessary and sufficient conditions for the smallest set of observers that makes a network observable, when the components are all trees, complete graphs, grids or cycles. When the components are of an arbitrary structure, in Section 3.1.2, we presented a way, based on the concept of graph boundary, to select observers such that the network becomes observable. For some special graphs, like trees and grids, the cardinality of the set of observers selected based on the presented condition is minimum, or close to a minimum. However, the simulation results on Erdős-Rényi graphs illustrated that this cardinality

can also be far from the smallest. Still, construction of such a set can be done easily, in polynomial time.

In Section 3.2, we have addressed the problem of source localization in partially known graphs. We have formulated a binary integer linear program, whose feasibility should be verified  $N$  times, each time assuming a different node to be the source. Each node for which the proposed optimization problem is feasible represents a source candidate. Although binary integer linear program is computationally very intensive, the proposed formulation does not require explicitly enumerating an exponential number of topologies that are compatible with the partially known network.



## Chapter 4

# Node selection for stochastic infection times

In this chapter, we address the observer selection problem in the presence of uncertainty in the infection times. In Chapters 2 and 3, we have assumed that there is no uncertainty in the observations, and the *observed* infection times match the *true* times of infection. The time taken by a node to infect its neighbor was considered a known constant, and there was no observation noise. Now, we relax these assumptions, and analyze separately three different diffusion scenarios, either modeling the propagation delay along the edges between two neighboring nodes as a random variable, as it is done in Subsection 4.1.2, or still considering the delay to be a constant, but introducing observation noise, as it is done in Subsections 4.1.3 and 4.1.4. Due to uncertainty in the observations, disambiguation of the source now cannot be guaranteed and instead the error probability of source localization needs to be considered. As the choice of observers also influences the source localization process, a question of interest is identifying the subset of observers that would minimize the error probability. However, obtaining an exact analytical expression for error probability is generally not a tractable problem, and, therefore, finding an optimal subset of observers that minimizes this error is not feasible.

Instead, in Subsection 4.1, we present a metric that acts as a surrogate for error probability and could be used to compare the performance of different subsets of observers in source localization, considering that all observers are selected at the same time. We apply the large deviations approach to derive error exponents that characterize the asymptotic behavior of the error probability of source localization. The analyzed asymptotics refers not to an increasing number of observations, but to vanishing uncertainty. In the settings that we consider, the number of observations is limited, as each observation comes from a different node, and the number of nodes in a network is fixed and finite. Hence, we evaluate the rate of error decay as uncertainty in the observations decreases and use it as a tool for comparison of observer subsets. Subset

selection based on this criterion is optimal from the perspective of fastest error decay when randomness decreases. However, as we show in Subsection 4.1.5, simulation results illustrate that the proposed metric is also very useful in a more realistic setting for non-negligible noise, as those subsets characterized by a higher error exponent generally yield lower error probability than others.

The metric that we develop in Subsection 4.1 can also be used for other applications. One of them is defense of networks, a very active research field as networks are subject to various forms of attacks [66, 67]. Even if the network nodes include their sender identification in the messages, this can be forged in order to conceal the true identity of the sender, which may send malicious packets. Hence, when designing a network, it may be useful to compare different topologies regarding their ability to identify the sender node. Assuming there are certain points in the network where packets are examined and the identity of any flagged packet is ascertained based on the packet arrival times, different topologies may yield different error probabilities. Since calculating the error probability is not feasible, there is a need for a surrogate metric for selecting topologies, which is exactly the metric that we propose. In another potential application, the goal is to preserve the anonymity of the sender [68]. If an individual, like a whistleblower or an activist, needed to publish online certain information, knowing that some sites are monitored, an important question would be from which site to post this sensitive information in order to preserve anonymity. Even though the identity of the sender may be forged, an additional level of anonymity may be introduced by the sender by publishing from a point in the network that gives the most uncertainty in sender localization based on the message arrival times. Our theoretically based metric provides an effective means of assessing which nodes are harder to pinpoint for a given network and defined monitoring points.

In Section 4.2, we return to the problem of dynamic observer selection, but now in a stochastic setting. We propose a sequential algorithm for source localization and apply a criterion developed for deterministic infection times. We demonstrate the applicability of the localization algorithm and the merit of the criterion for observer selection on a real-world data set of a cholera outbreak in Subsection 4.2.1.

## 4.1 Block selection

When the infection times are stochastic, even if the infection times of all the nodes are available, there is a certain level of error probability associated with source localization which depends on the stochasticity of observations. Now, if observations are available from only a subset of nodes, the error probability not only depends on the uncertainty in the infection times, but also on the choice of observers, whose infection times are used to localize the source. Hence, in this setting, identifying which observers lead to a low error probability of source localization becomes an important issue. For stochastic infection times, not only the combinatorial aspect of this problem makes this task challenging, but also the absence of a general expression

for the error probability. Since deriving an expression for error probability is typically not tractable, we need to develop a substitute metric, related to the error probability, yet analytically tractable.

Motivated by asymptotic analysis of error probability in multiple hypothesis testing, we also resort to the asymptotic study of error probability. However, a common approach in the asymptotic analysis is a characterization of the behavior of error probability as the number of observation keeps increasing. Then, the rate of error probability decay for an asymptotically large number of observations is derived [69]. However, for the problem of observer selection, this approach is not applicable, as each new observation represents a new observer, and, in our case, the number of observers is fixed, and the impact of a particular set of observers on error probability is exactly what needs to be evaluated, relative to some other set of observers. Another approach for asymptotic analysis in networks is considering a growing sequence of graphs whose number of nodes tends to infinity [70]. Analysis for growing number of nodes is performed for graph classes such as wireless ad-hoc networks [71] or randomly growing graphs [70], where the graph grows according to a specific rule: either all nodes are uniformly distributed and have the same range for connection, or each new node connects to a fixed number of randomly chosen nodes, with a probability of a connection to an old node depending on its degree. Applying this type of graph - growing analysis to our observer selection problem comes with an issue of how to keep increasing the graph, such that it reflects the error probability even though the number of observations is fixed and the number of potential sources is asymptotically increasing. Depending on how new nodes are added, graph distances between observers and all the other nodes are changing accordingly, which in turn affects the observers' infection times and, consequently, the error probability. Therefore, in order to avoid this issue, we resort to a different type of asymptotic analysis, where the number of observers is fixed and the topology is preserved while the uncertainty is the one that is asymptotically decreasing. We analyze how the error probability decreases as the uncertainty in the observations diminishes and evaluate the rate of this decrease in error probability. For each subset of observers of interest, we determine the rate of change in error probability, considering that the observations are becoming decreasingly random or noisy, and then we use the obtained rate to compare different subsets. The observer subset with a higher rate achieves a faster decrease in error probability as uncertainty in the observations decreases, compared to a subset with a lower rate.

Before we can apply the asymptotic analysis, we frame source localization as multiple hypothesis testing, where for each node in a network we have a different hypothesis. A hypothesis  $H_s$  corresponds to the assumption that node  $s$  is the actual source. Then the error probability of choosing the wrong hypothesis corresponds to the probability of localizing the source incorrectly, which is exactly what we wish to analyze. Let us fix the subset of observer nodes  $O$  and denote with  $\mathbf{x}$  the observations from the set  $O$ . This might, for example, correspond to a vector of infection times of nodes from the set  $O$ . The probability distribution associated with each hypothesis  $H_s$  is the conditional probability density of observations  $p(\mathbf{x}; s)$  given that

node  $s$  is the source. Without any prior knowledge of the source position, we assume that all network nodes are equally likely source candidates and hence, each hypothesis has the same prior probability  $\pi = 1/N$ . The maximum a posteriori probability decision rule minimizes the Bayesian probability of error, and in our case of uniform priors, it corresponds to the maximum likelihood estimator [69]. As discussed before, the corresponding probability of error is typically difficult to calculate and usually not tractable. Consequently, determining the subset of observers that globally minimizes the error is generally not analytically feasible. Instead, to guide us in the selection process of observers that would lead to the lowest error probability of source localization, we analyze asymptotic behavior or error probability. We will show that for the class of distributions that we consider, the error probability achieves exponential decay with decreasing uncertainty. Then, the metric that we will use to compare performances of different observer subsets is the value of the exponent, i.e., the rate of exponential decay.

Currently in the literature, the strategies for observer selection are based on centrality measures [5, 6, 10, 11], which take into consideration how central a node is within a given topology. As we show in later subsections, our proposed metric, based on exponents, encompasses not only the effect of topology, but also depends on the parameters of propagation. As uncertainty vanishes, infection times become deterministic, and even in this setting, centralities are not optimal selection strategies. Instead, as we have showed in Chapter 2, the concept of a resolving set is what plays a crucial role for observer selection. We will show experimentally, in Subsection 4.1.5, that even for non-zero level of uncertainty, using exponents as selection criterion leads to lower error probability than using centrality measures, even though exponents are derived for vanishing uncertainty.

#### 4.1.1 A general framework for deriving error exponents

In this subsection, we derive a general framework for evaluating the error exponents that control the decrease of error probability as the uncertainty in the observations vanishes. First, we will prove the main steps, and then, we complete the proofs for specific diffusion models, in subsequent subsections. The class of distributions that we consider is of the form

$$p(\mathbf{x}; i) = h(\eta)e^{-\frac{1}{\eta}g(\mathbf{x}, \mathbf{a}^i)}, \quad (4.1)$$

for  $i = 1, \dots, N$ , which belong to a wider class of elliptical distributions [72] and includes the most commonly used distributions: Gaussian, Laplace and exponential. Here  $\eta$  is the noise parameter such that the uncertainty decreases when  $\eta \rightarrow 0$ . We have that  $h(\eta)$  is a function with  $\eta \log(h(\eta)) \rightarrow 0$  for  $\eta \rightarrow 0$  and  $g(\mathbf{x}, \mathbf{a}^i)$  is a non-negative, continuous, function of  $\mathbf{x}$  that equals zero only when  $\mathbf{x} = \mathbf{a}^i$ . In the case of Gaussian distribution  $\mathcal{N}(\mu_i, \sigma^2)$ ,  $\eta$  represents the variance  $\sigma^2$ ,  $\mathbf{a}^i$  is the mean  $\mu_i$  and  $g(\mathbf{x}, \mathbf{a}^i)$  corresponds to  $\frac{(\mathbf{x}-\mu_i)^2}{2}$ .

In a binary hypothesis case, the error probability of the maximum-likelihood estimator,  $P_e$ , is bounded as

$$P_e \leq \int \left( \frac{1}{\pi} p(\mathbf{x}; k) \right)^\alpha \left( \frac{1}{\pi} p(\mathbf{x}; l) \right)^{1-\alpha} d\mathbf{x}, \quad (4.2)$$

for  $0 \leq \alpha \leq 1$  [69]. Extending to the multiple hypothesis case, the bound on the overall error probability is

$$P_e \leq \sum_{k=1}^N \sum_{l>k} P_e(k, l) = \sum_{i=1}^N \sum_{j>i} e^{\log P_e(k, l)}, \quad (4.3)$$

where  $P_e(k, l)$  is the pairwise error probability for hypotheses  $H_k$  and  $H_l$ , bounded as shown in (4.2). Let us denote with  $c_\alpha(k, l, \eta)$  the  $\alpha$ -Chernoff divergence between two distributions  $p(\mathbf{x}; k)$  and  $p(\mathbf{x}; l)$  [73]

$$c_\alpha(k, l, \eta) = -\log \int p(\mathbf{x}; k)^\alpha p(\mathbf{x}; l)^{1-\alpha} d\mathbf{x}. \quad (4.4)$$

The maximum value attained for  $0 \leq \alpha \leq 1$  represents the Chernoff distance between two distributions and it does not always have a closed form expression

$$C(k, l, \eta) = \max_{0 \leq \alpha \leq 1} c_\alpha(k, l, \eta). \quad (4.5)$$

For each specific value of noise parameter  $\eta$ , the corresponding Chernoff distance might be different, and we highlight this dependence explicitly in  $C(k, l, \eta)$ . We can rewrite (4.3) as

$$P_e \leq \frac{1}{N} \sum_{k=1}^N \sum_{l>k} e^{-C(k, l, \eta)}. \quad (4.6)$$

Let us denote with  $\gamma(k, l)$  the following limit

$$\gamma(k, l) = \lim_{\eta \rightarrow 0} \frac{C(k, l, \eta)}{1/\eta}. \quad (4.7)$$

The existence of the limit is shown in the next sections for three popular noise models. Let  $(i, j)$  be a pair of nodes such that the limit  $\gamma(k, l)$  is the lowest, i.e.,

$$\gamma(i, j) = \min_{(k, l)} \gamma(k, l). \quad (4.8)$$

The choice of a node pair  $(i, j)$  does not depend on the value of  $\eta$ , and there might be more than one pair of nodes that minimize (4.7). Applying the results of Lemma 15 below, we will show that  $\gamma(i, j)$  upper bounds

the error exponent as

$$\lim_{\eta \rightarrow 0} \frac{\log P_e}{1/\eta} \leq -\gamma(i, j). \quad (4.9)$$

**Lemma 15.** *Let the following inequality hold*

$$P_e(t) \leq \kappa \sum_{i=1}^n e^{-\beta_i(t)}, \quad (4.10)$$

where  $\kappa$  is a constant. If the functions  $\beta_i(t)$  exhibit an asymptotic linear growth, i.e., the following limits exist

$$\beta_i = \lim_{t \rightarrow \infty} \frac{\beta_i(t)}{t} \geq 0, \quad (4.11)$$

then the following inequality holds

$$\overline{\lim}_{t \rightarrow \infty} \frac{\log(P_e(t))}{t} \leq -\beta_p, \quad (4.12)$$

where  $\beta_p = \min\{\beta_1, \dots, \beta_n\}$ .

*Proof.* Since (4.11) holds, we can rewrite  $\beta_i(t)$  as

$$\beta_i(t) = \beta_i t + b_i(t), \quad (4.13)$$

where  $b_i(t)$  is a sublinear function for which  $\lim_{t \rightarrow \infty} \frac{b_i(t)}{t} = 0$  holds. Now, plugging (4.13) into (4.10), and we have

$$P_e(t) \leq \kappa \sum_{i=1}^n e^{-\beta_i t - b_i(t)}. \quad (4.14)$$

From here, we have

$$\begin{aligned} \frac{\log(P_e(t))}{t} &\leq \frac{\log(\kappa)}{t} + \frac{1}{t} \log \left( \sum_{i=1}^n e^{-\beta_i t - b_i(t)} \right) \\ &= \frac{\log(\kappa)}{t} + \frac{1}{t} \log \left( e^{-\beta_p t} \sum_{i=1}^n e^{-(\beta_i - \beta_p)t - b_i(t)} \right) \\ &= \frac{\log(\kappa)}{t} - \beta_p + \frac{1}{t} \log \left( \sum_{i=1}^n e^{-(\beta_i - \beta_p)t - b_i(t)} \right) \\ &\leq \frac{\log(\kappa)}{t} - \beta_p + \frac{1}{t} \log \left( \sum_{i=1}^n e^{-b_i(t)} \right), \end{aligned} \quad (4.15)$$

where the last inequality of (4.15) holds since  $\beta_p \leq \beta_i$ , for all  $i$ . Next, we will apply the following generic

inequality to (4.15)

$$\begin{aligned}
\log(A_1 + \dots + A_n) &\leq \log(n \max\{A_1, \dots, A_n\}) \\
&= \log(n) + \max\{\log(A_1), \dots, \log(A_n)\} \\
&\leq \log(n) + \max\{|\log(A_1)|, \dots, |\log(A_n)|\} \\
&\leq \log(n) + |\log(A_1)| + \dots + |\log(A_n)|.
\end{aligned}$$

Now, we obtain

$$\frac{\log(P_e(t))}{t} \leq \frac{\log(\kappa)}{t} - \beta_p + \frac{\log(n)}{t} + \sum_{i=1}^n \frac{|b_i(t)|}{t},$$

to which we apply  $\overline{\lim}_{t \rightarrow \infty}$  and prove the claim.  $\square$

Using (4.6) in place of (4.10), substituting  $1/\eta$  for  $t$ ,  $1/N$  for  $\kappa$ , indices  $k, l$  for  $i$  and  $C(k, l, \eta)$  for  $\beta_i(t)$ , provided that limits (4.7) exist— as we will later show — we can obtain the upper bound (4.9). With this we establish that  $\gamma(i, j)$  defined in (4.8) upper bounds our error exponent.

In order to claim that the exponent exactly equals  $\gamma(i, j)$ , we also need to establish a lower bound

$$\lim_{\eta \rightarrow 0} \frac{\log(P_e)}{1/\eta} \geq -\gamma(i, j). \quad (4.16)$$

Let  $P(e|H_s)$  denote the probability of an error given that hypothesis  $H_s$  is true. Then, we have

$$\begin{aligned}
P(e) &= \sum_{s=1}^N P(e|H_s)P(H_s) = \frac{1}{N} \sum_{s=1}^N P(e|H_s) \\
&\geq \frac{1}{N} P(e|H_i) \geq \frac{1}{N} \int_{\Omega_{ij}} p(\mathbf{x}; H_i) d\mathbf{x}
\end{aligned} \quad (4.17)$$

where  $\Omega_{ij} = \{\mathbf{x} : p(\mathbf{x}; H_i) \leq p(\mathbf{x}; H_j)\}$  defines a region of error where  $H_j$  is selected even though  $H_i$  is the true hypothesis. Then, plugging (4.17) into (4.16), the lower bound that we need to show becomes

$$\lim_{\eta \rightarrow 0} \eta \log \left( \frac{1}{N} \int_{\Omega} p(\mathbf{x}; H_i) d\mathbf{x} \right) \geq -\gamma(i, j), \quad (4.18)$$

for some region of error  $\Omega \subseteq \Omega_{ij}$ .

Before we state the Lemma needed to establish this lower bound, we introduce the necessary notation.

Let  $\text{vol}(S)$  denote the volume of a set  $S$  and we define a function  $f(\mathbf{a}, \Omega)$  as

$$f(\mathbf{a}, \Omega) = \inf \{g(\mathbf{x}, \mathbf{a}) \mid \mathbf{x} \in \Omega\}, \quad (4.19)$$

where again  $g(\mathbf{x}, \mathbf{a})$  is a non-negative function for  $\mathbf{x} \in \Omega$  and any  $\mathbf{a}$ , and  $g(\mathbf{x}, \mathbf{a}) = 0$  for  $\mathbf{x} = \mathbf{a}$ .

We also define a set  $\mathcal{R}$  that includes all the points  $\mathbf{x}$  where  $g(\mathbf{x}, \mathbf{a})$  is bounded as

$$\mathcal{R}(\ell, \ell + \epsilon) = \{\mathbf{x} : \ell < g(\mathbf{x}, \mathbf{a}) < \ell + \epsilon\}. \quad (4.20)$$

Now we state the lemma that proves the lower bound for the error exponent (4.18).

**Lemma 16.** *If the following holds*

$$P_e \geq h(\eta) \int_{\Omega} e^{-\frac{1}{\eta}g(\mathbf{x}, \mathbf{a})} d\mathbf{x}, \quad (4.21)$$

where  $\Omega$  is a set such that

i)  $\mathbf{a} \notin \Omega$

ii) for every  $\epsilon > 0$ , and for  $l = f(\mathbf{a}, \Omega)$

$$\text{vol}(\Omega \cap \mathcal{R}(l, l + \epsilon)) > 0, \quad (4.22)$$

and  $h(\eta)$  is a function such that

$$\lim_{\eta \rightarrow 0} \eta \log(h(\eta)) = 0, \quad (4.23)$$

then the following bound holds

$$\lim_{\eta \rightarrow 0} \frac{\log(P_e)}{1/\eta} \geq -f(\mathbf{a}, \Omega).$$

*Proof.* Let us first fix  $\epsilon > 0$ . Since (4.21) holds, we have

$$\begin{aligned} P_e &\geq h(\eta) \int_{\Omega \cap \mathcal{R}(l, l + \epsilon)} e^{-\frac{1}{\eta}g(\mathbf{x}, \mathbf{a})} d\mathbf{x} \\ &\geq h(\eta) \int_{\Omega \cap \mathcal{R}(l, l + \epsilon)} e^{-\frac{1}{\eta}(l + \epsilon)} d\mathbf{x} \end{aligned} \quad (4.24)$$

$$= h(\eta) e^{-\frac{1}{\eta}(l + \epsilon)} \text{vol}(\Omega \cap \mathcal{R}(l, l + \epsilon)), \quad (4.25)$$

where (4.24) holds since  $g(\mathbf{x})$  at any point in a set  $\mathcal{R}(l, l + \epsilon)$  is at most  $l + \epsilon$ , as defined by (4.20). Next, we

apply the limit and logarithm to (4.25) to obtain

$$\begin{aligned} \lim_{\eta \rightarrow 0} \frac{\log(P_e)}{1/\eta} &\geq \lim_{\eta \rightarrow 0} \left( \eta \log(h(\eta)) - \frac{1}{\eta}(l + \epsilon) \right. \\ &\quad \left. + \eta \text{vol}(\Omega \cap \mathcal{R}(l, l + \epsilon)) \right) \geq -(l + \epsilon). \end{aligned} \quad (4.26)$$

The last step of (4.26) holds due to the assumptions (4.22) and (4.23). Since (4.26) holds for any  $\epsilon > 0$ , now we take  $\epsilon \rightarrow 0$  which yields exactly our claim

$$\lim_{\eta \rightarrow 0} \frac{\log(P_e)}{1/\eta} \geq -l = -f(\mathbf{a}, \Omega). \quad (4.27)$$

□

In Lemma 16 we have shown that we can lower bound the error exponent for vanishing noise in terms of a function  $f(\mathbf{a}, \Omega)$  defined as (4.19). Using the results from the following Lemma, we will replace the set  $\Omega$  in the bound by its closure.

**Lemma 17.** *Let  $f(\mathbf{a}, \Omega)$  be a function defined as in (4.19). If  $g(\mathbf{x}, \mathbf{a})$  is a continuous function on  $\Omega$ , and  $\overline{\Omega}$  is a closure of the set  $\Omega$ , then  $f(\mathbf{a}, \Omega) = f(\mathbf{a}, \overline{\Omega})$ .*

*Proof.* Since  $\overline{\Omega} \supseteq \Omega$ , the following inequalities hold

$$f(\mathbf{a}, \overline{\Omega}) = \inf_{\mathbf{x} \in \overline{\Omega}} g(\mathbf{x}) \leq \inf_{\mathbf{x} \in \Omega} g(\mathbf{x}) = f(\mathbf{a}, \Omega).$$

Now we show the inequality  $f(\mathbf{a}, \overline{\Omega}) \geq f(\mathbf{a}, \Omega)$  by contradiction. Suppose that  $f(\mathbf{a}, \overline{\Omega}) < f(\mathbf{a}, \Omega)$ . Then there is a  $\bar{\mathbf{x}} \in \overline{\Omega} \setminus \Omega$  such that  $\inf_{\mathbf{x} \in \overline{\Omega}} g(\mathbf{x}, \mathbf{a}) < g(\bar{\mathbf{x}}, \mathbf{a}) < \inf_{\mathbf{x} \in \Omega} g(\mathbf{x}, \mathbf{a})$ , as  $g(\bar{\mathbf{x}}, \mathbf{a})$  is a continuous function. Therefore, we can find a  $\delta > 0$  such that the ball centered at  $\bar{\mathbf{x}}$  of radius  $\delta$  is contained inside  $\overline{\Omega} \setminus \Omega$ . However,  $\overline{\Omega} \setminus \Omega$  is the boundary of  $\Omega$  and by definition contains no interior points, so we arrive at a contradiction, and prove the claim. □

Now, based on the results of Lemma 17, we can further bound the error exponent from (4.27) as

$$\lim_{\eta \rightarrow 0} \frac{\log(P_e)}{1/\eta} \geq -f(\mathbf{a}, \overline{\Omega}). \quad (4.28)$$

Next, for a set  $\overline{\Omega}$  which is the closure of the set  $\Omega = \{\mathbf{x} : p(\mathbf{x}; i) < p(\mathbf{x}; j)\}$  if we show that the solution

of the minimization problem

$$\begin{aligned} \min_{\mathbf{x}} \quad & g(\mathbf{x}, \mathbf{a}^i) \\ \text{s.t.} \quad & \mathbf{x} \in \overline{\Omega}, \end{aligned} \tag{4.29}$$

exactly equals  $\gamma(i, j)$ , we can establish the lower bound (4.16). This is because Lemma 16 and 17 prove that the error exponent is lower bounded by  $f(\mathbf{x}, \overline{\Omega})$ , which is by definition the minimum of  $g(\mathbf{x}, \mathbf{a})$  for  $\mathbf{x} \in \overline{\Omega}$ . Then, showing that this same minimum equals  $\gamma(i, j)$  completes the proof that the error exponent is indeed lower bounded by  $\gamma(i, j)$ . Once we establish this, together with the upper bound (4.9), we have that the error exponent exactly equals our  $\gamma(i, j)$ . In the following section, for three different propagation models we complete these steps and derive exact expressions for the exponents. In these propagation models, infection times are modeled as either Gaussian, Laplace or exponential random variables. Although the details of derivation of the exponents are quite specific, the proofs follow the same general steps:

- $\alpha$ -Chernoff divergence from (4.4) is evaluated
- Chernoff distance as the maximum of  $\alpha$ -Chernoff divergence for  $0 \leq \alpha \leq 1$  is calculated
- $\gamma(k, l)$  is evaluated as (4.7), and  $\gamma(i, j)$  is defined as (4.8)
- The error exponent is upper bounded with  $\gamma(i, j)$  using the result of Lemma 15
- The error exponent is lower bounded with  $f(\mathbf{a}, \Omega)$  by applying Lemma 16, where  $f(\mathbf{a}, \Omega)$  is defined as (4.19)
- The closure of set  $\Omega$  is determined and the error exponent is lower bounded with  $f(\mathbf{a}, \overline{\Omega})$  by applying Lemma 17
- The value of  $f(\mathbf{a}, \overline{\Omega})$  is shown to be exactly equal to  $\gamma(i, j)$  using duality
- The error exponent is then lower bounded with  $\gamma(i, j)$ , since it is bounded by  $f(\mathbf{a}, \Omega)$  which equals  $\gamma(i, j)$
- The error exponent exactly equals  $\gamma(i, j)$ , since it is both lower and upper bounded by it

When the infection times are modeled as exponential random variables, derivation of  $\gamma(k, l)$  is more straightforward, while for other models, derivation is more involved. Application of Lemma 16 in Gaussian propagation model is again not straightforward and requires additional analysis, as set  $\Omega$  depends on the parameter  $\eta$ , unlike in the other two models. In Laplace model, the closure of set  $\Omega$  is not as intuitive as in other models, hence the duality result is established through multiple steps.

### 4.1.2 Observations are modeled as Gaussian random variables

In the first scenario that we analyze, we model the time taken for node  $u$  to infect its neighbor  $v$  along the edge  $u - v$ , i.e.,  $\theta_{u,v}$ , as a Gaussian random variable. Traditionally, in epidemic modeling, this propagation delay along the edges is taken to be a variable with exponential distribution [12]. However, in some recent work [5, 33, 40], this propagation time is approximated by a Gaussian variable. The central limit theorem is invoked for this approximation, as the infection time of an observer is a sum of the propagation times along the edges of the shortest path between the source and observer. As the infection times can be approximated with a Gaussian variable, then the individual propagation delays are also modeled as a Gaussian variable. We will also follow this reasoning. Hence, we assume that  $\theta_{uv}$ , for all  $u, v$  pairs where  $u$  and  $v$  are connected by an edge, are independent, identically distributed random variables with Gaussian distribution  $\mathcal{N}(\mu, \sigma^2)$  [5].

We assume that the underlying network is a tree, a graph with no cycles. Unlike general graphs, trees are tractable, as there is only a single path between any pair of nodes. For a general network, tree-based analysis is again used [4, 5, 8, 10, 22, 33, 40], by taking into consideration that the diffusion spreads through a network in the form of some spanning tree. The paths from the source to the nodes in a graph, for the first time when each node became infected or received information, actually corresponds to some spanning tree. However, the exact tree is unknown, and enumerating all of them is not feasible, as there is an exponential number of them. Typically, the breadth-first search (BFS) tree is used as an approximation of the true spanning tree, while in [33], cost and tree-based ranking algorithms are used to construct trees which perform better in experimental evaluations than BFS. We will now provide the analysis for a tree network, and the above mentioned approximations can be used to apply tree-based analysis for a general network.

We will analyze two scenarios: in the first we model the activation time of the source as a random variable and in the second we assume no knowledge of the activation time. As we will later show, evaluating the error exponent is actually simpler in the case no characterization of  $t_0$  is available.

#### *Scenario I*

We model the activation time of the source as a random variable with distribution  $\mathcal{N}(\mu_0, \sigma^2)$ , independent of the random propagation delays (where  $\mu_0$  is sufficiently large compared to  $\sigma^2$  to avoid negative activation time). We assume that the variance of the activation time is equal to the variance of the propagation delay in order to simplify the presentation, but, the model also admits a different variance. The infection time of a node  $o_l$  when  $s$  is the source is

$$t_{o_l} = t_0 + \sum_{i,j \in P(o_l, s)} \theta_{i,j},$$

where  $P(o_l, s)$  is the shortest path between  $o_l$  and  $s$ . The mean and the variance of the infection time of

node  $o_l$  are

$$\mathbb{E}(t_{o_l}) = \mu d(o_l, s) + \mu_0, \quad \text{var}(t_{o_l}) = (d(o_l, s) + 1)\sigma^2,$$

where  $d(o_l, s)$  denotes the graph distance between the nodes  $o_l$  and  $s$ . Even though the propagation delays associated with edges are independent, the infection times of any two nodes  $o_k$  and  $o_l$  may be correlated, due to the random activation time and the common edges between the paths from nodes  $o_k$  and  $o_l$  to the source node  $s$ . Now, the covariance of the infection times of nodes  $o_k$  and  $o_l$ , assuming the source is node  $s$ , is

$$\begin{aligned} \text{cov}(t_{o_k}, t_{o_l}) &= \mathbb{E} \left[ (t_{o_k} - \mu d(o_k, s) - \mu_0) (t_{o_l} - \mu d(o_l, s) - \mu_0) \right] \\ &= \sigma^2 (1 + |P(o_k, s) \cap P(o_l, s)|), \end{aligned} \quad (4.30)$$

where  $|\cdot|$  denotes the cardinality, and  $P(o_k, s) \cap P(o_l, s)$  denotes the common edges of paths  $P(o_k, s)$  and  $P(o_l, s)$ . The number of these common edges can be calculated as

$$|P(k, s) \cap P(l, s)| = \frac{1}{2} (d(k, s) + d(l, s) - d(k, l)). \quad (4.31)$$

Then, compactly, the covariance matrix associated with the source node  $s$ , and the set of observers  $O = \{o_1, \dots, o_r\}$  is

$$\Sigma_s = \frac{\sigma^2}{2} (\mathbf{d}\mathbf{1}^T + \mathbf{1}\mathbf{d}^T - \mathbf{D} + 2\mathbf{1}\mathbf{1}^T), \quad (4.32)$$

where  $\mathbf{d}$  depends on the vector of graph distances of the source to the observers as  $\mathbf{d} = \mu [d(o_1, s), \dots, d(o_r, s)]^T$ ,  $\mathbf{1}$  is a vector with all entries equal to 1 and  $\mathbf{D} \in \mathbb{R}^{r \times r}$  is the matrix of graph distances between observers. Finally, assuming node  $s$  to be the source, the infection times of the observers  $\mathbf{x} = [t_{o_1}, \dots, t_{o_r}]^T$ , are characterized by a multivariate Gaussian distribution  $\mathcal{N}(\boldsymbol{\mu}_s, \Sigma_s)$ , where

$$\boldsymbol{\mu}_s = \mathbf{d} + \mu_0 \mathbf{1}, \quad (4.33)$$

and  $\Sigma_s$  is given by (4.32). Therefore, for each network node  $s$ , we have a different hypothesis  $H_s$  with distribution  $\mathcal{N}(\boldsymbol{\mu}_s, \Sigma_s)$  describing the infection times of the observers.

### *Scenario II*

If no assumptions on  $t_0$  can be made, then one observer, say  $o_1$ , can be chosen as the reference, and instead of the infection times, their difference is used. Assuming the source to be node  $s$ , we denote with

$x_{o_k}$  this new observation for observer  $o_k$  to obtain [5]

$$x_{o_k} = t_{o_k} - t_{o_1} = \sum_{i,j \in P(o_k, s)} \theta_{i,j} - \sum_{i,j \in P(o_1, s)} \theta_{i,j}. \quad (4.34)$$

Now the infection times of the observers, assuming node  $s$  to be the source, are again characterized with multivariate Gaussian distribution, but with different parameters. The mean equals

$$\boldsymbol{\mu}_s = \mu [d(s, o_2) - d(s, o_1), \dots, d(s, o_r) - d(s, o_1)]^T, \quad (4.35)$$

while the covariance no longer depends on the source and is

$$[\boldsymbol{\Sigma}]_{k,i} = \sigma^2 \begin{cases} d(o_1, o_{k+1}), & k = i \\ |P(o_1, o_{k+1}) \cap P(o_1, o_{i+1})|, & k \neq i \end{cases}. \quad (4.36)$$

Having the statistical characterization of the observed infection times, for each possible source, for both scenarios, we proceed to derive the exact expression for  $\gamma(k, l)$  given by (4.7). The variance of the random propagation delay,  $\sigma^2$ , takes the role of the randomness parameter  $\eta$ . Since the densities  $p(\mathbf{x}; k)$  and  $p(\mathbf{x}; l)$  are multivariate Gaussian with equal priors, the  $\alpha$ -Chernoff divergence from (4.4) evaluates to [73]

$$c_\alpha(k, l, \sigma^2) = \frac{1}{2} \log \frac{\det(\alpha \boldsymbol{\Sigma}_k + (1 - \alpha) \boldsymbol{\Sigma}_l)}{(\det \boldsymbol{\Sigma}_k)^\alpha (\det \boldsymbol{\Sigma}_l)^{1-\alpha}} + \frac{\alpha(1 - \alpha)}{2} (\boldsymbol{\mu}_k - \boldsymbol{\mu}_l)^T (\alpha \boldsymbol{\Sigma}_k + (1 - \alpha) \boldsymbol{\Sigma}_l)^{-1} (\boldsymbol{\mu}_k - \boldsymbol{\mu}_l). \quad (4.37)$$

Next, we can decouple each covariance matrix as  $\boldsymbol{\Sigma}_i = \sigma^2 \tilde{\boldsymbol{\Sigma}}_i$ , where  $\tilde{\boldsymbol{\Sigma}}_i$  depends only on the graph structure (and possibly on the source node), but not on the variance of the propagation delay along the edges. Then,  $\alpha$ -Chernoff divergence from (4.37) can be rewritten as

$$\begin{aligned} c_\alpha(k, l, \sigma^2) &= \frac{1}{2} \log \frac{\det(\alpha \tilde{\boldsymbol{\Sigma}}_k + (1 - \alpha) \tilde{\boldsymbol{\Sigma}}_l)}{(\det \tilde{\boldsymbol{\Sigma}}_k)^\alpha (\det \tilde{\boldsymbol{\Sigma}}_l)^{1-\alpha}} + \frac{\alpha(1 - \alpha)}{2\sigma^2} (\boldsymbol{\mu}_k - \boldsymbol{\mu}_l)^T (\alpha \tilde{\boldsymbol{\Sigma}}_k + (1 - \alpha) \tilde{\boldsymbol{\Sigma}}_l)^{-1} (\boldsymbol{\mu}_k - \boldsymbol{\mu}_l) \\ &= f_1(\alpha, k, l) + \frac{1}{\sigma^2} f_2(\alpha, k, l), \end{aligned} \quad (4.38)$$

where  $\det(\mathbf{M})$  is the determinant of a matrix  $\mathbf{M}$  and

$$f_1(\alpha, k, l) = \frac{1}{2} \log \frac{\det(\alpha \tilde{\boldsymbol{\Sigma}}_k + (1 - \alpha) \tilde{\boldsymbol{\Sigma}}_l)}{(\det \tilde{\boldsymbol{\Sigma}}_k)^\alpha (\det \tilde{\boldsymbol{\Sigma}}_l)^{1-\alpha}},$$

$$f_2(\alpha, k, l) = \frac{\alpha(1-\alpha)}{2} (\boldsymbol{\mu}_k - \boldsymbol{\mu}_l)^T \boldsymbol{\Gamma}^{-1} (\boldsymbol{\mu}_k - \boldsymbol{\mu}_l) \quad (4.39)$$

and

$$\boldsymbol{\Gamma} = \alpha \tilde{\boldsymbol{\Sigma}}_k + (1-\alpha) \tilde{\boldsymbol{\Sigma}}_l. \quad (4.40)$$

Using the results of the following lemmas, we will show that analysis of the asymptotic behavior can be restricted only to analysis of  $f_2(\alpha, k, l)$  of  $\alpha$ -Chernoff divergence given by (4.38).

**Lemma 18.** *Let  $\Phi(\alpha, \theta) = g_1(\alpha) + \theta g_2(\alpha)$ , where  $g_1$  and  $g_2$  are continuous functions of  $\alpha$  for  $0 \leq \alpha \leq 1$ . Let  $\alpha^*(\theta_k)$  denote the maximizer of  $\Phi(\alpha, \theta)$  for fixed value  $\theta = \theta_k$ . Then*

$$\lim_{\theta \rightarrow 0} \max_{0 \leq \alpha \leq 1} \Phi(\alpha, \theta) = g_1(\alpha^*(0)).$$

*Proof.* Since  $g_2$  is a continuous function in the interval  $0 \leq \alpha \leq 1$ , it can be bounded by some constant  $h$ , i.e.,

$$|g_2(\alpha)| < h, \quad (4.41)$$

for  $0 \leq \alpha \leq 1$ . For the sequence  $\theta_k \rightarrow 0$ , let  $\alpha_k$  denote the corresponding maximizer of  $\Phi(\alpha, \theta_k)$ , i.e.,  $\alpha_k = \alpha^*(\theta_k)$ . Then we have that the following bounds hold

$$\Phi(\alpha_k, \theta_k) \geq \Phi(\alpha^*(0), \theta_k) \quad (4.42)$$

$$= g_1(\alpha^*(0)) + \theta_k g_2(\alpha^*(0)) \geq g_1(\alpha^*(0)) - \theta_k h. \quad (4.43)$$

Inequality (4.42) holds as  $\alpha_k$  maximizes  $\Phi(\alpha, \theta_k)$ , while inequality (4.43) holds since function  $g_2$  can be bounded as (4.41).

Then, from (4.43), we further have

$$\liminf_{k \rightarrow \infty} \Phi(\alpha_k, \theta_k) \geq \liminf_{k \rightarrow \infty} g_1(\alpha^*(0)) - \theta_k h = g_1(\alpha^*(0)). \quad (4.44)$$

Next, we also have

$$\begin{aligned} g_1(\alpha^*(0)) = \Phi(\alpha^*(0), 0) &\geq \Phi(\alpha_k, 0) = g_1(\alpha_k) = g_1(\alpha_k) + \theta_k g_2(\alpha_k) - \theta_k g_2(\alpha_k) \\ &\geq \Phi(\alpha_k, \theta_k) - \theta_k h. \end{aligned} \quad (4.45)$$

From (4.45) we obtain

$$\Phi(\alpha_k, \theta_k) \leq g_1(\alpha^*(0)) + \theta_k h$$

and

$$\limsup_{k \rightarrow \infty} \Phi(\alpha_k, \theta_k) \leq \limsup_{k \rightarrow \infty} g_1(\alpha^*(0)) - \theta_k h = g_1(\alpha^*(0)). \quad (4.46)$$

Combining the upper (4.44) and lower (4.46) bound, finally yields

$$\lim_{k \rightarrow \infty} \Phi(\alpha_k, \theta_k) = g_1(\alpha^*(0)).$$

□

Lemma 18 holds for functions of the form  $g_1(\alpha) + \theta g_2(\alpha)$ , while we have  $c_\alpha(k, l, \sigma^2) = f_1(\alpha, k, l) + \frac{1}{\sigma^2} f_2(\alpha, k, l)$ . Therefore, we will also need the result of the following lemma that holds for the functions of the form  $g_1(\alpha) + \frac{1}{\theta} g_2(\alpha)$ .

**Lemma 19.** *Let  $F(\alpha, \theta) = g_1(\alpha) + \frac{1}{\theta} g_2(\alpha)$ , where  $g_1$  and  $g_2$  are continuous functions of  $\alpha$  for  $0 \leq \alpha \leq 1$ . Let  $\alpha^*(\theta_k)$  denote the maximizer of  $F(\alpha, \theta)$  for fixed value  $\theta = \theta_k$ . Then*

$$\lim_{k \rightarrow \infty} \theta_k \max_{0 \leq \alpha \leq 1} F(\alpha, \theta) = g_2(\alpha^*(0)).$$

*Proof.* We can rewrite  $F(\alpha, \theta)$  as  $\frac{1}{\theta}(g_2(\alpha) + \theta g_1(\alpha)) = \frac{1}{\theta} \tilde{\Phi}(\alpha, \theta)$ . Then  $\alpha^*(\theta_k)$  is the maximizer of  $F(\alpha, \theta)$ , as well as of  $\tilde{\Phi}(\alpha, \theta)$  for  $0 \leq \alpha \leq 1$ . Again, for the sequence  $\theta_k \rightarrow 0$ , let  $\alpha_k$  denote the corresponding maximizer  $\alpha^*(\theta_k)$ . Then, applying the results of Lemma 18, we obtain

$$\lim_{k \rightarrow \infty} F(\alpha_k, \theta_k) \theta_k = \lim_{k \rightarrow \infty} \theta_k \frac{1}{\theta_k} \tilde{\Phi}(\alpha_k, \theta_k) = g_2(\alpha^*(0)).$$

□

In order to finish evaluating the exact expression for  $\gamma(k, l)$  from (4.7) we can now apply the results of Lemma 19 as follows

$$\begin{aligned} \gamma(k, l) &= \lim_{\sigma^2 \rightarrow 0} \frac{C(k, l, \sigma^2)}{1/\sigma^2} \\ &= \lim_{\sigma^2 \rightarrow 0} \sigma^2 \left( f_1(\alpha^*(\sigma^2), k, l) + \frac{1}{\sigma^2} f_2(\alpha^*(\sigma^2), k, l) \right) \\ &= f_2(\alpha^*(0), k, l) = \max_{0 \leq \alpha \leq 1} f_2(\alpha, k, l) \\ &= \max_{0 \leq \alpha \leq 1} \frac{\alpha(1-\alpha)}{2} (\boldsymbol{\mu}_k - \boldsymbol{\mu}_l)^T \boldsymbol{\Gamma}^{-1} (\boldsymbol{\mu}_k - \boldsymbol{\mu}_l), \end{aligned} \quad (4.47)$$

where  $\boldsymbol{\Gamma}$  is defined as (4.40).

Now, following (4.8), we denote with  $\gamma(i, j)$  the smallest exponent  $\gamma(k, l)$  given by (4.47). Establishing that  $\gamma(i, j)$  upper bounds the error exponent is already given by Lemma 15, while the lower bound requires additional steps. First, we will show that analysis of a problem for arbitrary matrices  $\Sigma_i$  and  $\Sigma_j$  can be simplified by applying simultaneous diagonalization of positive definite matrices [74]. We diagonalize  $\Sigma_i$  and  $\Sigma_j$  as

$$\tilde{\Sigma}_i = \mathbf{S}\mathbf{S}^T \text{ and } \tilde{\Sigma}_j = \mathbf{S}\mathbf{\Lambda}_{ij}\mathbf{S}^T,$$

where  $\mathbf{\Lambda}_{ij}$  is a real diagonal matrix with non-negative diagonal elements. Now we can rewrite  $f_2(\alpha, i, j)$  as

$$\frac{\alpha(1-\alpha)}{2} (\boldsymbol{\mu}_i - \boldsymbol{\mu}_j)^T \mathbf{S}^{-T} (\alpha\mathbf{I} + (1-\alpha)\mathbf{\Lambda})^{-1} \mathbf{S}^{-1} (\boldsymbol{\mu}_i - \boldsymbol{\mu}_j).$$

Then, instead of analyzing the error exponent for distinguishing between distributions  $\mathcal{N}(\boldsymbol{\mu}_i, \sigma^2\tilde{\Sigma}_i)$  and  $\mathcal{N}(\boldsymbol{\mu}_j, \sigma^2\tilde{\Sigma}_j)$ , we can analyze the equivalent problem of determining the error exponent for distributions  $\mathcal{N}(\mathbf{S}^{-1}\boldsymbol{\mu}_i, \sigma^2\mathbf{I})$  and  $\mathcal{N}(\mathbf{S}^{-1}\boldsymbol{\mu}_j, \sigma^2\mathbf{\Lambda})$ . Hence, we focus our attention to the case when  $\tilde{\Sigma}_i = \mathbf{I}$  and  $\tilde{\Sigma}_j = \mathbf{\Lambda}$  and denote  $\boldsymbol{\mu}'_i = \mathbf{S}^{-1}\boldsymbol{\mu}_i$  and  $\boldsymbol{\mu}'_j = \mathbf{S}^{-1}\boldsymbol{\mu}_j$ . Also, before we apply Lemma 16 to lower bound the error exponent, we need the result of the following lemma.

**Lemma 20.** *Let  $\{B_n\}$  be a monotone increasing sequence of sets and  $g(\mathbf{x}, \mathbf{a})$  is a non-negative continuous function for  $\mathbf{x} \in \Omega$  and any  $\mathbf{a}$ . Then the following holds*

$$\lim_{n \rightarrow \infty} \inf \{g(\mathbf{x}, \mathbf{a}) | \mathbf{x} \in B_n\} = \inf \left\{ g(\mathbf{x}, \mathbf{a}) | \mathbf{x} \in \lim_{n \rightarrow \infty} B_n \right\}.$$

*Proof.* Let  $B = \lim_{n \rightarrow \infty} B_n = \cup_{n \rightarrow \infty} B_n$ , and  $b = \inf \{g(\mathbf{x}, \mathbf{a}) | \mathbf{x} \in B\}$ . Let  $b_n = \inf \{g(\mathbf{x}, \mathbf{a}) | \mathbf{x} \in B_n\}$ . Then we need to show  $\lim_{n \rightarrow \infty} b_n = b$ . Since  $B_n \subseteq B_{n+1}$ , we have  $b = \inf_{\mathbf{x} \in B} g(\mathbf{x}, \mathbf{a}) \leq \inf_{\mathbf{x} \in B_n} g(\mathbf{x}, \mathbf{a}) = b_n$ , from which  $b \leq \lim_{n \rightarrow \infty} b_n$  follows. To prove the inequality in the other direction, since  $B = \cup_{n \rightarrow \infty} B_n$ , we have the following: for each  $\mathbf{x} \in B$ , there is some  $n$  such that  $\mathbf{x} \in B_n$ , hence  $b_n \leq b$ , and  $\lim_{n \rightarrow \infty} b_n \leq b$ .  $\square$

We now use Lemmas 16 and 20 to prove the Theorem that establishes a lower bound on the exponent, and then we relate this bound to our expression of  $\gamma(i, j)$  through Theorem 23.

**Theorem 21.** *The following bound holds*

$$\lim_{\sigma^2 \rightarrow 0} \frac{\log(P_e)}{1/\sigma^2} \geq - \inf_{\mathbf{x} \in \Omega} \frac{\|\mathbf{x} - \boldsymbol{\mu}'_i\|^2}{2}, \quad (4.48)$$

$$\text{for } \Omega = \left\{ \mathbf{x} : \frac{1}{2} \|\mathbf{x} - \boldsymbol{\mu}'_i\|^2 > \frac{1}{2} (\mathbf{x} - \boldsymbol{\mu}'_j)^T \boldsymbol{\Lambda}^{-1} (\mathbf{x} - \boldsymbol{\mu}'_j) \right\}. \quad (4.49)$$

*Proof.* First, comparing the distribution  $p(\mathbf{x}; i)$  to (4.1), we note that the function  $h(\sigma^2) = 1/(2\pi\sigma^2)^{r/2}$ . Then

$$\sigma^2 \log(h(\sigma^2)) = -\sigma^2 r/2 \log(2\pi\sigma^2) \xrightarrow{\sigma^2 \rightarrow 0} 0,$$

thereby satisfying the assumption (4.23) of Lemma 16. Function  $g(\mathbf{x}, \boldsymbol{\mu}'_i) = \|\mathbf{x} - \boldsymbol{\mu}'_i\|^2/2$  is surely non-negative and continuous. Let us denote  $\Omega_{\sigma^2} = \left\{ \mathbf{x} : p(\mathbf{x}; H_i) < p(\mathbf{x}; H_j) \right\}$ , which can be rewritten as

$$\Omega_{\sigma^2} = \left\{ \mathbf{x} : \sigma^2 K + \frac{\|\mathbf{x} - \boldsymbol{\mu}'_i\|^2}{2} > \frac{(\mathbf{x} - \boldsymbol{\mu}'_j)^T \boldsymbol{\Lambda}^{-1} (\mathbf{x} - \boldsymbol{\mu}'_j)}{2} \right\},$$

where  $K = -\frac{1}{2}\sigma^2 \log \det \boldsymbol{\Lambda}$ . We cannot directly apply the result established by Lemma 16, as the set  $\Omega_{\sigma^2}$  depends on the value of  $\sigma^2$ , unlike the set  $\Omega$  from Lemma 16. Let us separately consider the cases  $K \geq 0$  and  $K < 0$ .

Case I:  $K \geq 0$

For any value of  $\sigma^2 > 0$ , we have that  $\Omega \subset \Omega_{\sigma^2}$ . Then

$$\begin{aligned} P_e &\geq \frac{1}{(2\pi\sigma^2)^{r/2}} \int_{\Omega_{\sigma^2}} e^{-\frac{1}{2\sigma^2} \|\mathbf{x} - \boldsymbol{\mu}'_i\|^2} d\mathbf{x} \\ &\geq \frac{1}{(2\pi\sigma^2)^{r/2}} \int_{\Omega} e^{-\frac{1}{2\sigma^2} \|\mathbf{x} - \boldsymbol{\mu}'_i\|^2} d\mathbf{x} \end{aligned}$$

In order to use the result of Lemma 16, we need to show that its assumptions hold. We have that  $\boldsymbol{\mu}'_i \notin \Omega$ , unless  $\boldsymbol{\mu}'_i = \boldsymbol{\mu}'_j$ , and we exclude this case and later discuss it. Next we will show that the intersection of the set  $\Omega$  and the set  $\mathcal{R}(l, l + \epsilon)$ , where  $l = \inf\{\|\mathbf{x} - \boldsymbol{\mu}'_i\|^2/2 \mid \mathbf{x} \in \Omega\}$  has a non-empty interior.

Let us first fix  $\epsilon > 0$ . Then, there exists  $\bar{\mathbf{x}} \in \Omega$  such that  $g(\boldsymbol{\mu}'_i, \bar{\mathbf{x}}) < f(\boldsymbol{\mu}'_i, \Omega) + \epsilon$ . Since  $\bar{\mathbf{x}} \in \Omega$ , there exist a  $\delta_1 > 0$  such that an open ball, centered at  $\bar{\mathbf{x}}$  of radius  $\delta_1$ , denoted as  $B(\bar{\mathbf{x}}, \delta_1)$ , is contained in  $\Omega$ . Also,  $\bar{\mathbf{x}} \in B(\boldsymbol{\mu}'_i, l + \epsilon)$ , and so there exists  $\delta_2 > 0$ , such that  $B(\bar{\mathbf{x}}, \delta_2) \subset B(\boldsymbol{\mu}'_i, l + \epsilon)$ . Let  $\delta = \min\{\delta_1, \delta_2\}$ . Then for any  $\epsilon > 0$ , we have a point  $\bar{\mathbf{x}}$  and a radius  $\delta$ , such that  $B(\bar{\mathbf{x}}, \delta)$  is both in the set  $\Omega$  and the ring  $\mathcal{R}(l, l + \epsilon)$ , implying that  $\bar{\mathbf{x}}$  is an interior point of the intersection. Hence, the assumption  $\text{vol}(\Omega \cap \mathcal{R}_{\boldsymbol{\mu}'_i}(l, l + \epsilon)) > 0$  holds and we can now apply Lemma 16.

Case II:  $K < 0$

Let us denote with  $\sigma_n^2$  a decreasing sequence which converges to 0. For each value  $\sigma_n^2$ , we have the corresponding  $\Omega_{\sigma_n^2}$ , with  $\Omega_{\sigma_p^2} \subset \Omega_{\sigma_q^2}$ , for  $p > q$ . Then  $\Omega = \cup_{\sigma_n^2 \rightarrow \infty} \Omega_{\sigma_n^2}$ . Now, we fix  $\sigma^2 > 0$ , and choose

$\bar{\sigma}^2 > \sigma^2$ , which gives  $\Omega_{\bar{\sigma}^2} \subset \Omega_{\sigma^2}$ . Then we can bound the error probability as

$$\begin{aligned} P_e &\geq \frac{1}{(2\pi\sigma^2)^{r/2}} \int_{\Omega_{\sigma^2}} e^{-\frac{1}{2\sigma^2}\|\mathbf{x}-\boldsymbol{\mu}'_i\|^2} d\mathbf{x} \\ &\geq \frac{1}{(2\pi\sigma^2)^{r/2}} \int_{\Omega_{\bar{\sigma}^2}} e^{-\frac{1}{2\sigma^2}\|\mathbf{x}-\boldsymbol{\mu}'_i\|^2} d\mathbf{x} \end{aligned}$$

Again, by excluding the case  $\boldsymbol{\mu}'_i = \boldsymbol{\mu}'_j$  and invoking the same arguments as in the previous case to verify that assumption (4.22) holds, we apply the results of Lemma 16 to obtain

$$\lim_{\sigma^2 \rightarrow 0} \frac{\log(P_e)}{1/\sigma^2} \geq -f(\boldsymbol{\mu}'_i, \Omega_{\bar{\sigma}^2}). \quad (4.50)$$

Again,  $\Omega = \cup_{\bar{\sigma}^2 \rightarrow \infty} \Omega_{\bar{\sigma}^2}$ , where  $\Omega_{\bar{\sigma}^2}$  are monotone increasing sets for  $\bar{\sigma}^2 \rightarrow \infty$ . Then we can apply Lemma 20 to obtain

$$\lim_{\bar{\sigma}^2 \rightarrow \infty} f(\boldsymbol{\mu}'_i, \Omega_{\bar{\sigma}^2}) = f(\boldsymbol{\mu}'_i, \Omega). \quad (4.51)$$

Plugging (4.51) into (4.50), we finally obtain the claim.  $\square$

Next, instead of the set  $\Omega$ , we will need to use its closure, which we state in the following lemma.

**Lemma 22.** *Set*

$$\bar{\Omega} = \left\{ \mathbf{x} : \frac{1}{2} \|\mathbf{x} - \boldsymbol{\mu}'_i\|^2 \geq \frac{1}{2} (\mathbf{x} - \boldsymbol{\mu}'_j)^T \boldsymbol{\Lambda}^{-1} (\mathbf{x} - \boldsymbol{\mu}'_j) \right\}$$

*is the closure of the set  $\Omega$  defined in (4.49).*

*Proof.* Since  $f(\mathbf{x}) = \frac{1}{2} \|\mathbf{x} - \boldsymbol{\mu}'_i\|^2 - \frac{1}{2} (\mathbf{x} - \boldsymbol{\mu}'_j)^T \boldsymbol{\Lambda}^{-1} (\mathbf{x} - \boldsymbol{\mu}'_j)$  is a continuous function, set  $\Omega$  is an open, while  $\bar{\Omega}$  is a closed set. What remains to be shown is that every point in the set

$$S = \left\{ \mathbf{x} : \frac{1}{2} \|\mathbf{x} - \boldsymbol{\mu}'_i\|^2 = \frac{1}{2} (\mathbf{x} - \boldsymbol{\mu}'_j)^T \boldsymbol{\Lambda}^{-1} (\mathbf{x} - \boldsymbol{\mu}'_j) \right\}$$

is a limit of sequences  $\mathbf{x}_k \in \Omega$  and  $\mathbf{y}_k \notin \Omega$ . First we will exclude the case  $\boldsymbol{\mu}'_i = \boldsymbol{\mu}'_j$ , as depending on the eigenvalues of  $\boldsymbol{\Lambda}$ , set  $\Omega$  could be an empty set or the whole space, and its boundary would then be an empty set. We can consider a sequence  $\mathbf{x}_k = \mathbf{x} + \mathbf{v}$ , where entries of  $\mathbf{v}$  are all zeros except the first entry which is  $s/k$ , and  $\mathbf{x} \in S$ . The sequence obviously converges to  $\mathbf{x}$ , and we will show that there is always a value of  $s$ ,

such that  $\mathbf{x}_k \in \Omega$ . Denoting  $m = [\mathbf{\Lambda}^{-1}]_{11}$ , we have

$$\begin{aligned} f(\mathbf{x}_k) &= \frac{1}{2} \|\mathbf{x} + \mathbf{v} - \boldsymbol{\mu}'_i\|^2 - \frac{1}{2} (\mathbf{x} + \mathbf{v} - \boldsymbol{\mu}'_j)^T \mathbf{\Lambda}^{-1} (\mathbf{x} + \mathbf{v} - \boldsymbol{\mu}'_j) \\ &= \frac{1}{k} \left( \frac{s^2}{k} \left( 1 - \frac{1}{m} \right) + 2s \left( x_1 - \mu'_{i1} - \frac{x_1}{m} + \frac{\mu'_{j1}}{m} \right) \right). \end{aligned}$$

If  $t = x_1 - \mu'_{i1} - x_1/m + \mu'_{j1}/m > 0$  and  $s = 1$ , for large enough  $k$ , such that the sign of the second term, term  $t$ , dominates, we have that  $f(\mathbf{x}_k) > 0$ . Otherwise, if  $t < 0$ , we set  $s = -1$  and obtain  $f(\mathbf{x}_k) > 0$ , hence showing that every point in  $S$  is a limit of some sequence in  $\Omega$ . Similarly, taking  $\mathbf{y}_k = \mathbf{x} + \mathbf{v}$ , but this time taking  $s = -1$  for  $t > 0$  and  $s = 1$  for  $t < 0$ , we generate a sequence  $\mathbf{y}_k \rightarrow \mathbf{x}$  as  $k \rightarrow \infty$ . Then for large enough  $k$ , we have that  $\mathbf{y}_k$  belongs to the complement of  $\Omega$ , as  $f(\mathbf{y}_k) < 0$ . For  $t = 0$ , we can construct the sequences by perturbing not the first entry of  $\mathbf{x}$ , as we have done so far, but any other entry for which  $t \neq 0$ , unless  $\mathbf{x} - \boldsymbol{\mu}'_i = \mathbf{\Lambda}^{-1}(\mathbf{x} - \boldsymbol{\mu}'_j)$  holds. If  $\mathbf{\Lambda}^{-1} - \mathbf{I}$  is either positive or negative definite matrix, the set  $S$  consists of  $\mathbf{x} = \boldsymbol{\mu}'_i = \boldsymbol{\mu}'_j$ , which is the case we have previously excluded. If  $\mathbf{\Lambda}^{-1} - \mathbf{I}$  is neither positive nor negative definite, it implies that some eigenvalues of  $\mathbf{\Lambda}^{-1}$  are greater than 1, while others are less. Then we take  $s = 1$  and form a sequence  $\mathbf{x}_k$  by perturbing the entry of  $\mathbf{x}$  for which the corresponding eigenvalue is greater than 1, and less than 1 to generate  $\mathbf{y}_k$ .  $\square$

The next Theorem uses an interesting duality phenomenon to relate the upper bound shown for error exponent in Theorem 21 to our expression for  $\gamma(i, j)$ , the minimum value of (4.47).

**Theorem 23.** *The optimization problem*

$$\max_{0 \leq \alpha \leq 1} \frac{\alpha(1-\alpha)}{2} (\boldsymbol{\mu}'_i - \boldsymbol{\mu}'_j)^T (\alpha \mathbf{I} + (1-\alpha)\mathbf{\Lambda})^{-1} (\boldsymbol{\mu}'_i - \boldsymbol{\mu}'_j). \quad (4.52)$$

*is the dual of the minimization problem*

$$\begin{aligned} & \min_{\mathbf{x}} \frac{\|\mathbf{x} - \boldsymbol{\mu}'_i\|^2}{2} \\ \text{s.t. } & \frac{1}{2} \|\mathbf{x} - \boldsymbol{\mu}'_i\|^2 \geq \frac{1}{2} (\mathbf{x} - \boldsymbol{\mu}'_j)^T \mathbf{\Lambda}^{-1} (\mathbf{x} - \boldsymbol{\mu}'_j). \end{aligned} \quad (4.53)$$

*Proof.* The Lagrangian dual function of (4.53) is

$$\begin{aligned} L(\mathbf{x}, \nu) &= \frac{1}{2} \mathbf{x}^T (\mathbf{I} + \nu(\mathbf{\Lambda}^{-1} - \mathbf{I})) \mathbf{x} + (-\boldsymbol{\mu}'_i + \nu(\boldsymbol{\mu}'_i - \mathbf{\Lambda}^{-1} \boldsymbol{\mu}'_j))^T \mathbf{x} \\ &+ \frac{1}{2} \nu (\boldsymbol{\mu}'_j{}^T \mathbf{\Lambda}^{-1} \boldsymbol{\mu}'_j - \boldsymbol{\mu}'_i{}^T \boldsymbol{\mu}'_i) + \frac{1}{2} \boldsymbol{\mu}'_i{}^T \boldsymbol{\mu}'_i. \end{aligned} \quad (4.54)$$

Denoting  $c = \frac{1}{2}\nu(\boldsymbol{\mu}'_j{}^T \boldsymbol{\Lambda}^{-1} \boldsymbol{\mu}'_j - \boldsymbol{\mu}'_i{}^T \boldsymbol{\mu}'_i) + \frac{1}{2}\boldsymbol{\mu}'_i{}^T \boldsymbol{\mu}'_i$ ,  $b = -\boldsymbol{\mu}'_i + \nu(\boldsymbol{\mu}'_i - \boldsymbol{\Lambda}^{-1} \boldsymbol{\mu}'_j)$  and  $\mathbf{M} = \mathbf{I} + \nu(\boldsymbol{\Lambda}^{-1} - \mathbf{I})$ , the dual function is

$$L(\nu) = \inf_{\mathbf{x}} L(\mathbf{x}, \nu) = \begin{cases} c - \frac{1}{2}b^T \mathbf{M}^+ b, & \mathbf{M} \geq 0 \\ -\infty, & \text{otherwise} \end{cases} \quad (4.55)$$

Then the dual problem of (4.53) is

$$\begin{aligned} & \max L(\nu) \\ & \text{s.t. } \nu \geq 0 \end{aligned} \quad (4.56)$$

Strong duality holds for problem (4.53) and its dual (4.56) based on the S-procedure [75] provided that Slater's condition is satisfied, even though it is not a convex problem. Since we can always take  $\mathbf{x} = \boldsymbol{\mu}'_j$ , and we assume  $\boldsymbol{\mu}'_i \neq \boldsymbol{\mu}'_j$ , the constraint is satisfied with strict inequality and strong duality holds. The KKT conditions are then

$$(\mathbf{I} + \nu(\boldsymbol{\Lambda}^{-1} - \mathbf{I})) \mathbf{x} - \boldsymbol{\mu}'_i + \nu(\boldsymbol{\mu}'_i - \boldsymbol{\Lambda}^{-1} \boldsymbol{\mu}'_j) = 0 \quad (4.57)$$

$$g(\mathbf{x}) = (\mathbf{x} - \boldsymbol{\mu}'_j)^T \boldsymbol{\Lambda}^{-1} (\mathbf{x} - \boldsymbol{\mu}'_j) - \|\mathbf{x} - \boldsymbol{\mu}'_i\|^2 \leq 0 \quad (4.58)$$

$$\nu \geq 0 \quad (4.59)$$

$$\nu g(\mathbf{x}) = 0. \quad (4.60)$$

From (4.60), we have either that  $\nu = 0$  or  $g(\mathbf{x}) = 0$ . If  $\nu = 0$ , from (4.57), we obtain  $\mathbf{x} = \boldsymbol{\mu}'_i$ . Plugging back this solution into the constraint (4.58), we obtain  $(\boldsymbol{\mu}'_i - \boldsymbol{\mu}'_j)^T \boldsymbol{\Lambda}^{-1} (\boldsymbol{\mu}'_i - \boldsymbol{\mu}'_j) \leq 0$ , which is a contradiction, for all  $\boldsymbol{\mu}'_i \neq \boldsymbol{\mu}'_j$  since  $\boldsymbol{\Lambda}^{-1} > 0$ . For  $\mathbf{x} = \boldsymbol{\mu}'_i = \boldsymbol{\mu}'_j$ , the value of both optimization problems, (4.53) and (4.52), is 0. For the general case,  $\boldsymbol{\mu}'_i \neq \boldsymbol{\mu}'_j$ , we have that  $g(\mathbf{x}) = 0$ .

Rearranging (4.55) gives

$$\begin{aligned} L(\nu) = & \nu(\nu - 1)\boldsymbol{\mu}'_i{}^T \mathbf{M}^{-1} \boldsymbol{\Lambda}^{-1} \boldsymbol{\mu}'_j - \frac{1}{2}(\nu - 1)^2 \boldsymbol{\mu}'_i{}^T \mathbf{M}^{-1} \boldsymbol{\mu}'_i \\ & - \frac{1}{2}(\nu - 1)\boldsymbol{\mu}'_i{}^T \boldsymbol{\mu}'_i + \frac{1}{2}\nu \boldsymbol{\mu}'_j{}^T \boldsymbol{\Lambda}^{-1} \boldsymbol{\mu}'_j - \frac{1}{2}\nu^2 \boldsymbol{\mu}'_j{}^T \boldsymbol{\Lambda}^{-1} \mathbf{M}^{-1} \boldsymbol{\Lambda}^{-1} \boldsymbol{\mu}'_j. \end{aligned} \quad (4.61)$$

After applying the equality  $(\mathbf{I} + \mathbf{A}\mathbf{B})^{-1} = \mathbf{I} - \mathbf{A}(\mathbf{I} + \mathbf{B}\mathbf{A})^{-1}\mathbf{B}$  and further rearranging, we finally obtain

$$L(\nu) = \frac{\nu(1-\nu)}{2} (\boldsymbol{\mu}'_i - \boldsymbol{\mu}'_j)^T (\nu\mathbf{I} + (1-\nu)\boldsymbol{\Lambda})^{-1} (\boldsymbol{\mu}'_i - \boldsymbol{\mu}'_j),$$

which is exactly the expression for Chernoff  $\alpha$ -divergence, where the Lagrangian multiplier has the role of the parameter  $\alpha$ , and this proves the claim.  $\square$

Theorem 23 was the last step needed to show that  $\gamma(i, j)$  lower bounds the error exponent. Since it also upper bounds the exponent, we conclude that the error exponent for vanishing noise when the observations are modeled as Gaussian variables is indeed

$$\gamma(i, j) = \max_{0 \leq \alpha \leq 1} \frac{\alpha(1-\alpha)}{2} (\boldsymbol{\mu}_i - \boldsymbol{\mu}_j)^T \boldsymbol{\Gamma}^{-1} (\boldsymbol{\mu}_i - \boldsymbol{\mu}_j),$$

for

$$\boldsymbol{\Gamma} = \alpha \tilde{\boldsymbol{\Sigma}}_i + (1-\alpha) \tilde{\boldsymbol{\Sigma}}_j.$$

Note that Theorem 23 proves that the value of the error exponent is a minimum that the exponent of the distribution function  $p(\mathbf{x}; i)$  reaches in the error region, where  $H_j$  is chosen, even though  $H_i$  is the true hypothesis.

For the observation model where no assumption on the activation time can be made, and the difference of infection times is used, the covariance matrix is the same for all the distributions of suspect nodes. It can be easily seen that  $\boldsymbol{\Gamma}$  from (4.40) then exactly equals  $\frac{1}{\sigma^2} \boldsymbol{\Sigma}$ , where  $\boldsymbol{\Sigma}$  is defined by (4.36). Then the optimal value of  $\alpha$  that maximizes  $\gamma(i, j)$  from (4.47) easily evaluates to  $\frac{1}{2}$ , giving a closed form for the exponent

$$\gamma(i, j) = \frac{1}{8} (\boldsymbol{\mu}_i - \boldsymbol{\mu}_j)^T \boldsymbol{\Gamma}^{-1} (\boldsymbol{\mu}_i - \boldsymbol{\mu}_j).$$

In the previous analysis, we have excluded the case of equal means  $\boldsymbol{\mu}_i = \boldsymbol{\mu}_j$ , and hence,  $\boldsymbol{\mu}'_i = \boldsymbol{\mu}'_j$ , as for this case there is no exponential error decay. However, the expression for the error exponent (4.7) is still valid, as it evaluates to zero.

### 4.1.3 Observations are modeled as Laplace random variables

In this scenario, we assume the propagation delay between two neighboring nodes  $u$  and  $v$ ,  $\theta_{u,v}$  to be a constant, and to simplify the notation, w.l.o.g. we assume it to be 1. Then, assuming  $s$  is the source, the *true* infection time of observer  $o_p$  equals its graph distance to the source node  $d(o_p, s)$ . However, we assume that the observations of infection times are corrupted with noise with Laplace distribution. This is motivated by

the use of Laplace noise in modeling outliers, because of its heavy-tail property, and the possible presence of outlier behavior in information networks [76]. Now, denoting the *observed* infection time of observer  $o_p$  as  $x_p$ , we have

$$x_p = d(o_p, s) + n_p,$$

where  $n_p$  is a random variable with density  $p(n_p) = \frac{1}{2b_p} e^{-\frac{|n_p - \mu'_p|}{b_p}}$ . Hence, the distribution characterizing the infection time of observer  $o_p$  is

$$p(x_p; s) = \frac{1}{2b_p} e^{-\frac{|n_p - \mu'_p - d(o_p, s)|}{b_p}},$$

where we allow the noise parameters to differ across different nodes, while the noise remains independent across nodes. Stacking the observations from all observer nodes into a vector  $\mathbf{x}$ , denoting  $\mu_p^s = \mu'_p + d(o_p, s)$ ,  $b = \min_p b_p$  and writing  $b_p = v_p b$ , for  $p = 1, \dots, r$ , we obtain

$$p(\mathbf{x}; s) = \prod_{p=1}^r \frac{1}{2bv_p} e^{-\frac{|x_p - \mu_p^s|}{bv_p}}. \quad (4.62)$$

Now  $b$  takes the role of the noise parameter  $\eta$ . Next, we evaluate the  $\alpha$ -Chernoff divergence (4.4) to obtain

$$\begin{aligned} c_\alpha(k, l, b) &= -\log \prod_{p=1}^r \int \frac{1}{2bv_p} e^{-\frac{\alpha|x_p - \mu_p^k| + (1-\alpha)|x_p - \mu_p^l|}{v_p b}} dx_p \\ &= -\log \prod_{p=1}^r \frac{1}{2bv_p} \left( bv_p e^{-(1-\alpha)\frac{|\mu_p^k - \mu_p^l|}{bv_p}} + \frac{bv_p}{1-2\alpha} \left( e^{-\alpha\frac{|\mu_p^k - \mu_p^l|}{bv_p}} - e^{-(1-\alpha)\frac{|\mu_p^k - \mu_p^l|}{bv_p}} \right) + bv_p e^{-\alpha\frac{|\mu_p^k - \mu_p^l|}{bv_p}} \right) \\ &= -\log \prod_{p=1}^r \frac{(1-\alpha) e^{-\alpha\frac{|\mu_p^k - \mu_p^l|}{bv_p}} - \alpha e^{-(1-\alpha)\frac{|\mu_p^k - \mu_p^l|}{bv_p}}}{1-2\alpha}. \end{aligned} \quad (4.63)$$

In order to derive the expression for  $\gamma(k, l)$ , and consequently for the error exponent, we will use the following lemmas.

**Lemma 24.** *Given  $c_\alpha(k, l, b)$  as in (4.63), the following holds*

$$c = \lim_{b \rightarrow 0} bc_\alpha(k, l, b) = \begin{cases} \alpha \sum_{p=1}^r \frac{|\mu_p^k - \mu_p^l|}{v_p}, & \alpha \leq \frac{1}{2} \\ (1-\alpha) \sum_{p=1}^r \frac{|\mu_p^k - \mu_p^l|}{v_p}, & \alpha \geq \frac{1}{2} \end{cases}. \quad (4.64)$$

*Proof.* We have the following

$$c = \lim_{b \rightarrow 0} b r \log(1 - 2\alpha) - b \sum_{p=1}^r \log \left( (1 - \alpha) e^{-\alpha \frac{|\mu_p^k - \mu_p^l|}{bv_p}} - \alpha e^{-(1-\alpha) \frac{|\mu_p^k - \mu_p^l|}{bv_p}} \right).$$

Changing the variables as  $y = 1/b$  and  $t_p = |\mu_p^k - \mu_p^l|/v_p$ , we further have

$$\begin{aligned} c &= \lim_{b \rightarrow 0} - \sum_{p=1}^r \frac{\log \left( (1 - \alpha) e^{-\alpha y t_p} - \alpha e^{-(1-\alpha) t_p} \right)}{y} \\ &= \lim_{b \rightarrow 0} - \sum_{p=1}^r \frac{\alpha t_p (1 - \alpha) \left( 1 - e^{-(1-2\alpha) t_p y} \right)}{-1 + \alpha + \alpha e^{-(1-2\alpha) t_p y}}, \end{aligned} \quad (4.65)$$

where in (4.65) we used L'Hopital's rule. For  $\alpha < \frac{1}{2}$ , we have that  $e^{-(1-2\alpha) t_p y} \rightarrow 0$ , as  $y \rightarrow \infty$ , hence

$$c = \sum_{p=1}^r \alpha t_p = \alpha \sum_{p=1}^r \frac{|\mu_p^k - \mu_p^l|}{v_p}, \text{ for } \alpha < \frac{1}{2}.$$

For  $\alpha < \frac{1}{2}$ , again we apply L'Hopital's rule to (4.65) to obtain

$$c = \sum_{p=1}^r (1 - \alpha) t_p = (1 - \alpha) \sum_{p=1}^r \frac{|\mu_p^k - \mu_p^l|}{v_p}, \text{ for } \alpha > \frac{1}{2}.$$

For  $\alpha = \frac{1}{2}$ , we look at  $\lim_{\alpha \rightarrow \frac{1}{2}} c_\alpha(k, l, b)$ . Since logarithm is a continuous function, we exchange it with the limit to obtain

$$\lim_{\alpha \rightarrow \frac{1}{2}} c_\alpha(k, l, b) = - \sum_{p=1}^r \log \lim_{\alpha \rightarrow \frac{1}{2}} \frac{(1 - \alpha) e^{-\alpha \frac{t_p}{b}} - \alpha e^{-(1-\alpha) \frac{t_p}{b}}}{1 - 2\alpha}.$$

Applying L'Hopital's rule we obtain

$$\lim_{\alpha \rightarrow \frac{1}{2}} c_\alpha(k, l, b) = - \sum_{p=1}^r \log e^{\frac{-t_p}{2b} \frac{b + \frac{1}{2} t_p}{b}} = - \sum_{p=1}^r \left( \frac{t_p}{2b} + \log \left( 1 + \frac{t_p}{2b} \right) \right). \quad (4.66)$$

From here, we have

$$c = \sum_{p=1}^r \frac{t_p}{2b} = \sum_{p=1}^r \frac{|\mu_p^k - \mu_p^l|}{2v_p}, \text{ for } \alpha = \frac{1}{2},$$

which completes the proof. □

**Lemma 25.** Given  $c_\alpha(k, l, b)$  as in (4.63), the following holds

$$\gamma(k, l) = \lim_{b \rightarrow 0} b \max_{0 \leq \alpha \leq 1} c_\alpha(k, l, b) = \sum_{p=1}^r \frac{|\mu_p^k - \mu_p^l|}{2\nu_p}. \quad (4.67)$$

*Proof.* First we need to show that for  $0 < x \leq \bar{x}$  and  $k \geq 0$  the following inequality holds

$$x \log \left( 1 + \frac{k}{x} \right) \leq \bar{x} \log \left( 1 + \frac{k}{\bar{x}} \right) + \frac{k}{1 + \frac{k}{\bar{x}}}. \quad (4.68)$$

Applying the Mean Value Theorem, for  $\bar{y} < y, z \in [\bar{y}, y]$  we have

$$\log(1 + y) \leq \log(1 + \bar{y}) + \frac{y - \bar{y}}{1 + \bar{y}} \leq \log(1 + \bar{y}) + \frac{y}{1 + \bar{y}}. \quad (4.69)$$

Substituting  $y = k/x$  and multiplying by  $x$  in (4.69), we obtain

$$x \log \left( 1 + \frac{k}{x} \right) \leq x \log \left( 1 + \frac{k}{\bar{x}} \right) + \frac{k}{1 + \frac{k}{\bar{x}}}.$$

Using  $x \leq \bar{x}$ , we obtain (4.68). Let  $c$  be as defined in (4.64). In order to switch the order of the operators  $\lim$  and  $\max$  in (4.67), we first need to show that  $b c_\alpha(k, l, b)$  uniformly converges to  $c$ , for  $b \rightarrow 0$ . Denoting  $t_p = |\mu_p^k - \mu_p^l|/\nu_p$ , we have

$$b c_\alpha(k, l, b) = - \sum_{p=1}^r b \log \left( e^{-\alpha \frac{t_p}{b}} \frac{1 - \alpha - \alpha e^{\frac{t_p}{b}(2\alpha-1)}}{1 - 2\alpha} \right).$$

For  $\alpha < \frac{1}{2}$ , we have

$$b c_\alpha(k, l, b) = \sum_{p=1}^r \alpha t_p - G_1(\alpha, b),$$

where

$$G_1(\alpha, b) = \sum_{p=1}^r \log \frac{1 - \alpha - \alpha e^{\frac{t_p}{b}(2\alpha-1)}}{1 - 2\alpha}.$$

Next, since  $e^{\frac{t_p}{b}(2\alpha-1)} < 1$  we have

$$G_1(\alpha, b) \geq \sum_{p=1}^r b \log \frac{1 - \alpha - \alpha}{1 - 2\alpha} = 0.$$

Applying the inequality  $e^x \geq x + 1$ , we can also lower bound  $G_1(\alpha, b)$  for  $0 \leq \alpha \leq \frac{1}{2}$  to get

$$\begin{aligned} G_1(\alpha, b) &\leq \sum_{p=1}^r b \log \frac{1 - \alpha - \alpha \left(1 + \frac{t_p}{b}(2\alpha - 1)\right)}{1 - 2\alpha} \\ &= \sum_{p=1}^r b \log \left(1 + \alpha \frac{t_p}{b}\right) \leq rb \log \left(1 + \frac{\max_p t_p}{2b}\right). \end{aligned}$$

Next, we substitute  $x = b$  and  $k = \frac{1}{2} \max_p t_p$  in (4.68) to obtain

$$G_1(\alpha, b) \leq r\bar{b} \log \left(1 + \frac{\max_p t_p}{2\bar{b}}\right) + \frac{r \max_p t_p}{2 + \frac{\max_p t_p}{\bar{b}}} \xrightarrow{\bar{b} \rightarrow 0} 0.$$

Therefore, for every  $\epsilon > 0$ , there is a  $\bar{b} > 0$  such that  $0 \leq G_1(\alpha, b) < \epsilon$ , which shows  $b c_\alpha(k, l, b)$  uniformly converges to  $\alpha \sum_{p=1}^r \frac{|\mu_p^k - \mu_p^l|}{v_p}$ , for  $\alpha < \frac{1}{2}$ .

Now for  $\alpha > \frac{1}{2}$ , we have

$$\begin{aligned} b c_\alpha(k, l, b) &= - \sum_{p=1}^r b \log \left( e^{-(1-\alpha)\frac{t_p}{b}} \frac{-(1-\alpha)e^{\frac{t_p}{b}(1-2\alpha)} + \alpha}{2\alpha - 1} \right) \\ &= \sum_p (1-\alpha)t_p - \sum_{p=1}^r b \log \left( \frac{\alpha - (1-\alpha)e^{\frac{(1-2\alpha)t_p}{b}}}{2\alpha - 1} \right). \end{aligned}$$

Now, denoting

$$G_2(\alpha, b) = \sum_{p=1}^r \log \left( \frac{\alpha - (1-\alpha)e^{\frac{(1-2\alpha)t_p}{b}}}{2\alpha - 1} \right),$$

using the same reasoning as for the case of  $\alpha < \frac{1}{2}$ , we have

$$0 < G_2(\alpha, b) \leq \sum_{p=1}^r b \log \left(1 + \frac{(1-\alpha)t_p}{b}\right) \leq rb \log \left(1 + \frac{\max_p t_p}{2b}\right),$$

Again using (4.68) we can show that  $b c_\alpha(k, l, b)$  uniformly converges to  $(1-\alpha) \sum_{p=1}^r \frac{|\mu_p^k - \mu_p^l|}{v_p}$ , for  $\alpha > \frac{1}{2}$ .

For  $\alpha = \frac{1}{2}$ , we use (4.66) and apply (4.68) to obtain the remainder of the claim on uniform convergence.

Now, since  $b c_\alpha(k, l, b)$  uniformly converges to  $c$ , we have

$$\gamma(k, l) = \max_{0 \leq \alpha \leq 1} \lim_{b \rightarrow 0} b c_\alpha(k, l, b) = \max_{0 \leq \alpha \leq 1} c = \sum_{p=1}^r \frac{|\mu_p^k - \mu_p^l|}{2v_p}.$$

□

As previously done, we select a node pair  $(i, j)$  such that  $\gamma(i, j)$  from (4.67) is the lowest. In the following steps, we will show that  $\gamma(i, j)$  exactly equals the error exponent. The upper bound on the exponent by  $\gamma(i, j)$  is established by Lemma 15, but we need, once again, to complete the proof for the lower bound. Comparing the probability density function (4.62) with the generalized form (4.1) we note that  $g(x, a) = \sum_{p=1}^r \frac{|x_p - a_p|}{2v_p}$ , and  $h(b) = \prod_{p=1}^r \frac{1}{2bv_p}$ . Now we state the Theorem that lower bounds the error exponent, and the subsequent Theorems 27 and 28 will relate this lower bound to  $\gamma(i, j)$ .

**Theorem 26.** *The following bound holds*

$$\lim_{b \rightarrow 0} \frac{\log(P_e)}{1/b} \geq - \inf_{\mathbf{x} \in \Omega} \sum_{p=1}^r \frac{|x_p - \mu_p^i|}{v_p}, \quad (4.70)$$

$$\text{for } \Omega = \left\{ \mathbf{x} : \sum_{p=1}^r \frac{|x_p - \mu_p^i|}{v_p} > \sum_{p=1}^r \frac{|x_p - \mu_p^j|}{v_p} \right\}. \quad (4.71)$$

*Proof.* We note that  $\Omega = \{ \mathbf{x} : p(\mathbf{x}; H_i) < p(\mathbf{x}; H_j) \}$  is equivalent with (4.71), and does not depend on the noise parameter  $b$ . Therefore, we just need to verify the conditions to apply Lemma 16. First we note that  $\mu^i \notin \Omega$ . Function  $g(\mathbf{x}, \mu^i) = \sum_{p=1}^r \frac{|x_p - \mu_p^i|}{2v_p}$  is non-negative and continuous. We follow the same reasoning as in Case I of Theorem 21 to show that the intersection of the sets  $\Omega$  and  $\mathcal{R}(l, l + \epsilon)$ , where  $l = \inf\{g(\mathbf{x}, \mu^i) | \mathbf{x} \in \Omega\}$ , has a non-empty interior. We also confirm that

$$b \log(h(b)) = b \log\left(\prod_{p=1}^r \frac{1}{2bv_p}\right) = -b \sum_{p=1}^r \log(2bv_p) \xrightarrow{b \rightarrow 0} 0,$$

thereby satisfying all the assumptions of Lemma 16. Applying it proves the claim. □

Unlike in the Gaussian case, the closure of set  $\Omega$  given by (4.71) is not obtained by substituting inequality for equality, which we need to apply duality. Therefore, we will first use duality in Theorem 27 to prove that the derived  $\gamma(i, j)$  equals the minimum value of the density function exponent in the error set  $\Omega' = \{ \mathbf{x} : p(\mathbf{x}; H_i) \leq p(\mathbf{x}; H_j) \}$ . Then in Theorem 28, we prove that this minimum value is the same even if the minimization is in the closure of the set  $\Omega$  given by (4.71). This shows that the lower bound on the exponent established previously by Theorem 26 can be restated in terms of  $\gamma(i, j)$ .

**Theorem 27.** *The optimal value of the minimization*

$$\min_{\mathbf{x} \in \Omega'} \sum_{p=1}^r \frac{|x_p - \mu_p^i|}{v_p} \quad (4.72)$$

equals exactly

$$\sum_{p=1}^r \frac{|\mu_p^j - \mu_p^i|}{2v_p},$$

where

$$\Omega' = \left\{ \mathbf{x} : \sum_{p=1}^r \frac{|x_p - \mu_p^i|}{v_p} \geq \sum_{p=1}^r \frac{|x_p - \mu_p^j|}{v_p} \right\}. \quad (4.73)$$

*Proof.* We can analyze problem (4.72), which is non-convex, by treating the non-convex constraint set as a union of convex sets  $\Omega' = \cup_m \Omega_m$ ,  $m = 1, \dots, 2^{2r}$ , then by solving the problem in each convex set and selecting the minimum of all solutions. The Lagrangian dual function for a problem with a convex constraint  $\mathbf{x} \in \Omega_m$  is

$$L(x_1, \dots, x_r, \nu) = (1 - \nu) \sum_{p=1}^r f_p^i(x) + \nu \sum_{p=1}^r f_p^j(x),$$

where if we have  $x_p \geq \mu_p^i$  in  $\Omega_m$ , then  $f_p^i(x) = \frac{x_p - \mu_p^i}{v_p}$ , and otherwise, it is  $f_p^i(x) = \frac{\mu_p^i - x_p}{v_p}$ , with  $f_p^j(x)$  defined analogously. We can then split the sum into 4 sums to obtain

$$\begin{aligned} L(x_1, \dots, x_r, \nu) = & \sum_{p \in \mathcal{I}_1 \cup \mathcal{I}_2} \frac{x_p - \mu_p^i(1 - \nu) - \mu_p^j}{v_p} + \sum_{p \in \mathcal{I}_3} \frac{(1 - 2\nu)x_p - \mu_p^i(1 - \nu) + \mu_p^j}{v_p} + \\ & + \sum_{p \in \mathcal{I}_4} \frac{(2\nu - 1)x_p + \mu_p^i(1 - \nu) - \mu_p^j}{v_p} + \sum_{p \in \mathcal{I}_5 \cup \mathcal{I}_6} \frac{-x_p + \mu_p^i(1 - \nu) + \mu_p^j}{v_p}, \end{aligned} \quad (4.74)$$

where  $\mathcal{I}_1 = \{l : \mu_p^i < \mu_p^j < x_p\}$ ,  $\mathcal{I}_2 = \{l : \mu_p^j < \mu_p^i < x_p\}$ ,  $\mathcal{I}_3 = \{l : \mu_p^i < x_p < \mu_p^j\}$ ,  $\mathcal{I}_4 = \{l : \mu_p^j < x_p < \mu_p^i\}$ ,  $\mathcal{I}_5 = \{l : x_p < \mu_p^j < \mu_p^i\}$  and  $\mathcal{I}_6 = \{l : x_p < \mu_p^i < \mu_p^j\}$ . Next we find the dual function as

$$L(\nu) = \inf_{\mathbf{x} \in \Omega_p} L(x_1, \dots, x_r, \nu).$$

Finding  $x_p$  that minimizes (4.74) for each sum, and denoting  $t_q = \sum_{p \in \mathcal{I}_q} |\mu_p^i - \mu_p^j|/v_p$ , for  $q = 1, \dots, 6$ , we

obtain the following form for the dual function

$$L(\nu) = \begin{cases} \nu(-t_1 + t_2 + t_3 + t_4 - t_5 + t_6) - t_2 - t_6, & 0 \leq \nu < \frac{1}{2} \\ \frac{1}{2}(-t_1 - t_2 + t_3 + t_4 - t_5 - t_6), & \nu = \frac{1}{2} \\ \nu(-t_1 + t_2 - t_3 - t_4 - t_5 + t_6) - t_2 + t_3 + t_4 - t_6, & \nu > \frac{1}{2} \end{cases}.$$

The maximum value of the dual function in  $\Omega_m$  is  $\frac{1}{2}(-t_1 - t_2 + t_3 + t_4 - t_5 - t_6)$ , for  $\nu = \frac{1}{2}$ . Analyzing this maximum over different  $\Omega_m$ , we see that the maximum is attained for  $\mathcal{I}_q = \emptyset$ ,  $q = 1, 2, 5, 6$ , as each term  $t_q$  is non-negative. Then the maximum of the dual function is exactly  $\sum_{p=1}^r \frac{|\mu_p^i - \mu_p^j|}{2\nu_p}$ , as claimed.  $\square$

Next, we show that the optimal value of the problem (4.72) is the same when the optimization is carried out in the closure of set  $\Omega$  given by (4.71), instead of the set  $\Omega'$  from (4.73).

**Theorem 28.** *The optimal value of the minimization*

$$\min_{\mathbf{x} \in \bar{\Omega}} \sum_{p=1}^r \frac{|x_p - \mu_p^i|}{\nu_p} \quad (4.75)$$

where  $\bar{\Omega}$  is the closure of the set  $\Omega$  defined in (4.71), equals the optimal value of the problem (4.72).

*Proof.* Let  $\mathbf{x}^*$  denote an optimal solution of (4.72). Then, from the proof of Theorem 27, we have that  $\mu_p^i \leq x_p^* \leq \mu_p^j$ , for  $\mu_p^i < \mu_p^j$ , and  $\mu_p^j \leq x_p^* \leq \mu_p^i$ , for  $\mu_p^j < \mu_p^i$ . We also have

$$\sum_{p=1}^r \frac{|x_p^* - \mu_p^i|}{\nu_p} = \sum_{p=1}^r \frac{|\mu_p^j - \mu_p^i|}{2\nu_p}. \quad (4.76)$$

Next, we claim that each such point  $\mathbf{x}^*$  is a limit point of some sequence from the set  $\Omega$ . Let  $\mathbf{y}_k = \mathbf{x}^* + \mathbf{c}$ , where  $\mathbf{c}$  is a vector with entries  $c_p = \frac{\text{sgn}(\mu_p^j - \mu_p^i)\epsilon_p}{k}$ , with  $\text{sgn}$  representing the sign function and  $\epsilon_p \geq 0$ . We will show that  $\mathbf{y}_k \xrightarrow{k \rightarrow \infty} \mathbf{x}^*$  and  $\mathbf{y}_k \in \Omega$ . Let  $\delta_p = |\mu_p^j - \mu_p^i|$ ,  $d_p = |x_p^* - \mu_p^i|$ , then  $|x_p^* - \mu_p^j| = \delta_p - d_p$ . Then we have  $|y_p - \mu_p^i| = d_p + |c_p|$  and  $|y_p - \mu_p^j| = \delta_p - d_p - |c_p|$ , for  $\epsilon_p$  small enough that  $x_p^* + c_p \leq \mu_p^j$ , for  $\mu_p^i < \mu_p^j$  and  $x_p^* + c_p \geq \mu_p^j$  otherwise. Then, using the above and (4.76), we have  $\sum_{p=1}^r \frac{|y_p - \mu_p^i|}{\nu_p} - \sum_{p=1}^r \frac{|y_p - \mu_p^j|}{\nu_p} = \sum_{p=1}^r \frac{|c_p|}{\nu_p} > 0$ . Strict inequality holds as not all  $\epsilon_p$  can be equal to 0, since the points  $\mu^i$  and  $\mu^j$  do not satisfy the condition (4.76) for  $\mathbf{x}^*$ . From here we have that each solution  $\mathbf{x}^*$  is a limit point of a sequence  $\mathbf{y}_k \in \Omega$ , hence  $\mathbf{x}^* \in \bar{\Omega}$ . We also have that  $\bar{\Omega} \subset \Omega'$ , where  $\Omega'$  is defined in (4.73). This holds since  $\Omega'$  is a closed set and contains all its limit points, which includes all the limit points of  $\Omega$ , and therefore includes the closure of  $\Omega$ . Thus, we have that  $\mathbf{x}^*$  is also the solution to (4.75), which completes the claim.  $\square$

With Theorem 26, we established that the error exponent is bounded by the minimum of the function  $g(\mathbf{x}, \mathbf{a})$  in the set  $\Omega$ , while Theorems 27 and 28 show that this minimum exactly equals  $\gamma(i, j)$ . Establishing this lower bound completes the proof that the error exponent for vanishing noise when the observations are modeled as random variables with Laplace distribution is indeed

$$\gamma(i, j) = \sum_{p=1}^r \frac{|\mu_p^i - \mu_p^j|}{2v_p},$$

for

$$(i, j) = \arg \min_{k, l} \gamma(k, l).$$

In the case of  $\mu^i = \mu^j$  there is no exponential error decay. However, the expression for the exponent is still valid, as it evaluates to zero.

#### 4.1.4 Observations are modeled as exponential random variables

In this diffusion model, we again assume that a constant time is needed for an infection to spread from a node to its neighbor, i.e.,  $\theta_{u,v}$  is a constant. To simplify the notation, w.l.o.g, we assume the constant to be 1. However, now we consider that each node shows infection symptoms only after some random time. This models the existence of an incubation period, which is the time that passes between the moment when an individual contracts a virus until the symptoms are exhibited. Similarly, a person might hear about a product and continue spreading the news about it before actually purchasing it. As the exponential noise is the worst possible non-negative additive noise [77], we model the duration of this incubation period as a random variable with exponential distribution, independent across observers. Since individuals might vary in purchasing behavior or in showing symptoms, we characterize each node with its own noise parameter.

We compactly denote the *true* infection time of each observer  $o_p$  as  $a_p^s = d(o_p, s)$ , for a source node  $s$ . Denoting the *observed* infection time of observer  $o_p$  as  $x_p$ , we have

$$x_p = d(o_p, s) + n_p = a_p^s + n_p,$$

where  $n_p$  is an exponential random variable with density  $p(n_p) = \lambda_p e^{-\lambda_p n_p} u(n_p)$ ,  $u(n_p)$  is the discrete step function ( $u(n_p) = 1$  for  $n_p \geq 0$  and  $u(n_p) = 0$  for  $n_p < 0$ ). Stacking the observations from all observers into a vector, we obtain  $\mathbf{x} = \mathbf{a}^s + \mathbf{n}$ . Since we assume the noise in different nodes to be independent, the

observation density is given by

$$p(\mathbf{x}; \mathbf{s}) = \prod_{p=1}^r \lambda_p e^{-\lambda_p(x_p - a_p^s)} u(x_p - a_p^s). \quad (4.77)$$

Let  $\lambda = \min_p \lambda_p$ . Then we can write  $\lambda_p = v_p \lambda$ , for  $p = 1, \dots, r$ . Now, the parameter  $1/\lambda$  has the role of the randomness parameter  $\eta$ , as noise decreases for  $\lambda \rightarrow \infty$ . Next, we evaluate  $\alpha$ -Chernoff divergence (4.4) and obtain

$$\begin{aligned} c_\alpha(k, l, \lambda) &= -\log \left( \prod_{p=1}^r \int p(x_p; k)^\alpha p(x_p; l)^{1-\alpha} dx_p \right) \\ &= -\log \left( \prod_{p=1}^r v_p \lambda e^{v_p \lambda (\alpha a_p^k + (1-\alpha) a_p^l)} \int_{\max\{a_p^k, a_p^l\}}^\infty e^{-v_p \lambda x_p} dx_p \right) \\ &= -\log \left( \prod_{p=1}^r e^{v_p \lambda (\alpha a_p^k + (1-\alpha) a_p^l) - v_p \lambda \max\{a_p^k, a_p^l\}} \right). \end{aligned} \quad (4.78)$$

In this case, we can find a closed form solution for the optimization problem (4.5), to obtain the Chernoff distance between distributions  $p(\mathbf{x}; k)$  and  $p(\mathbf{x}; l)$  [78]

$$C(k, l, \lambda) = \lambda \beta(k, l) \quad (4.79)$$

where

$$\beta(k, l) = \begin{cases} \sum_{p=1}^r \mathbb{I}_{\{a_p^k > a_p^l\}} v_p (a_p^k - a_p^l), & \mathbf{v}^T \mathbf{a}^k \geq \mathbf{v}^T \mathbf{a}^l \\ \sum_{p=1}^r \mathbb{I}_{\{a_p^k < a_p^l\}} v_p (a_p^l - a_p^k), & \mathbf{v}^T \mathbf{a}^k < \mathbf{v}^T \mathbf{a}^l \end{cases}, \quad (4.80)$$

$\mathbb{I}$  is an indicator function for the condition in  $\{\cdot\}$  and  $\mathbf{v} = [v_1, \dots, v_r]^T$ . Now, we can evaluate the limit (4.7) to easily obtain the expression

$$\gamma(k, l) = \beta(k, l). \quad (4.81)$$

As done before, we select a pair  $(i, j)$  that minimizes  $\gamma(k, l)$  to obtain  $\gamma(i, j)$ , which we will now prove to be exactly the error exponent. We follow the same line of reasoning as before and in the next Theorem, we obtain a lower bound on the exponent, while in Theorem 30, we relate this bound to our  $\gamma(i, j)$ .

**Theorem 29.** *The following bound holds*

$$\lim_{\lambda \rightarrow \infty} \frac{\log(P_e)}{\lambda} \geq -\inf_{\mathbf{x} \in \Omega} \mathbf{v}^T (\mathbf{x} - \mathbf{a}^i), \quad (4.82)$$

for

$$\Omega = \{\mathbf{x} : p(\mathbf{x}; i) < p(\mathbf{x}; j)\}. \quad (4.83)$$

*Proof.* Before we apply Lemma 16, we first verify its assumptions. In this case  $h(\lambda) = \prod_{p=1}^r \lambda v_p$ , and we have

$$\frac{1}{\lambda} \log(h(\lambda)) = \sum_{p=1}^r \frac{\log(\lambda v_p)}{\lambda} \xrightarrow{\lambda \rightarrow \infty} 0,$$

thereby satisfying assumption (4.23). The set that characterizes the region of error can be written as  $\Omega = \{\mathbf{x} | \mathbf{x} > \max\{\mathbf{a}^i, \mathbf{a}^j\}\}$ , for  $\mathbf{v}^T \mathbf{a}^i < \mathbf{v}^T \mathbf{a}^j$ . For  $\mathbf{x} \in \Omega$ , the function  $g(\mathbf{x}, \mathbf{a}^i) = \mathbf{v}^T (\mathbf{x} - \mathbf{a}^i)$  is non-negative, continuous and evaluates to 0 for  $\mathbf{x} = \mathbf{a}^i$ . It is easy to see that  $\mathbf{a}^i \notin \Omega$ . Again, for  $l = \inf\{\mathbf{v}^T (\mathbf{x} - \mathbf{a}^i) | \mathbf{x} \in \Omega\}$ , as  $g(\mathbf{x}, \mathbf{a}^i)$  is continuous in the sets  $\Omega$  and  $\mathcal{R}$ , the same arguments apply as in Case I of Theorem 21 to verify that the assumption (4.22) holds. We apply the result of Lemma 16 to obtain the claim.  $\square$

The set  $\Omega$  can be rewritten as  $\Omega = \{\mathbf{x} | \mathbf{x} > \mathbf{a}^i, \mathbf{x} > \mathbf{a}^j\}$ . Since we have linear inequalities that define the open set  $\Omega$ , the closure of the set is then simply  $\bar{\Omega} = \{\mathbf{x} | \mathbf{x} \geq \mathbf{a}^i, \mathbf{x} \geq \mathbf{a}^j\}$ , for  $\mathbf{v}^T \mathbf{a}^i < \mathbf{v}^T \mathbf{a}^j$ .

The following Theorem shows that the lower bound shown in the previous Theorem has the same value as  $\gamma(i, j)$  (4.81).

**Theorem 30.** *The optimal value of the minimization*

$$\begin{aligned} & \min_{\mathbf{x}} \mathbf{v}^T (\mathbf{x} - \mathbf{a}^i) \\ & \text{s.t. } \mathbf{x} \geq \mathbf{a}^i, \mathbf{x} \geq \mathbf{a}^j, \end{aligned} \quad (4.84)$$

when  $\mathbf{v}^T \mathbf{a}^i \leq \mathbf{v}^T \mathbf{a}^j$  holds, equals  $\beta(i, j)$  defined in (4.80).

*Proof.* The Lagrangian dual function of (4.84) is

$$L(\mathbf{x}, \mathbf{v}_1, \mathbf{v}_2) = (\mathbf{v} - \mathbf{v}_1 - \mathbf{v}_2)^T \mathbf{x} + \mathbf{v}_1^T \mathbf{a}^i + \mathbf{v}_2^T \mathbf{a}^j - \mathbf{v}^T \mathbf{a}^i. \quad (4.85)$$

The dual function is

$$\begin{aligned} L(\mathbf{v}_1, \mathbf{v}_2) &= \inf_{\mathbf{x}} L(\mathbf{x}, \mathbf{v}_1, \mathbf{v}_2) \\ &= \begin{cases} \mathbf{v}_1^T \mathbf{a}^i + \mathbf{v}_2^T \mathbf{a}^j - \mathbf{v}^T \mathbf{a}^i, & \mathbf{v}_1 + \mathbf{v}_2 = \mathbf{v} \\ -\infty, & \text{otherwise} \end{cases}. \end{aligned}$$

Then the dual problem of (4.84) is

$$\begin{aligned} & \max (\boldsymbol{v}_1 - \boldsymbol{v})^T \boldsymbol{a}^i + \boldsymbol{v}_2^T \boldsymbol{a}^j \\ & \text{s.t. } \boldsymbol{v}_1, \boldsymbol{v}_2 \geq \mathbf{0}, \quad \boldsymbol{v}_1 + \boldsymbol{v}_2 = \boldsymbol{v}. \end{aligned} \quad (4.86)$$

Strong duality holds for problem (4.84) and its dual (4.86) [75]. KKT conditions are

$$\begin{aligned} & \boldsymbol{v} - \boldsymbol{v}_1 - \boldsymbol{v}_2 = \mathbf{0} \\ & \boldsymbol{a}^i - \boldsymbol{x} \leq \mathbf{0}, \quad \boldsymbol{a}^j - \boldsymbol{x} \leq \mathbf{0} \\ & \boldsymbol{v}_1, \boldsymbol{v}_2 \geq \mathbf{0}, \quad \boldsymbol{v}_1^T (\boldsymbol{a}^i - \boldsymbol{x}) = 0 \\ & \boldsymbol{v}_2^T (\boldsymbol{a}^j - \boldsymbol{x}) = 0. \end{aligned} \quad (4.87)$$

From (4.87), we have either that  $v_{1p} = 0, v_{2p} = v_p, x_p = a_p^i$  for  $a_p^j \geq a_p^i$ , or  $v_{1p} = v_p, v_{2p} = 0, x_p = a_p^i$  for  $a_p^i \geq a_p^j$ . This exactly gives us the first row of  $\beta(i, j)$  from (4.80) when  $\boldsymbol{v}^T \boldsymbol{a}^i \leq \boldsymbol{v}^T \boldsymbol{a}^j$ . Now, reversing  $i$  and  $j$ , and assuming  $\boldsymbol{v}^T \boldsymbol{a}^j \leq \boldsymbol{v}^T \boldsymbol{a}^i$  from the beginning, we get the second row of (4.80).  $\square$

With this we conclude that the error exponent is also lower bounded by  $\gamma(i, j)$ . Hence the error exponent for vanishing noise when the observations are modeled as variables with exponential distribution is indeed

$$\gamma(i, j) = \begin{cases} \sum_{p=1}^r \mathbb{I}_{\{a_p^i > a_p^j\}} v_p (a_p^i - a_p^j), & \boldsymbol{v}^T \boldsymbol{a}^i \geq \boldsymbol{v}^T \boldsymbol{a}^j \\ \sum_{p=1}^r \mathbb{I}_{\{a_p^i < a_p^j\}} v_p (a_p^j - a_p^i), & \boldsymbol{v}^T \boldsymbol{a}^i < \boldsymbol{v}^T \boldsymbol{a}^j \end{cases}, \quad (4.88)$$

for

$$(i, j) = \arg \min_{k, l} \gamma(k, l).$$

In the case of  $\boldsymbol{a}^i = \boldsymbol{a}^j$  the error decay is not exponential. However, the expression for the error exponent (4.80) is still valid, as it evaluates to zero.

### Properties of the exponent

We have shown that the error exponent for vanishing noise when the observations are modeled as variables with exponential distribution equals (4.88). In the next Theorem, we show that the exponent has an interesting property.

**Theorem 31.**  $\gamma(i, j)$ , given by (4.88), is a metric.

*Proof.* To show that  $\gamma(i, j)$  satisfies all the conditions for a metric, we first reformulate (4.88). Let  $\mathbf{q}^+$  denote a vector where negative entries of  $\mathbf{q}$  are replaced with 0, i.e.,  $q_i^+ = \max\{0, q_i\}$ . Similarly, let  $\mathbf{q}^-$  denote a vector where positive entries of  $\mathbf{q}$  are set to 0, but instead of negative values, their absolute values are taken. Let  $\cdot$  denote an operator of a pointwise product. Then for any vector  $\mathbf{q}$ , we have  $\mathbf{q} = \mathbf{q}^+ - \mathbf{q}^-$  and for a positive vector  $\mathbf{v} > \mathbf{0}$  we have

$$\begin{aligned}\|\mathbf{v} \cdot \mathbf{q}\|_1 &= \mathbf{v}^T \mathbf{q}^+ + \mathbf{v}^T \mathbf{q}^- \\ \mathbf{v}^T \mathbf{q} &= \mathbf{v}^T \mathbf{q}^+ - \mathbf{v}^T \mathbf{q}^-. \end{aligned} \quad (4.89)$$

Summing the two expressions of (4.89) gives

$$\mathbf{v}^T \mathbf{q}^+ = \frac{1}{2} (\|\mathbf{v} \cdot \mathbf{q}\|_1 + \mathbf{v}^T \mathbf{q}). \quad (4.90)$$

Now we can rewrite (4.88) as

$$\begin{aligned}\gamma(i, j) &= \mathbb{I}_{\{\mathbf{v}^T \mathbf{a}^i > \mathbf{v}^T \mathbf{a}^j\}} \mathbf{v}^T (\mathbf{a}^i - \mathbf{a}^j)^+ + \\ &\mathbb{I}_{\{\mathbf{v}^T \mathbf{a}^i = \mathbf{v}^T \mathbf{a}^j\}} \mathbf{v}^T (\mathbf{a}^i - \mathbf{a}^j)^+ + \mathbb{I}_{\{\mathbf{v}^T \mathbf{a}^i < \mathbf{v}^T \mathbf{a}^j\}} \mathbf{v}^T (\mathbf{a}^j - \mathbf{a}^i)^+. \end{aligned} \quad (4.91)$$

When  $\mathbf{v}^T \mathbf{a}^i = \mathbf{v}^T \mathbf{a}^j$  holds, then  $\mathbf{v}^T (\mathbf{a}^i - \mathbf{a}^j) = 0$  and substituting  $\mathbf{q} = \mathbf{a}^i - \mathbf{a}^j$  in (4.90), we obtain  $\mathbf{v}^T (\mathbf{a}^i - \mathbf{a}^j)^+ = \frac{1}{2} \|\mathbf{v} \cdot (\mathbf{a}^i - \mathbf{a}^j)\|_1$ . Again, using (4.90), we can rewrite (4.88) as

$$\begin{aligned}\gamma(i, j) &= \mathbb{I}_{\{\mathbf{v}^T \mathbf{a}^i > \mathbf{v}^T \mathbf{a}^j\}} \frac{1}{2} (\|\mathbf{v} \cdot (\mathbf{a}^i - \mathbf{a}^j)\|_1 + \mathbf{v}^T (\mathbf{a}^i - \mathbf{a}^j)) \\ &+ \mathbb{I}_{\{\mathbf{v}^T \mathbf{a}^i = \mathbf{v}^T \mathbf{a}^j\}} \frac{1}{2} \|\mathbf{v} \cdot (\mathbf{a}^i - \mathbf{a}^j)\|_1 \\ &+ \mathbb{I}_{\{\mathbf{v}^T \mathbf{a}^i < \mathbf{v}^T \mathbf{a}^j\}} \frac{1}{2} (\|\mathbf{v} \cdot (\mathbf{a}^j - \mathbf{a}^i)\|_1 + \mathbf{v}^T (\mathbf{a}^j - \mathbf{a}^i)) \end{aligned}$$

Finally, we have

$$\gamma(i, j) = \frac{1}{2} \|\mathbf{v} \cdot (\mathbf{a}^i - \mathbf{a}^j)\|_1 + \frac{1}{2} |\mathbf{v}^T \mathbf{a}^i - \mathbf{v}^T \mathbf{a}^j|. \quad (4.92)$$

From (4.92), we directly see that positive-definiteness and symmetry hold. Substituting  $\mathbf{x} = \mathbf{v} \cdot (\mathbf{a}^i - \mathbf{a}^j)$  and  $\mathbf{y} = \mathbf{v} \cdot (\mathbf{a}^j - \mathbf{a}^k)$  into  $\|\mathbf{x} + \mathbf{y}\|_1 \leq \|\mathbf{x}\|_1 + \|\mathbf{y}\|_1$ , and  $\mathbf{x} = \mathbf{v}^T \mathbf{a}^i - \mathbf{v}^T \mathbf{a}^j$  and  $\mathbf{y} = \mathbf{v}^T \mathbf{a}^j - \mathbf{v}^T \mathbf{a}^k$  into  $|\mathbf{x} + \mathbf{y}| \leq |\mathbf{x}| + |\mathbf{y}|$ , we see that  $\gamma(i, k) \leq \gamma(i, j) + \gamma(j, k)$  also holds. Thus  $\gamma(i, j)$  is a metric.  $\square$

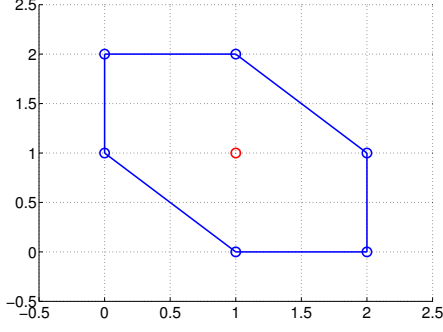


Figure 4.1: Unit ball in two-dimensional space for  $\gamma(i, j)$ , centered at a point  $\mathbf{a}^i = \mathbf{1}$  and  $\mathbf{a}^j = \mathbf{1}$  denoted with a red circle.

In the proof of Theorem 31, we have made no assumption on the arguments  $\mathbf{a}^i$  and  $\mathbf{a}^j$ , and we have shown that  $\gamma(i, j)$  is a metric for any two real vectors.

Next, we further examine the properties of the derived exponent  $\gamma(i, j)$ , for the simplified case of  $\mathbf{v} = \mathbf{1}$ . A unit ball defined in this case is shown in Figure 4.1. The blue line in Figure 4.1 contains all the points which are at distance 1 from the red point, where distance is defined with  $\gamma(i, j)$ , for two vectors  $\mathbf{a}^i$  and  $\mathbf{a}^j$ . Since in our specific case spatial coordinates represent graph distances to observer nodes, which are integers, only the vertices of the unit ball are possible values for  $\mathbf{a}^i$  at distance 1 (given that the ball is centered at a point with integer coordinates).

Although each  $\gamma(k, l)$  can be calculated in  $\mathcal{O}(r)$  time, still  $\binom{N}{2}$  pairwise values of  $\gamma(k, l)$  need to be calculated for each of  $\binom{N}{r}$  different subsets that are examined in order to select an optimal subset. Next, we present some basic bounds for the error exponent, given that  $\mathbf{v} = \mathbf{1}$ . Let  $\gamma(O_r)$  denote the smallest  $\gamma(i, j)$  for all  $i, j$  pairs for a fixed subset  $O_r$ , while  $\gamma(r)$  denotes the smallest  $\gamma(i, j)$  for all  $i, j$  pairs for any observer subset of cardinality  $r$ .

**Theorem 32.** *The following bounds hold*

$$\gamma(O_r) > 0 \iff O_r \text{ is a resolving set.} \quad (4.93)$$

$$\gamma(O_r) \leq \gamma(O_r \cup o_{r+1}) \quad (4.94)$$

$$\gamma(r) \leq r. \quad (4.95)$$

*Proof.* From (4.88) it follows that  $\gamma(i, j) = 0$  if and only if  $\mathbf{a}^i = \mathbf{a}^j$ , i.e., if nodes  $i$  and  $j$  are equidistant to all the observer nodes. Then the set  $O_r$  cannot be a resolving set, which is by definition a set of nodes  $O$  such that each pair of nodes has a different distance to at least one node from  $O$  [52].

The following inequality (4.94) is intuitive, as it states that the distances between distributions that characterize source candidates will not decrease if a new node is observed, and consequently, the error will not decrease any slower if an additional observation is included. Including a new observer node adds a new

entry to  $\mathbf{a}^i$  and  $\mathbf{a}^j$ , which cannot decrease either  $(\mathbf{a}^i - \mathbf{a}^j)^+$  or  $(\mathbf{a}^j - \mathbf{a}^i)^+$ . Then each pairwise distance as seen from (4.91) does not decrease. This also holds for the smallest distance. Note that here we only claim that for a fixed subset, a new observer cannot decrease the distance, and hence we also have  $\gamma(r) \leq \gamma(r+1)$ , but it is not generally true that  $\gamma(O_r) \leq \gamma(O_{r+1})$ , if  $O_r \not\subset O_{r+1}$ .

Inequality (4.95) comes from analyzing  $\gamma(i, j)$ , when  $i$  and  $j$  are neighbor nodes. For any observer  $o_l$ , we have that  $d(i, o_l) \in \{d(j, o_l) - 1, d(j, o_l), d(j, o_l) + 1\}$  when  $i$  and  $j$  are connected by an edge. Hence  $|a_l^i - a_l^j| = |d(i, o_l) - d(j, o_l)| \leq 1$ , and for  $r$  observers we have  $\|\mathbf{a}^i - \mathbf{a}^j\|_1 \leq r$  and  $|\mathbf{1}^T \mathbf{a}^i - \mathbf{1}^T \mathbf{a}^j| \leq r$ . Using these in (4.92), we have that  $\gamma(i, j) \leq r$ , when  $i$  and  $j$  are neighbors, and the same then holds for the minimal  $\gamma(i, j)$ .  $\square$

In order to understand how the source localization error differs across different topologies and what is the best possible exponent that can be reached with any subset selection for a given topology, we analyze the idealized case when all nodes are monitored.

**Theorem 33.** *For a complete network  $\gamma(N) = 1$ , for a star  $\gamma(N) = 2$ , for a path  $\gamma(N) = \lceil \frac{N}{2} \rceil$  and for a tree  $\gamma(N) \leq \max\{2(\tau_a + 1), 2(\tau_b + 1)\}$ , where  $a$  and  $b$  are nodes at distance 1 to a common ancestor, and  $\tau_s$  is the number of descendants of node  $s$ .*

*Proof.* Observing all nodes in a complete graph, for any two nodes  $i$  and  $j$ , we have that  $\mathbf{d}(i, O_N)$  and  $\mathbf{d}(j, O_N)$  differ only in two entries, as  $0 = d(i, i) \neq d(i, j) = 1$  and vice versa, hence  $\gamma(N) = \gamma(i, j) = 1$ .

In a star network,  $\mathbf{d}(i, O_N)$  and  $\mathbf{d}(j, O_N)$  for any two leaf nodes differ only in the entries  $i$  and  $j$ . Since  $d(i, j) = 2$ , this pair determines the minimal  $\gamma(i, j)$ , as  $\mathbf{d}(i, O_N)$  and  $\mathbf{d}(c, O_N)$ , where  $c$  represents the central node, differ in all the entries.

In a path network, we label the nodes sequentially, and denote with  $\beta = \lceil \frac{d(i, j)}{2} \rceil^2$  if  $d(i, j)$  is an odd number, and  $\beta = \frac{d(i, j)}{2} \left( \frac{d(i, j)}{2} - 1 \right)$  otherwise. Then it can be shown that  $C(i, j) = \beta + d(i, j) + d(i, j) \max\{i - 1, N - i - d(i, j)\}$ . The minimum is reached for  $d(i, j) = 1$  and  $i = \lceil \frac{N}{2} \rceil$ , and equals  $\lceil \frac{N}{2} \rceil$ .

The bound for  $\gamma(N)$  in trees is obtained by analyzing  $\gamma(i, j)$ , when  $a$  and  $b$  are both at a distance 1 to a common ancestor. Then, nodes  $a$  and  $b$  are equidistant to all the nodes except themselves and their descendants. For any node  $o$  that is a descendent of  $a$ , we have  $d(o, a) - d(o, b) = d(a, b) = 2$ , from which the bound follows. Although not straightforward, this bound is useful in cases such as when a tree has two leaves connected to the same node (like in a star network). Then, regardless of the remaining structure of the tree, or selected observer subset, the error exponent can be at most 2.  $\square$

#### 4.1.5 Simulation results

In the previous section we have derived exact expressions for error exponents for three different propagation models. Selecting the subsets that achieve the highest error exponent would guarantee the fastest error decay

for vanishing noise. Now, we illustrate the applicability of the proposed framework in the case of non-negligible noise. We show that selecting the subsets with higher exponents leads to lower error probability through two sets of simulations, the first modeling the infection times as Gaussian, and the second as exponential variables. The results are similar to the case of infection times modeled as Laplace variables, hence, to avoid repetition, we omit this case.

The first application we simulated is the selection of a spanning tree when infection times are modeled as multivariate Gaussian variables. We generated 100 random 20-node trees and from each tree we selected 9 of its leaves, assuming they are the data collection points. We assumed the propagation delay along the edges and activation time to be random variables with distribution  $\mathcal{N}(1, \sigma^2)$ , where  $\sigma \in [0.1, 0.5]$ . Since calculating the exact error probability is not computationally feasible, we ran 2000 Monte Carlo trials for each tree to get the error estimate. For each tree, we calculated its error exponent.

The second set of simulations illustrates the merits of the proposed metric for the selection of a subset of nodes in an Erdős-Rényi graph when observed infection times are modeled as exponential random variables. We generated 100 Erdős-Rényi graphs with 20 nodes, and within each graph we selected 500 sets of 5 different observers. For each subset in each graph, we evaluated the exact error probability, which is computationally very intensive, and hence smaller size graphs were used. Also, for each subset, its error exponent was calculated. The simulated observation noise had mean in the range  $[0.2, 3.3]$ . Since the graphs had true infection times in the range  $[0, 6]$ , this represents significant noise.

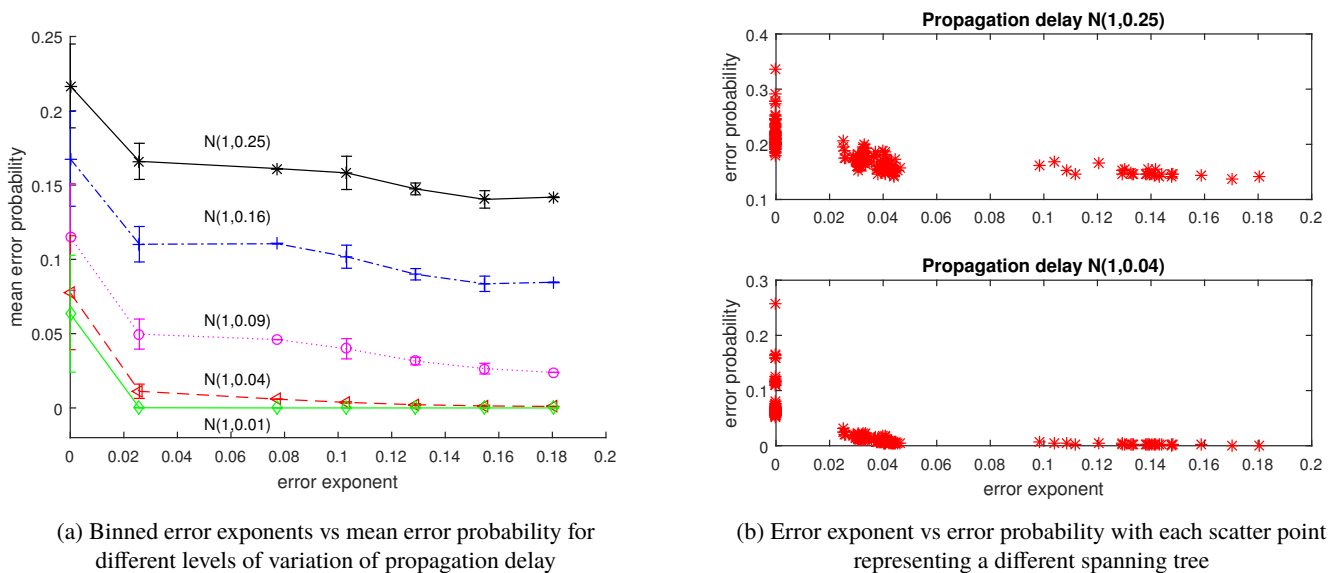


Figure 4.2: Relationship between error probability and error exponents for 200 trees of 20 nodes and 9 observers where infection times of the observers are modeled as variables with multivariate Gaussian distribution

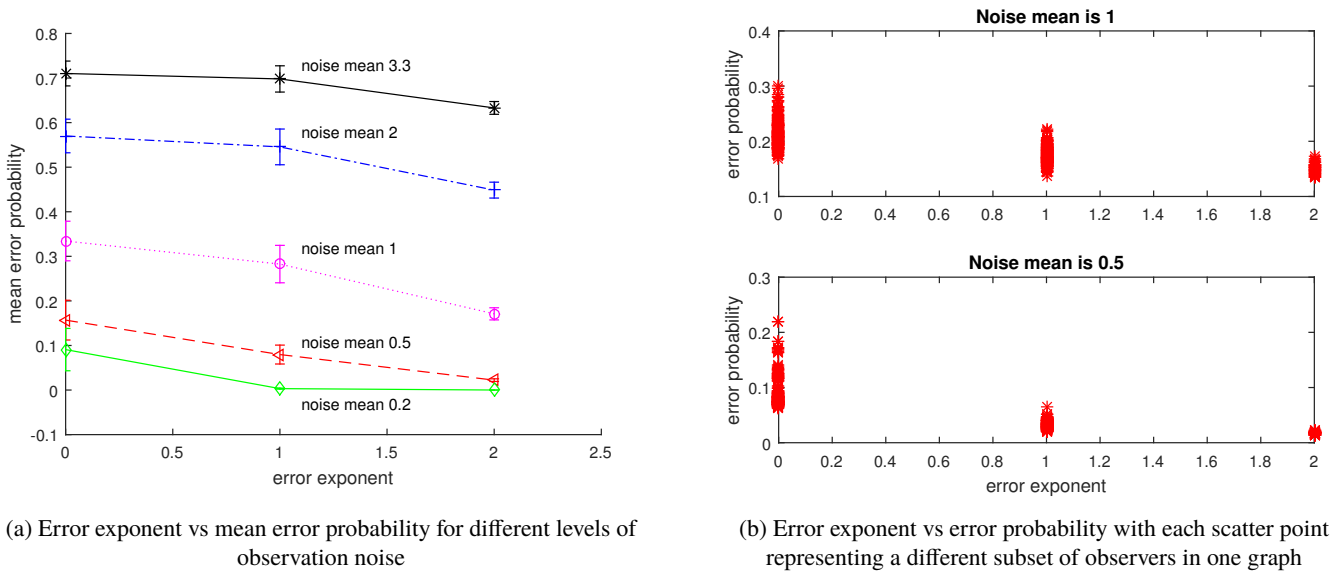


Figure 4.3: Relationship between error probability and error exponents for 100 Erdős-Rényi graphs of 20 nodes and 500 different subsets of 5 observers where infection times of the observers are modeled as variables with exponential distribution

Figure 4.2 shows the relationship between the error probability and our error exponent for the first setup, while Figure 4.3 illustrates it for the second. For Figure 4.2a, for each value of  $\sigma^2$ , we bin the exponents of trees in 8 equally spaced groups, and for each group, we find the average error probability. For Figure 4.3a, for each value of  $\lambda$ , the error probability of the subsets with the same exponent was averaged. Both figures clearly show that trees (subsets) with a higher error exponent have a lower error probability. Plotted error

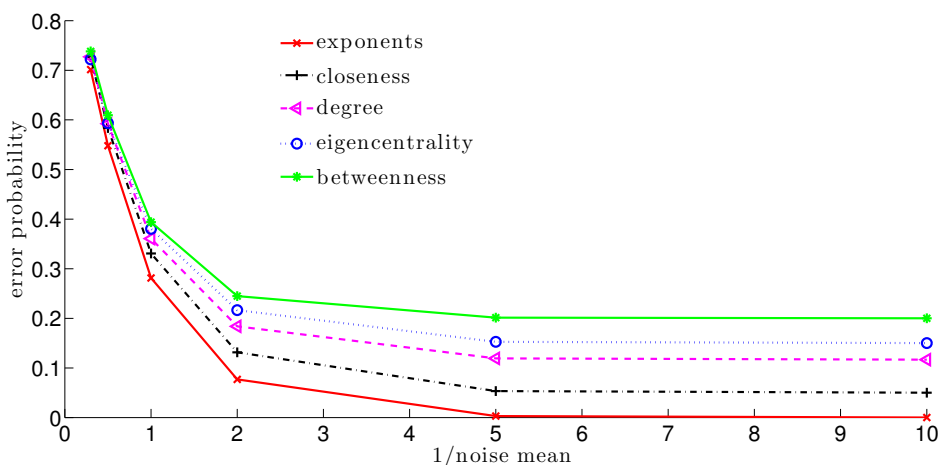


Figure 4.4: Comparison of average error probability achieved by subsets with the highest exponents with subsets that have the highest centrality measures

bars show the standard deviation of the error probability within each exponent group. It can be seen that this deviation decreases with the decrease of the randomness of observations. For very small randomness, for non-zero exponent groups, the error probability approaches zero. This decay is faster for groups with higher exponents. Zero exponent means that there are nodes characterized by the same probability distribution, i.e.,  $p(i) = p(j)$ , for some  $i \neq j$ , and hence they cannot be distinguished even in a deterministic setting. Then, the subsets that have a zero value exponent correspond to a non-resolving set of a give graph, as they cannot distinguish all the nodes in a deterministic setting.

Figure 4.2b shows two scatter plots, one where propagation along the edge is a random variable with distribution  $\mathcal{N}(1, 0.25)$ , and the second with  $\mathcal{N}(1, 0.04)$ , where each point represents one of 200 trees. Figure 4.3b also shows two scatter plots, one for  $\lambda = 1$ , and the second for  $\lambda = 1/0.5$ , where each point represents one of 500 subsets of one specific graph. Both plots show that selection of a tree (subset) with a higher exponent, generally leads to a lower error probability, even with higher randomness of infection times. Again, a decrease in randomness decreases the error, with faster decay experienced by trees (subsets) with higher exponents.

Figures 4.2 and 4.3 illustrate that the proposed metric indeed provides a useful tool for selection of a subset that achieves low error probability. Next, we compare the error probability of the subset with the highest exponent with subsets that have the highest centrality measures, which is the current state of the art for subset selection. We looked at the following centralities: degree (how connected a node is), closeness (how easily a node can reach other nodes), betweenness (how important a node is in terms of connecting other nodes), and eigencentrality (how central are node's neighbors) [61]. We used the same 100 random Erdős-Rényi graphs with 20 nodes generated for the setup where observed infection times are modeled as exponential random variables. For each graph, the same 500 sets of 5 different observers were analyzed and the subset with the highest exponent was selected. Additionally, subsets with the highest degree, closeness, betweenness and eigencentrality were selected. The error probabilities of these subsets were evaluated for a fixed level of noise, and the results were averaged for all graphs. This was repeated for different levels of noise and the obtained plot is shown in Figure 4.4. It clearly shows that the average error probability of the subset with the highest exponent is lower than of the subset chosen by any centrality, regardless of the noise level. Therefore, the simulation results indicate that the proposed metric achieves better performance than all the strategies currently present in the literature. One possible explanation could be because the centrality based strategies take into consideration only the network structure, while the proposed metric additionally depends on the parameters of the propagation hence, it incorporates more information on which the error probability depends on.

## 4.2 Sequential selection

In this section, we return to the problem of dynamic observer selection, but now for stochastic infection times. We will again adopt a diffusion model described in Subsection 4.1.2 where the infection times are modeled as correlated Gaussian random variables. In this model, the propagation delay along the edge that connects two neighboring nodes is modeled as a Gaussian variable with known parameters. The model allows for either known statistical characterization of the source activation time, as well as for completely unknown time. What differs in these two scenarios is that the observations in the first scenario are directly observed infection times, while for the second, differences of infection times are used instead. These differences are again modeled as Gaussian correlated variables.

In the sequential selection, we are interested in finding a strategy of choosing observers such that the source is localized with the smallest cost, as observing each node has a cost associated with obtaining its infection times. If all nodes have equal cost, we are simply interested in determining the source using the smallest number of observers. As the observations have uncertainty, obtaining the source candidates from the observations is not as straightforward as it was for the deterministic case, and we need to resort to source estimation. Also, a stopping criterion needs to be defined, in order to determine when sufficient certainty in the source identity has been reached. In order to design an algorithm for sequential observer selection for stochastic observations, we again resort to multiple hypothesis testing, but this time, to the sequential settings.

The goal of hypothesis testing is to classify a sequence of observations into one of  $M \geq 2$  hypothesis, using the statistical characterization of observations under each hypothesis [79]. In sequential settings, the number of observations used to reach a decision is variable and there is a trade-off between decision accuracy and the number of observations used. While for the binary case  $M = 2$ , there exists a sequential test that is optimal in the sense that it minimizes the average number of observations among all sequential and non-sequential tests, there are no such available general results for  $M \geq 3$  [79]. Even in the case when there is such a test, determining its parameters is not tractable [79]. Instead, sub-optimal sequential tests have been developed that have a simple structure and asymptotic optimality. Two tests have been proposed [80, 81, 82] that are asymptotically optimal relative to the expected number of observations when the error probabilities are vanishingly small, even when the observations are neither identical nor identically distributed, under certain conditions. For sequential source localization, we apply a sequential test whose stopping time is lower for given thresholds [79]. Next, we provide the details of the test from [79, 82].

Let  $H_s$ , for  $s = 1, \dots, M$  be a hypothesis characterized with density function  $p(\mathbf{x}; s)$  and a prior

distribution  $\pi_i > 0$ . Let  $\alpha_i$  be the probability of accepting hypothesis  $H_i$  incorrectly. Then we have

$$\alpha_i = \sum_{\substack{j=1, \\ j \neq i}}^M \pi_j \alpha_{ji}, \quad (4.96)$$

where  $\alpha_{ji}$  is the probability of accepting  $H_i$  when  $H_j$  is the true hypothesis. Next, for

$$a_i = \log \frac{\pi_i}{\alpha_i}, \quad (4.97)$$

the stopping threshold is defined as

$$b_i = \frac{e^{a_i}}{1 + e^{a_i}}. \quad (4.98)$$

Let  $\mathbf{x}_k$  be a vector of observations obtained up to a time step  $k$ . Then,  $\Pi_i(k)$  is the posterior probability distribution of the hypothesis  $H_i$  after obtaining  $k$  observations. It can be written as

$$\Pi_i(k) = \frac{\pi_i p(\mathbf{x}_k; i)}{\sum_{j=1}^M \pi_j p(\mathbf{x}_k; j)}. \quad (4.99)$$

The stopping time  $\tau$  of the sequential test is then defined as the first  $k$  such that

$$\Pi_i(k) > b_i, \quad (4.100)$$

for at least one  $i$ . The decision is made in favor of hypothesis  $H_m$ , where  $m$  is

$$m = \arg \max_j \Pi_j(\tau).$$

Defined as such, the test outputs a decision without exceeding the previously specified probability of accepting  $H_i$  incorrectly which is given by (4.96), for each  $i = 1, \dots, M$ . Next, we apply the above-described sequential test for source localization.

We frame source localization as a multiple hypothesis testing problem, where each hypothesis represents a different node being the source, as described in Section 4.1. Each hypothesis  $H_s$ ,  $s = 1, \dots, N$ , is described with the conditional density of the observations  $p(\mathbf{x}; s)$  of a given set of observers and for a fixed source  $s$ . We can obtain the statistical characterization of the observations  $p(\mathbf{x}; s)$  as described in Subsection 4.1.2. When certain knowledge of source activation times is assumed, observations correspond to the infection times and are Gaussian variables, with mean given by (4.33) and covariance defined by (4.32). In the absence

of any knowledge of activation time, the mean is given by (4.35) while the covariance is defined by (4.36), as the observations are again modeled as correlated Gaussian variables. In both cases, we are assuming the underlying topology is a tree, based on the same reasoning as in Subsection 4.1.2. It is important to note that for a different set of observers the density  $p(\mathbf{x}; s)$ , characterizing a hypothesis  $H_s$ , changes. As more observers are selected, the dimension of observations  $\mathbf{x}$  increases, and densities of all hypotheses change accordingly.

Now, the process of sequential source localization is performed as follows. In the absence of prior knowledge, initially, all nodes are assumed to be equally likely the source and we have  $\pi_i = 1/N$ , for  $i = 1, \dots, N$ . We set the  $\alpha_{ji} = \beta$  as the probability of accepting  $H_i$  when  $H_j$  is the true hypothesis, for all  $i \neq j$  pairs. Then, from (4.96), the probability of accepting  $H_i$  incorrectly is set to

$$\alpha_i = \frac{N-1}{N} \beta, \quad (4.101)$$

and from (4.97), we obtain

$$a = -\log(\beta(N-1)). \quad (4.102)$$

The stopping threshold from (4.98) equals

$$b = \frac{1}{1 + \beta(N-1)}. \quad (4.103)$$

The posterior probability distribution for hypothesis which represents node  $i$  being the source is updated after  $k$  observations as

$$\Pi_i(k) = \frac{(\det \Sigma_i)^{-\frac{1}{2}} e^{-\frac{1}{2}(\mathbf{x}_k - \mu_i)^T \Sigma_i^{-1} (\mathbf{x}_k - \mu_i)}}{\sum_{j=1}^N (\det \Sigma_j)^{-\frac{1}{2}} e^{-\frac{1}{2}(\mathbf{x}_k - \mu_j)^T \Sigma_j^{-1} (\mathbf{x}_k - \mu_j)}}. \quad (4.104)$$

The stopping time from (4.100) now simplifies to

$$\tau = \inf \left\{ k : \max_i \Pi_i(k) > b \right\}, \quad (4.105)$$

and the test decides in favor of  $H_m$ , the hypothesis for which the threshold is reached.

After the first observer is selected, the posterior probability distribution of each hypothesis,  $\Pi_i(1)$  is updated and the condition for stopping is checked, i.e., whether  $\max_i \Pi_i(1) > b$  holds. If the condition is met, the hypothesis  $H_m$  which exceeds the threshold is chosen as the true one, meaning that node  $m$  is the most likely source candidate. If the condition is not met for any hypothesis after the first observation, the test proceeds, another observation is obtained and the condition is checked again. The process is repeated

until the criterion is met, or all the nodes have been observed. Although the sequential test can be applied to the context of sequential source localization as described, there are a few issues that need to be resolved.

For a small number of observers, it might happen that not all nodes are characterized by unique densities  $p(\mathbf{x}; s)$ . Instead, there may exist nodes  $i \neq j$  for which  $p(\mathbf{x}; i) = p(\mathbf{x}; j)$  holds. Then, no observation from the current set of observers can distinguish between hypotheses  $H_i$  and  $H_j$ , as their characterization of the observations is the same, and, hence, nodes  $i$  and  $j$  cannot be distinguished. If such nodes are not the ones whose evaluated posterior distribution crosses the threshold, then inability to distinguish them has no consequence on determining the source identity. Otherwise, other observers should be selected until there is only a single hypothesis that crosses the threshold. Therefore, after selecting each observer, densities  $p(\mathbf{x}; s)$  are formulated for the current observer set. Nodes that are characterized by the same  $p(\mathbf{x}; s)$  are grouped into an equivalence class. Updated posterior distributions of these classes are checked to see if any one of them crosses the threshold. If the distribution that crosses the threshold characterizes a group of nodes, or if no distribution crosses the threshold, another observer is selected. Otherwise, the test is considered complete.

Now, that a method for determining the source and the stopping criterion have been established, we again address the question of observer selection. As the observations are not known in advance, we cannot select at time step  $k$  a node which would directly maximize  $\max_i \Pi_i(k)$  in order to meet the stopping criterion (4.105) with the fewest possible observers. The metric based on error exponents proposed in Section 4.1 can be used for selecting the subsequent observer, but is more suitable for the block, than for sequential selection as explained next. For very few observers, as previously discussed, there might be nodes characterized by the same density and forming an equivalence class. The error exponent can be used to compare the performance of different observer subsets from the perspective of distinguishing between different classes. However, in sequential settings, the number of nodes belonging to an equivalence class is also very important, as the goal is to select a single source candidate with a pre-specified certainty, starting from a single observer. Therefore, choosing the subsequent observer such that it maximizes the error exponent for the current source candidates could be a selection strategy, but it might be more beneficial when the number of observers is not very low. In order to take into consideration the number of nodes belonging to an equivalence class, i.e., the nodes that are characterized by the same density  $p(\mathbf{x}; s)$ , we resort to the observer selection method for deterministic infection times, presented in Subsection 2.2.2.

For sequential observer selection when the infection times have no uncertainty, it was shown that selecting an observer that maximizes the weighted expected decrease in the number of source candidates incurs a source localization cost that is bounded in terms of optimal cost. As such greedy observer selection was shown to be efficient and with performance comparable to optimal, we again apply it for sequential selection, with only a slight adaptation. Let  $O = \{o_1, \dots, o_k\}$  be a set of currently selected observers and  $S(O)$  a set of the current source candidates as determined by the sequential test. With

---

**Algorithm 7** Greedy algorithm for sequential source localization when the infection times are stochastic

---

```
1:  $O \leftarrow \emptyset$  //  $O$  is the current observer set
2:  $S(O) \leftarrow \{1, \dots, N\}$  //  $S(O)$  is the set of current source candidates
3: continue  $\leftarrow 1$  // continue is the flag for proceeding with the test
4: set  $\beta$  and determine  $b$  from (4.103) //  $\beta$  is the probability of accepting  $H_i$  when  $H_j$  is true
5: set  $k = 0$  //  $k$  is the number of selected observers

6: while  $|S(O)| > 1$  OR continue = 1 do
7:    $k \leftarrow k + 1$ 
8:   if  $k = 1$  AND difference of infection times are used as observations then
9:     // Initially, when the differences are used, two observers have to be selected at the same time
10:    foreach  $o_i, o_j \in V \setminus O$  do  $\Delta(o_i, o_j | S(O)) = |S(O)| - \frac{1}{|S(O)|} \sum_{s \in S(O)} |S_d^s(O \cup \{o_i, o_j\})|$ 
11:    Select  $(o_1^*, o_2^*) \in \arg \max_{o_i, o_j} \frac{\Delta(o_i, o_j | S(O))}{c(o_i) + c(o_j)}$ 
12:     $O \leftarrow O \cup \{o_1^*, o_2^*\}$ 
13:     $k \leftarrow k + 1$ 
14:    Observe  $o_1^*, o_2^*$  and form the vector of all the available observations  $\mathbf{x}_k$ 
15:  else
16:    foreach  $o \in V \setminus O$  do  $\Delta(o | S(O)) = |S(O)| - \frac{1}{|S(O)|} \sum_{s \in S(O)} |S_d^s(O \cup o)|$ 
17:    Find all  $o' \in \arg \max_o \frac{\Delta(o | S(O))}{c(o)}$ 
18:    foreach  $o'$  do  $\delta(o' | S(O)) = - \sum_{s \in V \setminus S(O)} |S_d^s(O \cup o')|$ 
19:    Select  $o^* \in \arg \max_{o'} \delta(o' | S(O))$ 
20:     $O \leftarrow O \cup \{o^*\}$ 
21:    Observe  $o^*$  and form the vector of all the available observations  $\mathbf{x}_k$ 
22:  end if
23:  foreach  $i = 1$  to  $N$  do construct  $p(\mathbf{x}; i)$ 
24:  Group nodes with same  $p(\mathbf{x}; i)$  into an equivalence class
25:  foreach equivalence class  $j$  update the posterior probability distribution  $\Pi_j(k)$  given by (4.104)
26:  Find  $m = \arg \max_j \Pi_j(k)$ 
27:  Find the set  $\mathcal{S}$  of all nodes that belong to an equivalence class  $m$ 
28:   $S(O) \leftarrow \mathcal{S}$ 
29:  if  $\Pi_m(k) > b$  then
30:    continue = 0
31:  else
32:    continue = 1
33:  end if
34: end while
```

---

$S_d(O \cup o)$  we denote a set of source candidates that would remain, if additionally node  $o$  was selected as the observer and source candidates were evaluated for deterministic propagation times. Therefore, assuming node  $s$  is the source we have  $S_d^s(O \cup o) = \{s' : \mathbf{d}(O \cup o, s') = \mathbf{d}(O \cup o, s)\}$  when infection times are used directly as observations and when the difference of distances are used, we have  $S_d^s(O \cup o) = \{s' : [d(o_2, s') - d(o_1, s'), \dots, d(o_k, s') - d(o_1, s')] = [d(o_2, s) - d(o_1, s), \dots, d(o_k, s) - d(o_1, s)]\}$ . Then, plugging in (2.16) new expressions for  $S_d^s(O \cup o)$ , and assuming all source candidates equally likely, we have that at each time step, an expected decrease in the number of source candidates is

$$\Delta(o|S(O)) = |S(O)| - \frac{1}{|S(O)|} \sum_{s \in S(O)} |S_d^s(O \cup o)|. \quad (4.106)$$

At each time step, an observer is selected that maximizes  $\Delta(o|S(O))/c(o)$ , as the cost of nodes should also be considered. If there is more than one node that achieves the maximum, we select the one that contributes the most to distinguishing the remainder of the nodes  $V \setminus S(O)$ . This step is added in the stochastic settings, as, even though  $S(O)$  are the most likely candidates at a given time step, the true source node might be one of the remaining nodes, due to the uncertainty in the observations. Hence, for each node that maximizes the weighted expected benefit, we also calculate

$$\delta(o|S(O)) = - \sum_{s \in V \setminus S(O)} |S_d^s(O \cup o)|, \quad (4.107)$$

and select the node that maximizes (4.107). Selected as such, the subsequent observer contributes the most to distinguishing among the current source candidates, while also, among the nodes with the same performance, distinguishes the most remaining nonsource candidate nodes. The pseudocode for the complete sequential source localization proposed approach is given in Algorithm 7. In the following subsection, we illustrate the merit of the proposed algorithm on a real data set of cholera outbreak.

### 4.2.1 Real-world case study: Cholera Outbreak

We test the merits of the proposed Algorithm 7 on the actual data from a real-world epidemic outbreak. We use information collected for a cholera outbreak in the KwaZulu-Natal province, South Africa, in 2000. The epidemic was caused by a strain of the bacterium *Vibrio cholerae*, which colonizes the human intestine and is transmitted through contamination of aquatic environments [1]. The epidemic lasted for 2 years and involved about 140,000 confirmed cholera cases. The data were provided by the KwaZulu-Natal Health Department and consist of a record of each single cholera case specified by the date and health subdistrict where it occurred, starting from August 2000. We use the network model, developed in [1], for the basin of

river Thukela, the largest of the region, where the number of cholera cases recorded amounted to 29,000. All the channels of perennial rivers are considered edges and all the endpoints of these channels are considered as nodes. A hydrographic map of the KwaZulu-Natal province with the Thukela river basin indicated is shown in Figure 4.5a. The population and the cholera cases of a subdistrict were assigned to the nearest network node. Some network nodes ended up with no population nor cholera cases assigned to it. The most affected nodes were those with intermediate population size. As stated in [1], this is probably due to the fact that the highest population density regions correspond, in this particular case, with the most developed ones. These cities can then rely on wastewater treatment and treated water supply that help to reduce cholera transmission as well. The bacteria can spread along stream both upstream and downstream with a slightly biased propagation downstream, hence, the graph is modeled as undirected. The graphical model describes spreading of bacteria through waterways, but actual cholera spreading depends on seasonal parameters, as well as on human-to-human transmission.

The same data set was also used to illustrate the performance of an algorithm for source localization in [5]. The authors of [5] developed a model for describing the propagation of cholera between two nodes connected by an edge. The propagation delay along the edge between nodes  $u$  and  $v$  is modeled as a Gaussian random variable  $\mathcal{N}(\mu_{u,v}, \sigma_{u,v}^2)$ . The mean  $\mu_{u,v}$  is approximated by  $r_{uv}\Theta/p$ , where  $r_{uv}$  is the physical distance between communities  $u$  and  $v$ ,  $p$  is the spatial drift of cholera, estimated at approximately 3 km/day in [1], and  $\Theta$  is a threshold that corresponds to the number of registered cholera cases needed to consider a community infected, and was set at 50. The standard deviation  $\sigma_{u,v}$  is considered proportional to the mean  $\mu_{u,v}$  with a fixed propagation ratio  $\sigma_{u,v}/\mu_{u,v} = 0.5$ . The time when the first community became infected is considered unknown, and the difference of infection times are used to estimate the source. To accommodate for a non-negligible measurement delay between infection by the vibrios and reporting to local health authorities, the covariance of the infection time of an observer is modified by adding an additional noise term to each entry as follows [5]

$$\Lambda = \Sigma + (\mathbf{M} + \mathbf{I})\sigma_m^2,$$

where  $\Sigma$  is as defined in (4.36),  $\mathbf{M}$  is a matrix of all ones,  $\mathbf{I}$  is an identity matrix and  $\sigma_m$  is the standard deviation of the measurement delay set to 1 day. The source localization in [5] was performed by finding the most likely source node within 2 hops of the first infected observer. It should also be noted that the first community to become infected might not actually be the source of the outbreak due to the delay between the infection and the actual reporting of the disease [5]. Still, we will refer to the first infected community as the true source node.

We apply the proposed Algorithm 7 for the same cholera network and propagation model. In order to incorporate the same prior knowledge as it was used in [5], where the search for the source node was

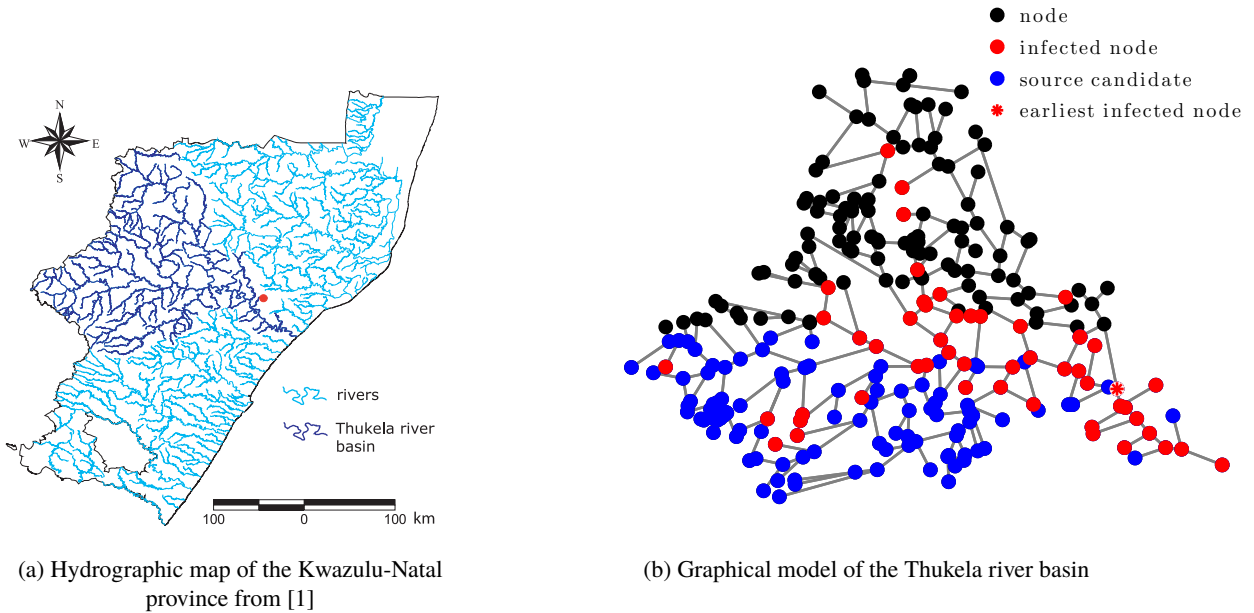


Figure 4.5: Map and a graph model of the Thukela river basin

highly localized within a small neighborhood of the first infected observer, we assume to have a form of prior knowledge, where the source candidates are considered only those nodes in the southern part of the region, below geographical longitude of 28.6, as in this region lies the true source. Still, out of  $N = 287$  nodes, a total of 161 nodes were considered possible source candidates. Applying the same threshold of  $\Theta = 50$ , we ended up with 52 infected nodes, i.e., nodes that have at least 50 registered cholera cases. Only these nodes were considered as potential observers. The graphical model of the Thukela river basin, with indicated infected nodes, possible source candidates and the earliest infected node is shown in Figure 4.5b. We set the parameter  $\beta = 1/N$  and determine the threshold for stopping from (4.103). Since the activation time of the source is unknown, the difference of infection times are used as observations. In the first round of the algorithm, two nodes are selected as observers, according to step 14 of Algorithm 7. The first of these observers is set as a reference node. When checking whether the posterior distribution that characterizes a certain node being the source crosses the threshold, we only look at the 161 possible candidates, not all the nodes. Also, when calculating the benefits of an observer, we first calculate for each observer the average decrease in the number of current source candidates, and for the observers that maximize this value, we also evaluate the benefit related only to the remaining possible candidates. Since there is no available information on the cost of finding the number of cholera cases within each community, we consider the cost of all the observers to be the same and equal 1. The goal of the sequential source localization is to determine the source using the smallest number of observers.

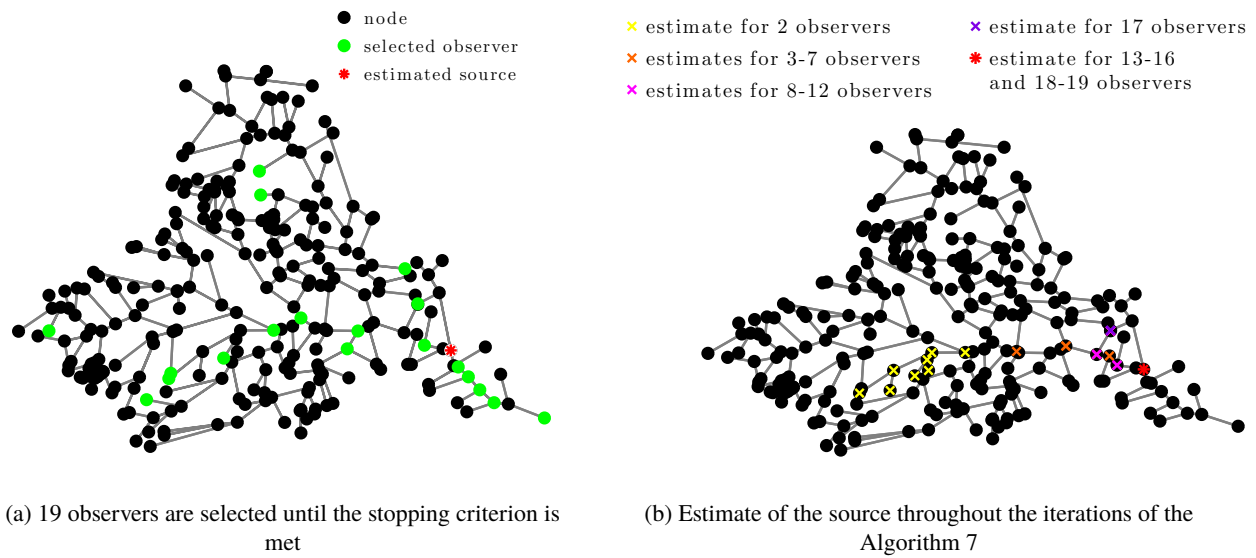


Figure 4.6: The results of applying Algorithm 7 to the dataset of Cholera outbreak in KwaZulu Natal

Once applied, the Algorithm 7 stops after selecting in total 19 observers which are indicated in Figure 4.6a. It correctly estimates the source as the first infected community. Figure 4.7b shows how the estimate of the source changed throughout the iterations of the algorithm. After the initial step and the first two selected observers, there was not a single equivalence class that reached the threshold, the most likely class contained 7 nodes and those became the most likely source candidates. As more and more observers were included, the estimates kept getting closer to the true source. After 13 selected observers, the most likely source candidate was indeed the true source, but its posterior probability distribution still did not cross the threshold. The true source node remained the most likely candidate after a few more observers were added. However, after 17 observers, the estimate was shifted towards another node, 2 hops away from it. With 18 observers, both nodes, the true source and the node 2 hops away from it, became the most likely candidates. After including the observation of the 19-th observer, the true source became the most likely candidate, its posterior distribution crossed the threshold and the sequential test terminated with the true source correctly identified. If instead of stopping, the test proceeded and more observers were selected in the same way, the true source would remain the most likely source candidate until the observation of the 22nd observer was included. Then, the most likely candidate would proceed to be another node that is also 2 hops away from the earliest infected node and this would remain to be the estimated source even after including infection times of all 52 infected nodes. Thus, if all available infection times were used for maximum-likelihood estimation, the estimate of the source, i.e., the most likely source node, would not be the true source, but a node 2 hops away from it. This might be a consequence of true data deviating from the used model, as true infection times do not come from the Gaussian distribution that is used to describe it. As a node is considered infected only

if more than 50 cholera cases have been registered, we have that, for example, the source node was infected at day 85, and its neighbor at day 141, while the neighbor’s neighbor (a node two hops away from the source) was infected at 94th day, i.e., earlier than a node preceding it on the path to the source. Also, as discussed earlier, spreading of cholera occurs not only through waterways, but depends on seasonal parameters, quality of water treatment and mobility of infected individuals.

To evaluate the merits of selecting observers using the proposed criterion based on the expected number of discarded candidates, we repeat the process of sequential source localization, using the same model and the parameters, except, at each iteration, observers are now selected randomly among the infected nodes. We repeat the sequential test 100 times, each time selecting observers randomly and the results of the random selection are shown in Figure 4.7. Whereas with the proposed observer selection criterion the threshold is reached with 19 observers, on average 34.4 observers were needed if they were selected randomly. The histogram of the number of randomly selected observers needed to reach the threshold is shown in Figure 4.7a. In more than 50% of the runs, the algorithm stopped after selecting more than 38 observers and with more than 30% of the runs ending up with more than 44 observers. Figure 4.7b shows the histogram of the distance between the true source and the estimate of the sequential algorithm with random observer selection. In 30% of the runs, the source was estimated as one of the nodes at least 3 hops away from the actual source. The estimate was the true source node in 9% of the cases. In 39% of the cases, the terminated algorithm determined the source to be the same node that is 2 hops away from the actual source, as would be determined by selecting all the potential observers. The comparison with random selection illustrates the benefits of using the proposed selection criterion motivated by adaptive submodularity. Selecting observers

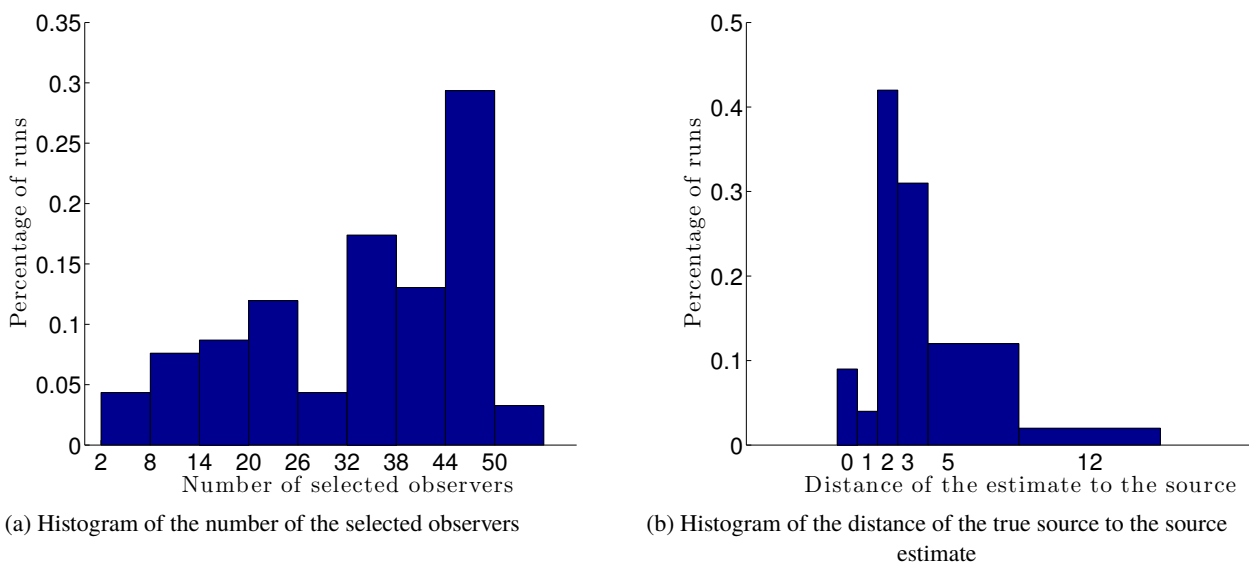


Figure 4.7: The performance of the random observer selection

such that they distinguish the most between possible candidates contributes to the stopping criterion of the sequential test at an earlier time.

### 4.3 Summary

In this Chapter, we have analyzed the problem of selecting the nodes that contribute the most to the localization of the source, now when the infection times are stochastic. Infection time of a node is no longer considered exactly equal to the node's distance to the source. Instead, we model it as a random variable. Determining the source identity is performed with a certain error probability. Exact analytical characterization of the error probability is typically not available. Hence, selecting the nodes that yield the lowest error probability is not feasible. Therefore, in Section 4.1, we have proposed a surrogate metric for error probability – the error exponent that characterizes the rate of decay for vanishing uncertainty. Source localization was framed as a multiple hypothesis problem and we have analyzed the asymptotic behavior of the error. We have exactly evaluated the error exponent for three different diffusion scenarios; in each, the infection times are modeled as random variables with different distributions. In the first scenario, we have adopted a common approximation of a propagation delay between two neighboring nodes with a Gaussian variable of known mean and variance. In the second and the third scenario we return to the assumption of constant propagation delay, but we consider the presence of uncertainty in observing the infection times. Motivated by the modeling of the outliers with Laplace noise, in the second scenario, we introduce Laplace observation noise to model outlier behavior in networks, with each node characterized by different parameters. In order to model the presence of an incubation period in the onset of symptoms, we assume that observations are corrupted by exponential noise in the third scenario that we have considered. Again, as individuals exhibit different behaviors, each node was characterized by different noise parameters. We have shown that the error exponent in this case of infection times modeled exponential variables is a metric and we have presented some interesting bounds for the exponent for some special graphs. For all three diffusion scenarios, the error exponent for vanishing uncertainty was determined using the same framework. The proofs deviated from the standard ones in large deviations as we have encountered two intriguing phenomena. First, in the derivation of exponents, straightforward approaches cannot be applied, since the decision region associated with each hypothesis changes with diminishing noise. Second, we have discovered an interesting duality result for three above-mentioned distributions: the optimization problem for finding the error exponent has a pleasingly simple dual that consists of minimizing the exponent of the density function in the error region. Selecting observer subsets based on the proposed criterion is certainly optimal from the perspective of the fastest error decay as uncertainty decreases. In Subsection 4.1.5, we have illustrated with simulations that the proposed metric is also very useful in a more realistic setting for non-negligible noise, as the subsets

characterized by a higher error exponent generally yield lower error probability than other subsets. We have also demonstrated that selecting subsets based on error exponents leads to lower average error probability compared to subset selection based on the current state of the art, which is centrality based measures. We have also noted that the proposed metric can be used in other applications related to the identification of a sender: for selecting a topology that leads to higher probability of a sender identification in the field of the defense of networks and for selecting a sender node that preserves the anonymity the most.

In Section 4.2, we have addressed the problem of sequential observer selection when the infection times are modeled as correlated Gaussian random variables. We have developed an algorithm for sequential source localization by applying sequential multiple hypothesis testing, once again considering each node in the network as a different alternative for the source. As an observer selection criterion we have adopted a criterion developed for deterministic infection times based on adaptive submodularity from Subsection 2.2.2. At each time step of a sequential test, we have proposed to select a node that decreases the most an expected number of nodes that are characterized by the same density of observations as the current, most likely, source candidates. In case there is more than one such node, the selected observer is the one that contributes the most towards distinguishing the distributions that characterize the nodes that are not the current source candidates. This was added, as due to the presence of uncertainty, the most likely source candidates at a certain time step, might not be also the most likely at the subsequent time step. The merits of the proposed algorithm were illustrated on a real data from a cholera outbreak in a South African province in 2000. We have used an available graphical model [1] of the Thukela river basin that describes the spreading of cholera through rivers and a previously developed model for times of infection by cholera for the same dataset [5]. Used models do not take into consideration all the aspects of cholera spreading, as they do not include the parameters associated with the seasonal aspect of spreading, the possibility of cholera spreading through mobility of infected individuals and the influence of the quality of water treatment in communities. Therefore, as done in previous work, we have incorporated prior knowledge on the source location, that still leaves more than half of nodes as possible, equally likely, source candidates. Also, for observers nodes we have only taken into account those nodes that have crossed a threshold for infection. Our proposed algorithm correctly identifies the earliest infected node. The benefits of the proposed criterion for observer selection were illustrated by comparing with the performance of a random observer selection. When selected randomly, on average, 81% more observers were needed to determine the source and the source estimate was in around 50% of the runs neither the earliest infected node nor the node, 2 hops away from it, that would be the estimate if all the infection times were used for estimation. Hence, we have showed that the proposed algorithm for source localization and observer selection can successfully be applied to real-world diffusion data.

## Chapter 5

# Thesis conclusions and future work

This thesis addresses the question of how to select the observer nodes that contribute the most to the task of source localization on graphs. In this chapter we summarize the contributions we have made in addressing this question for various diffusion scenarios. We conclude by discussing the limitations of the work and some possible future directions.

### 5.1 Conclusions

In order to understand the exclusive effect of the choice of observers on the ability to disambiguate the source, we have first analyzed the observer selection strategies in a deterministic scenario, where the infection times are not corrupted by noise and the network structure is fully known. The observations used to localize the source were the infection times of the observers, which correspond to their graph distance to the source node.

We have modeled the dynamics of the diffusion process as a linear time-varying system for the case of block selection, when all the observer nodes are selected at the same time and assuming the activation time of the source is known. Analogously to characterizing the observability of a system without considering the observation noise, we have defined the concept of network observability to denote the ability to infer the source location from the timestamps of observers in a deterministic, noiseless scenario. We have constructed a network observability matrix and using this matrix, we have provided a necessary and sufficient conditions for network observability. Additionally, we have shown that a network is observable if and only if the set of observers forms a resolving set. Then, we have related the problem of selecting the smallest set of nodes that achieves observability to a known problem of finding the smallest resolving set, which is an NP-Hard problem for general graphs. Leveraging on the results from graph theory, we have determined this smallest set of

nodes for special graph classes. We have proposed two greedy algorithms for observer selection by applying the fact that the problem of finding the smallest resolving set can be framed as a set cover problem and known approximations can be used. The first approximation algorithm determines a set of nodes that would lead to source localization with the smallest cost and the second selects a set of nodes of a given cardinality that would lead to the smallest uncertainty in the source identity. Both algorithms have performance guarantees based on the known greedy cover approximation.

Still for the deterministic setting, we have also analyzed dynamic observer selection strategies which are relevant in applications when observations of the previous observer are used to select the subsequent one. We have also considered that each node might have a different cost, where the cost is associated with resources, like time and effort, required to learn the node's infection time. Using dynamic programming with imperfect state knowledge we have obtained optimal strategies for node selection, again for two problems: localizing a source with the smallest cost and achieving the smallest uncertainty in the source identity for a pre-specified number of observers. As the optimal approach is computationally very intensive, we have developed efficient approximation algorithms for both problems. We have reformulated the problems to fit the adaptive submodularity framework in order to obtain performance guarantees for the greedy approach. Initially, the dynamic strategies were analyzed under the assumption of a known source activation time. Then, we have shown that both the optimal and the greedy approach can be applied for unknown time when the differences of infection times are used instead of infection times. We have proved that the adaptive submodular property still holds under the new assumptions.

After analyzing the observer selection problem with no uncertainty present, we have relaxed the assumption of a completely known network structure, while still assuming deterministic infection times. The structure of local communities is often well known, while the connections between different communities can be hidden, as it may be a weak friendship connection, a random contact or an offline information exchange. Hence, we have studied the observer selection problem in a graph where the edges in each connected components are known, but not the edges that connect different components. We have shown that the number of connected graphs that can be constructed by adding inter-component edges scales exponentially with the number of components. Therefore, we have concluded that the analysis of network observability is not feasible by individual study of all of the compatible topologies. Thus, we have extended the concept of network observability in the context of partially known diffusion graph. Now, a partially known network is considered observable if any source can be determined from the infection times of the observers even without knowing where are the missing edges. When all the components belong to the same graph type - either all trees, complete graphs, grids or cycles - we have determined the necessary and sufficient conditions for the smallest set of observers that makes such a network observable. For example, we have proved that knowing the infection times of all the leaf nodes on all but one tree component and of the nodes that form a

resolving set of the last tree component is both necessary and sufficient to uniquely identify the source node, even without knowing how the tree components are interconnected. When the components have arbitrary structure, we have presented a strategy for observer selection, based on the concept of graph boundary, that achieves network observability. If this strategy is applied for some special graphs, like trees and grids, the cardinality of the set of observers selected is indeed the smallest, or close to it. However, this might not be the case for general graphs, as we have illustrated through simulations for Erdős-Rényi graphs. Selection of nodes based on the proposed condition can easily be done in polynomial time by considering each component separately.

We have also addressed the problem of source localization considering that the inter-component edges are hidden. We have framed the source localization problem as a binary integer linear program modeling it as multicommodity flow problem with side constraints. The feasibility of the proposed optimization problem should be verified for each node in a network. If the problem is feasible for a given node, the node is considered a source candidate. Although the binary integer linear program is computationally very intensive, the proposed formulation does not require explicitly enumerating an exponential number of topologies that are compatible with the partially known network.

After considering the uncertainty in network topology, we have analyzed the observer selection problem in the presence of uncertainty in the observations. The infection time of a node is no longer considered exactly equal to the node's distance to the source and, instead, it is modeled as a random variable. Ideally, we would like to select the nodes that minimize the source localization error. However, an analytical expression for the error probability of source localization is typically not available. Therefore, we have developed a surrogate measure for source localization error, by framing the source localization as a multiple hypothesis testing problem, where each potential source candidate represents a hypothesis. We have analyzed the asymptotic behavior of the error probability of hypothesis testing, considering that the uncertainty vanishes, and not that the number of observations increase, which is the standard approach, as it was not applicable in our case. The metric that we have proposed represents the error exponent that characterizes the rate of error decay for vanishing uncertainty. We have exactly evaluated the error exponent for three different diffusion scenarios. In each of these scenarios the infection times are modeled as random variables with different distributions: Gaussian, Laplacian and exponential. Our derivation showed that selecting an observer subset with the largest exponent leads to the fastest error decay as uncertainty in the observations decreases. We have illustrated with simulations that the proposed metric is also very useful in a more realistic setting for non-negligible noise, as the subsets characterized by a higher error exponent generally yield lower error probability than the other subsets. Additionally, we have demonstrated that selection of subsets based on error exponents leads to lower average error probability compared to subset selection based on the current state of the art, which is centrality based measures. We have also noted that the proposed metric is useful for

other applications that include the task of sender identification: for selecting a topology that leads to higher probability of a sender identification in the field of the defense of networks and for selecting a sender node that preserves the most its anonymity.

Finally we have addressed the problem of sequential observer selection for a common model where the propagation delay along an edge, over which the contagion spreads from a node to its neighbor, is modeled as a Gaussian random variables. We have developed an algorithm for sequential source localization by applying the sequential multiple hypothesis testing procedure, once again considering each node in the network as a different hypothesis. As an observer selection criterion we have adopted a criterion developed for deterministic infection times based on the adaptive submodularity framework. The proposed sequential algorithm was validated on real data from a cholera outbreak in a South African province in 2000 where it successfully localized the first infected community. The number of observer nodes was on average 81% lower than if the choice of observers was random, for even higher accuracy, thereby confirming that the proposed strategy for observer selection also has merit for stochastic infection times.

## 5.2 Limitations and future work

In this thesis we have addressed the problem of observer selection for the purpose of source localization by simplifying certain aspects of the network diffusion model. These simplifications were necessary in order to theoretically analyze the diffusion process in networks and gain crucial insight for tackling real-world scenarios. We have started with a very simple, purely deterministic, model, assuming exact knowledge of the infection times, source activation time and network structure. Later, we allowed uncertainty in the network structure, but still assuming perfect knowledge of the infection times. Separately, we have relaxed the restriction on perfect knowledge of the times, but now assuming exact knowledge of the network structure. We have also allowed the activation time to be unknown. Theoretical analysis of the deterministic model revealed important insights that were applied in subsequent work where uncertainty was present.

Actual diffusion takes place in the presence of multiple uncertainties at the same time. Additionally, the assumption that each node infects its neighbor deterministically, with probability one, typically does not hold. Some possible directions for future work include the analysis of selection strategies while accommodating both partial knowledge of times and topology, as well as considering probabilistic infection models. Moreover, when assuming the uncertainty in the diffusion topology, we have only considered that inter-component edges were hidden and the known network consisted of disconnected components, while it may be less restrictive to assume that an intra-component edge might be hidden as well and multiple inter-component edges might exist.

Besides adding more uncertainty to the diffusion model, another future direction could be the interpre-

tation of the results obtained so far in the context of graphs, for example, what are the graph properties of the subset of nodes that has the highest error exponent, or how the exponent changes for different graph classes. We have tackled some of these questions for the diffusion model with random incubation period, when the infection times are modeled as random variables with exponential distribution. However, it would be interesting to see what can be done for other diffusion models, as well as to further explore the network parameters (centrality or mutual distance) of the selected observer nodes.

Finally, we would like to adapt the proposed approaches in order to efficiently apply them on large-scale networks. For example, the proposed metric based on error exponents represents a surrogate metric for error probability for which no expression is available, and it can be used to compare performances of different subsets. However, if we would like to identify a subset of  $k$  observers that has the highest error exponent, a total of  $\binom{N}{k}$  possible subsets need to be checked, and for each  $\binom{N}{2}$  values need to be evaluated, which is not feasible even for moderate values of  $N$ . Hence, a possible research direction of significant practical relevance would be a modification of this, and other proposed strategies, such that they can easily be implemented on real networks with a large number of nodes.



## Chapter 6

# Bibliography

- [1] E. Bertuzzo, S. Azaele, A. Maritan, M. Gatto, I. Rodriguez-Iturbe, and A. Rinaldo, “On the space-time evolution of a cholera epidemic,” *Water Resources Research*, vol. 44, 2008.
- [2] M. Newman, “The spread of epidemic disease on networks,” *Physical Review E*, vol. 66, no. 1, pp. 16–28, July 2002.
- [3] A. G. M. Draief and L. Massoulié, “Thresholds for virus spread on networks,” *Annals of Applied Probability*, 2008, 2008.
- [4] D. Shah and T. Zaman, “Rumors in a network: who’s the culprit?” *IEEE Transactions on Information Theory*, 2011.
- [5] P. Pinto, P. Thiran, and M. Vetterli, “Locating the source of diffusion in large-scale networks,” *Physical Review Letters*, August 2012.
- [6] E. Seo, P. Mohapatra, and T. F. Abdelzaher, “Identifying rumors and their sources in social networks,” *SPIE DSS*, 2012.
- [7] N. Karamchandani and M. Franceschetti, “Rumor source detection under probabilistic sampling,” *ISIT*, 2013.
- [8] W. Luo, W. Tay, and M. Leng, “How to identify an infection source with limited observations,” *IEEE Journal of Selected Topics in Signal Processing*, vol. 8, no. 4, pp. 586–597, Aug 2014.
- [9] L. E. Celis, F. Pavetić, B. Spinelli, and P. Thiran, “Budgeted sensor placement for source localization on trees,” *LAGOS*, 2015.

- [10] X. Zhang, Y. Zhang, T. Lv, and Y. Yin, “Identification of efficient observers for locating spreading source in complex networks,” *Physica A*, vol. 442, pp. 100–109, 2016.
- [11] Z. Shen, S. Cao, W. Wang, Z. Di, and H. E. Stanley, “Locating the source of diffusion in complex networks by time-reversal backward spreading,” *Physical Review E*, vol. 93, 2016.
- [12] H. W. Hethcote, “The mathematics of infectious diseases,” *SIAM Review*, vol. 42, no. 4, pp. 599–653, 2000.
- [13] A. Ganesh, L. Massoulie, and D. Towsley, “The effect of network topology on the spread of epidemics,” *IEEE Infocom*, 2005.
- [14] M. Woolhouse, “How to make predictions about future infectious disease risks,” *Philosophical Transactions of the Royal Society B*, 2011.
- [15] D. Balcan, B. Gonçalves, H. Hu, J. J. Ramasco, V. Colizza, and A. Vespignani, “Modeling the spatial spread of infectious diseases: the GLObal Epidemic and Mobility computational model,” *Journal of Computational Science*, 2010.
- [16] S. Eubank, H. Guclu, V. S. A. Kumar, M. V. Marathe, A. Srinivasan, Z. Toroczkai, and N. Wang, “Modelling disease outbreaks in realistic urban social networks,” *Nature*, vol. 429, 2004.
- [17] V. Colizza, A. Barrat, M. Barthélemy, and A. Vespignani, “Predictability and epidemic pathways in global outbreaks of infectious diseases: the SARS case study,” *BMC Medicine*, 2007.
- [18] E. Valdano, C. Poletto, A. Giovannini, D. Palma, L. Savini, and V. Colizza, “Predicting epidemic risk from past temporal contact data,” *PLOS Computational Biology*, 2015.
- [19] M. Tildesley, N. Savill, D. Shaw, R. Deardon, S. Brooks, M. Woolhouse, B. Grenfell, and M. Keeling, “Optimal reactive vaccination strategies for a foot-and-mouth outbreak in Great Britain,” *Nature*, vol. 440, 2005.
- [20] S. Lee, L. E. C. Rocha, F. Liljeros, and P. Holme, “Exploiting temporal network structures of human interaction to effectively immunize populations,” *PLOS One*, 2012.
- [21] W. Dong, W. Zhang, and C.W.Tan, “Rooting out the rumor culprit from suspects,” *ISIT*, 2013.
- [22] W. Luo, W. P. Tay, and M. Leng, “Identifying infection sources and regions in large networks,” *IEEE Transactions on Signal Processing*, vol. 61, no. 11, pp. 2850–2864, June 2013.
- [23] Z. Wang, W. Dong, W. Zhang, and C.W.Tan, “Rumor source detection with multiple observations: Fundamental limits and algorithms,” *SIGMETRICS*, pp. 1–13, 2014.

- [24] K. Zhu and L. Ying, "Information source detection in the SIR model: A sample path based approach," *ITA Workshop*, 2013.
- [25] W. Luo and W. Tay, "Finding an infection source under the SIS model," *ICASSP*, 2013.
- [26] K. Zhu and L. Ying, "Information source detection in networks: Possibility and impossibility results," *IEEE Infocom*, 2016.
- [27] N. Antulov-Fantulina, A. Lancic, H. Stefancic, M. Sikic, and T. Smuc, "Statistical inference framework for source detection of contagion processes on arbitrary network structures," *SASOW*, 2014.
- [28] C. H. Comin and L. da Fontoura Costa, "Identifying the starting point of a spreading process in complex networks," *Physical Review E*, vol. 84, 2011.
- [29] B. Prakash, J. Vrekeen, and C. Faloutsos, "Spotting culprits in epidemics: How many and which ones?" *IEEE ICDM*, 2012.
- [30] V. Fioriti and M. Chinnici, "Predicting the sources of an outbreak with a spectral technique," *CoRR*, 2012.
- [31] A. Lokhov, M. Mézard, H. Ohta, and L. Zdeborova, "Inferring the origin of an epidemic with a dynamic message-passing algorithm," *Physical Review E*, vol. 90, 2014.
- [32] F. Yang, R. Zhang, Y. Yao, and Y. Yuan, "Locating the propagation source on complex networks with propagation centrality algorithm," *Knowledge-Based Systems*, 2016.
- [33] K. Zhu, Z. Chen, and L. Ying, "Locating contagion sources in networks with partial timestamps," *Data Mining and Knowledge Discovery*, pp. 1–32, 2015.
- [34] X. Chen, X. Hu, and C. Wang, "Approximability of the minimum weighted doubly resolving set problem," *Computing and Combinatorics, Proceedings of 20th International Conference COCOON*, 2014.
- [35] L. Lu and T. Zhou, "Link prediction in complex networks: A survey," *Physica A*, 2010.
- [36] M. Kim and J. Leskovec, "The network completion problem: Inferring missing nodes and edges in networks," *SDM*, pp. 47–58, 2011.
- [37] M. Gomez-Rodriguez, J. Leskovec, and A. Krause, "Inferring networks of diffusion and influence," *Knowledge Discovery from Data*, 2010.
- [38] S. A. Myers and J. Leskovic, "On the convexity of latent social network inference," *NIPS*, 2010.

- [39] Z. Shen, W. Wang, Y. Fan, Z. Di, and Y. Lai, “Reconstructing propagation networks with natural diversity and identifying hidden sources,” *Nature Communications*, vol. 5, no. 4323, 2013.
- [40] P. Zhang, J. He, G. Long, G. Huang, and C. Zhang, “Towards anomalous diffusion sources detection in a large network,” *ACM Trans. Internet Technol.*, vol. 16, no. 1, 2016.
- [41] M. Eslami, H. R. Rabiee, and M. Salehi, “DNE: A method for extracting cascaded diffusion networks from social networks,” *PASSAT*, 2011.
- [42] S. Zejnilović, J. Gomes, and B. Sinopoli, “Network observability and localization of the source of diffusion based on a subset of nodes,” *Allerton*, 2013.
- [43] —, “Sequential observer selection for source localization,” *GlobalSIP*, 2015.
- [44] S. Zejnilović, D. Mitsche, J. Gomes, and B. Sinopoli, “Network observability for source localization in graphs with unobserved edges,” *GlobalSIP*, 2014.
- [45] —, “Extending the metric dimension to graphs with missing edges,” *Theoretical Computer Science*, vol. 609, pp. 384–394, 2016.
- [46] S. Zejnilović, J. Gomes, and B. Sinopoli, “Network observability and localization of source of diffusion in tree networks with missing edges,” *EUSIPCO*, 2014.
- [47] S. Zejnilović, J. Xavier, J. Gomes, and B. Sinopoli, “Assessing node selection strategies for source localization on graphs via error exponents,” *to be submitted to IEEE Transactions on Signal Processing*, 2016.
- [48] N. Biggs, “Algebraic graph theory,” *Cambridge University Press*, 1993.
- [49] G. Chartrand, L. Eroha, M. A. Johnson, and O. R. Oellermann, “Resolvability in graphs and the metric dimension of a graph,” *Discrete Applied Mathematics*, vol. 105, pp. 99–113, 2000.
- [50] P. Slater, “Leaves of trees,” *Congressus Numerantium*, vol. 14, pp. 549–559, 1975.
- [51] W. Goddard and O. R. Oellermann, *Chapter Distance in Graphs in Structural Analysis of Complex Networks*. Birkhauser, 2009.
- [52] S. Khuller, B. Raghavachari, and A. Rosenfeld, “Landmarks in graphs,” *Discrete Applied Mathematics*, vol. 70, no. 3, pp. 217–229, 1996.
- [53] C. Hernando, M. Mora, I. M. Pelayo, C. Seara, J. Caceres, and M. L. Puertas, “On the metric dimension of some families of graphs,” *Electronic Notes in Discrete Mathematics*, vol. 22, pp. 129–133, 2005.

- [54] B. Bollobas, D. Mitsche, and P. Pralat, “Metric dimension for random graphs,” *The electronic journal of combinatorics*, Aug 2013.
- [55] V. V. Vazirani, *Approximation Algorithms*. Springer, 2001.
- [56] J. Caceres, C. Hernando, M. Mora, I. Pelayo, M. L. Puertas, C. Seara, and D. R. Wood, “On the metric dimension of cartesian products of graphs,” *SIAM J. Discrete Math.*, vol. 21(2), pp. 423–441, 2007.
- [57] D. Bertsekas, *Dynamic programming and Optimal Control*. Athena Scientific, 1995, vol. I.
- [58] D. Garijo, A. Gonzalez, and A. Marquez, “The resolving number of a graph,” *arXiv:1309.0252v1*, 2013.
- [59] D. Golovin and A. Krause, “Adaptive submodularity: Theory and applications in active learning and stochastic optimization,” *Journal of Artificial Intelligence Research*, vol. 42, pp. 427–486, 2011.
- [60] D. J. Watts and S. H. Strogatz, “Collective dynamics of ‘small-world’ networks,” *Letters to nature*, no. 393, pp. 440–442, June 1998.
- [61] M. Jackson, *Social and Economic Networks*. Princeton University Press, 2008.
- [62] A. Cayley, *The collected mathematical papers of Arthur Cayley, ScD., FRS*. Nabu Press, 2013.
- [63] G. Chartrand, D. Erwin, G. L. Johns, and P. Zhang, “Boundary vertices in graphs,” *Discrete Mathematics*, vol. 263, pp. 25–34, 2003.
- [64] C. Hernando, M. Mora, I. M. Pelayo, and C. Seara, “Some structural, metric and convex properties on the boundary of a graph,” *Electronic notes in Discrete Mathematics*, vol. 24, pp. 203–209, 2006.
- [65] D. P. Bertsekas, *Network Optimization: Continuous and Discrete Models*. Athena Scientific, 1998.
- [66] S. K. Singh, M. P. Singh, and D. K. Singh, “A survey on network security and attack defense mechanism for wireless sensor networks,” *International Journal of Computer Trends and Technology*, 2011.
- [67] T. Peng, C. Leckie, and K. Ramamohanarao, “Survey of network-based defense mechanisms countering the DoS and DDoS problems,” *ACM Comput. Surv.*, vol. 39, no. 1, 2007.
- [68] Global Voices Advocacy. [Online]. Available: <https://advox.globalvoices.org/>
- [69] T. Cover and J. Thomas, *Elements of Information Theory 2nd Edition*. Wiley Series in Telecommunications and Signal Processing, 2006.
- [70] L. Lovász, *Large networks and graph limits*. Colloquium Publications, 2012.

- [71] P. Gupta and P. Kumar, “The capacity of wireless networks,” *IEEE Transactions on Information Theory*, vol. 46, no. 2, pp. 388–404, 2000.
- [72] G. Frahm, “Generalized elliptical distributions: Theory and applications,” Ph.D. dissertation, Universität zu Köln, 2004.
- [73] F. Nielsen, “Generalized Bhattacharyya and Chernoff upper bounds on Bayes error using quasi-arithmetic means,” *Pattern Recognition Letters*, vol. 42, pp. 25–34, 2014.
- [74] Horn and Johnson, *Matrix Analysis*. Cambridge University Press, 1985.
- [75] S. Boyd and L. Vandenberghe, “Convex optimization,” *Cambridge University Press*, 2004.
- [76] J. Gao, F. Liang, W. Fan, C. Wang, Y. Sun, and J. Han, “On community outliers and their efficient detection in information networks,” *KDD*, 2010.
- [77] A. Martinez, “Communication by energy modulation: The additive exponential noise channel,” *IEEE Transactions on Information Theory*, vol. 57, no. 6, Jun 2011.
- [78] S. Zejnilović, J. Xavier, J. Gomes, and B. Sinopoli, “Selecting observers for source localization via error exponents,” *ISIT*, 2015.
- [79] V. P. Dragalin, A. G. Tartakovsky, and V. V. Veeravalli, “Multihypothesis sequential probability ratio tests—part i: Asymptotic optimality,” *IEEE Transactions on Information Theory*, vol. 45, no. 7, 1999.
- [80] A. G. Tartakovsky, “Asymptotic optimality of certain multihypothesis sequential tests: Non-i.i.d. case,” *Statistical Inference for Stochastic Processes*, 1999.
- [81] A. Tartakovsky, “Asymptotically optimal sequential tests for nonhomogeneous processes,” *Sequential Analysis*, vol. 17, 1998.
- [82] C. Baum and V. V. Veeravalli, “A sequential procedure for multihypothesis testing,” *IEEE Transactions on Information Theory*, vol. 40, no. 6, 1994.